

**DESIGN, 2D QSAR STUDIES SYNTHESIS AND  
PHARMACOLOGICAL EVALUATION OF NOVEL COUMARIN  
TETHERED PYRIMIDINE DERIVATIVES**

**A Dissertation submitted to**

**THE TAMILNADU Dr. M.G.R MEDICAL UNIVERSITY  
CHENNAI – 600032**

**In partial fulfilment of the requirements for the award of the  
degree of**

**MASTER OF PHARMACY**

**IN**

**BRANCH II- PHARMACEUTICAL CHEMISTRY**

**SUBMITTED BY**

**T.R. RAJADEVI RAVI (261915010)**

**Under the Guidance of**

**Dr. S. AMUTHALAKSHMI.M. Pharm., Ph.D.,  
ASSOCIATE PROFESSOR**

**DEPARTMENT OF PHARMACEUTICAL CHEMISTRY**



**C.L. BAID METHA COLLEGE OF PHARMACY.**

**(An ISO 9001-2008 certified Institute)**

**THORAIPAKKAM, CHENNAI-600097**

October 2021

Phone : 24960151, 24962592, 24960425  
e-mail : cbaidmethacollege@gmail.com  
Website : www.cbaidmethacollege.com



**C.L. Baid Metha College of Pharmacy**  
An ISO 9001:2008 approved institution  
Jyothi Nagar, Old Mahabalipuram Road,  
Thorapakkam, Chennai - 600 097.



ISO 9001 : 2008  
Reg. No : RQ91/3438

Affiliated to The Tamil Nadu Dr. M.G.R. Medical University, Chennai.  
Approved by Pharmacy Council of India, New Delhi, and  
All India Council for Technical Education, New Delhi

**L. Uday Metha**  
Secretary & Correspondent

**Dr. Grace Rathnam, M.Pharm, Ph.D**  
Principal

**Dr. Grace Rathnam, M.Pharm; Ph.D.**  
Principal & HOD,  
Department of Pharmaceutics,  
C.L. Baid Metha College of Pharmacy,  
Chennai-97

### CERTIFICATE

This is to certify that the project entitled “**DESIGN, 2D QSAR STUDIES SYNTHESIS AND PHARMACOLOGICAL EVALUATION OF NOVEL COUMARIN TETHERED PYRIMIDINE DERIVATIVES**” was submitted by **T.R.RAJADEVI RAVI (261915010)**, in partial fulfilment for the award of the degree of **Master of Pharmacy** during the academic year 2020–2021.it was carried out at C.L. BAID METHA COLLEGE OF PHARMACY, CHENNAI-600097 under the guidance and supervision of Dr. S.AMUTHALAKSHMI.M.PHARM,PH.D., associate professor Department Of Pharmaceutical Chemistry during the academic year 2020–2021

Date:  
Chennai-97

**Dr. Grace Rathnam, M.Pharm; Ph.D.**  
Principal & HOD,  
Department of Pharmaceutics,  
C.L. Baid Metha College of Pharmacy,  
Chennai-97



Affiliated to The Tamil Nadu Dr. M.G.R. Medical University, Chennai.  
Approved by Pharmacy Council of India, New Delhi, and  
All India Council for Technical Education, New Delhi

**L. Uday Metha**  
Secretary & Correspondent

**Dr. Grace Rathnam, M.Pharm, Ph.D**  
Principal

Dr. N.Ramalakshmi, M.Pharm; Ph.D;  
Prof & Head,  
Department of Pharmaceutical Chemistry,  
C.L. Baid Metha College of Pharmacy,  
Chennai-97

### CERTIFICATE

This is to certify that the project entitled “**DESIGN, 2D QSAR STUDIES SYNTHESIS AND PHARMACOLOGICAL EVALUATION OF NOVEL COUMARIN TETHERED PYRIMIDINE DERIVATIVES**” was submitted by **T.R.RAJADEVI RAVI (261915010)**, in partial fulfilment for the award of the degree of **Master of Pharmacy** during the academic year 2020–2021. It was carried out at C.L. BAID METHA COLLEGE OF PHARMACY, CHENNAI-600097 under the guidance and supervision of Dr. S.AMUTHALAKSHMI.M.PHARM,PH.D., associate professor Department Of Pharmaceutical Chemistry during the academic year 2020–2021

Date:  
Chennai-97

Dr. N.Ramalakshmi, M.Pharm; Ph.D;  
Prof & Head,  
Department of Pharmaceutical Chemistry,  
C.L. Baid Metha College of Pharmacy,  
Chennai-97

Phone : 24960151, 24962592, 24960425  
e-mail : clbaidmethacollege@gmail.com  
Website : www.clbaidmethacollege.com



# C.L. Baid Metha College of Pharmacy

An ISO 9001:2008 approved institution

Jyothi Nagar, Old Mahabalipuram Road,  
Thorapakkam, Chennai - 600 097.



Affiliated to The Tamil Nadu Dr. M.G.R. Medical University, Chennai.  
Approved by Pharmacy Council of India, New Delhi, and  
All India Council for Technical Education, New Delhi

**L. Uday Metha**  
Secretary & Correspondent

**Dr. Grace Rathnam, M.Pharm, Ph.D**  
Principal

**Dr.S .AMUTHALAKSHMI.M.PHARM, PH.D**  
Associate Professor,  
Department of Pharmaceutical Chemistry,  
C.L. Baid Metha College of Pharmacy,  
Chennai-97

## CERTIFICATE

This is to certify that the project entitled “**DESIGN, 2D QSAR STUDIES SYNTHESIS AND PHARMACOLOGICAL EVALUATION OF NOVEL COUMARIN TETHERED PYRIMIDINE DERIVATIVES**” as submitted by **T. R. RAJADEVI RAVI (261915010)**, in partial fulfillment for the award of the degree of **Master of Pharmacy** in the academic year **2019-21**. It was carried out at **C.L. BAID METHA COLLEGE OF PHARMACY, CHENNAI – 600097** under the guidance and supervision of **Dr.S.AMUTHALAKSHMI.M.Pharm, Ph.D.**, Associate Professor in the Department of Pharmaceutical Chemistry during the academic year 2019 –2021.

Date:  
Chennai-97

**Dr.S. AMUTHALAKSHMI.M. PHARM, PH. D**  
Associate Professor,  
Department of Pharmaceutical Chemistry,  
C.L. Baid Metha College of Pharmacy,  
Chennai-97

## DECLARATION

I do hereby declare that the thesis entitled “**DESIGN, 2D QSAR STUDIES SYNTHESIS AND PHARMACOLOGICAL EVALUATION OF NOVEL COUMARIN TETHERED PYRIMIDINE DERIVATIVES**” by **T.R. RAJADEVI RAVI (261915010)**, in partial fulfilment of the degree of **MASTER OF PHARMACY** was carried out at **C.L. BAID METHA COLLEGE OF PHARMACY, CHENNAI-600 097** under the guidance and Supervision of **Dr.S. AMUTHALAKSHMI.M. Pharm, Ph.D.**, Associate Professor during the academic year 2019-2021. The work embodied in this thesis is original & is not submitted in part or full for any other degree of this or any other University.

PLACE: CHENNAI-97

**T.R. RAJADEVI RAVI**

DATE:

**(261915010)**

**Department of Pharmaceutical Chemistry**

## **ACKNOWLEDGEMENT**

First and foremost, I would like to thank my father Almighty for giving me the strength, knowledge, ability and opportunity to undertake this research study and to persevere and complete it satisfactorily. Without his blessings, this achievement would not have been possible.

I express my sincere gratitude to my guide, **Dr. S. AMUTHALAKHSMI, Ph.D.**, Department of Pharmaceutical Chemistry, C.L. Baid Metha College of Pharmacy, Chennai who gave inspiration and guidance at every stage of my dissertation work, her valuable suggestion and discussion have enabled me to execute the present work successfully.

I sincerely thank **Dr. GRACE RATHNAM, M. Pharm, Ph.D., Principal**, C.L. Baid Metha College of Pharmacy, Chennai, for providing the necessary facilities for my project work.

It's my privilege to express my grateful and sincere gratitude to **Dr. N. RAMALAKSHMI, M.Pharm, Ph.D.**, Professor, HOD, Department of Pharmaceutical Chemistry and **Mrs. K. DUNMATHI M. Pharm**, Asst. Prof. Department of Pharmaceutical Chemistry for their valuable suggestions.

I acknowledge my sincere thanks to **Mrs. REMYA R.S M. Pharm**, Asst. Prof and **Mrs. E.SANKARI**, Asst. Prof Department of Pharmaceutical Chemistry to share the valuable points in this work.

I sincerely thank our Chief Librarian, **Mrs. RAJALAKSHMI**, for providing necessary reference material for my project work.

I owe special thanks to **Mr. Srinivasan and Mrs. Shanthi**, Stores in- charge, C.L. Baid Metha College of Pharmacy, Chennai, for their timely supply of all necessary chemicals and reagents required for the completion of my project work.

I am thankful to **Mrs. MUTHULAKSHMI**, Lab attender, Department of Pharmaceutical Chemistry, C.L. Baid Metha College of Pharmacy, Chennai, for providing clean and sophisticated environment during the work period.

I am thankful to **Mr. GANESH BAHADUR**, Chief Security, C.L. Baid Metha College of Pharmacy, Chennai, for providing an uninterrupted service at the college campus during the work period.

I am thankful to Miss. **PADMA K**, C.L. Baid Metha College of Pharmacy, Chennai, for providing a support and well wishes for their moral support.

The acknowledgement would be incomplete if I did not mention my **mother-S.Thenmozhiravi and sisters, Friends and Well Wishers** for their moral support and encouragement in completing this project work successful.

**Place:** Chennai

**T.R. RAJADEVI RAVI**

**(261915010)**

**Department of Pharmaceutical Chemistry**

## CONTENTS

S.No.	PARTICULARS	PAGE NO.
1	<b>INTRODUCTION</b>	1
	1.1 4-Methyl-7-Hydroxy Coumarin	4
	1.2 4-Methyl,-7-Hydroxy-8- Acetyl Coumarin	5
	1.3 4-Methyl-7-Hydroxy-8-Pyrimidine coumarin	6
	1.4 Peckman Condensation	7
	1.5 Antibacterial	8
	1.6 2D QSAR model	10
	1.7 Docking	11
	1.8 Drug filters	12
2	<b>REVIEW OF LITERATURE</b>	14
3	<b>AIM AND OBJECTIVE</b>	27
4	<b>PLAN OF THE STUDY</b>	29
5	<b>MATERIALS AND METHODS</b>	30
	5.1 2D QSAR model	31
	5.2 Design Of Compounds	34
	5.3 <i>InSilico</i> Screening of Designed Compounds	37
	5.4 Docking	47
	5.5 Synthesis	48
	5.6 Characterization	50
	5.7 Biological Evaluation	52



<b>S.No.</b>	<b>PARTICULARS</b>	<b>PAGE NO.</b>
6	<b>RESULTS AND DISCUSSION</b>	54
	6.1 2D QSAR model	55
	6.2 Design of Compounds	69
	6.3 <i>InSilico</i> Screening of Designed Compounds	73
	6.4 Docking	83
	6.5 Synthesis	89
	6.6 characterization	90
	6.7 biological evaluation	102
7	<b>CONCLUSION</b>	107
8	<b>BIBILIOGRAPHY</b>	108

## DESIGN, 2D QSAR STUDIES SYNTHESIS AND PHARMACOLOGICAL EVALUATION OF NOVEL COUMARIN TETHERED PYRIMIDINE DERIVATIVES

### 1. INTRODUCTION:

The design and synthesis of biologically active molecules to address unmet medical needs". However, this oversimplification ignores the larger historical context of medicinal chemistry and its ongoing evolution. To truly understand this discipline, we need to examine its past, present, and future to determine how it has come to encompass many different scientific domains, and how it is still shaping the world today. This significantly improves the scientific and economic efficiency of the drug screening process and broadens our library of potential drug candidates [1].

Medicinal chemists are no longer just mixing chemicals to make new drugs. They are utilizing the power of Nature to chemo enzymatically generate new compounds (Garneau-Tsodikova). Even though most people today still consider medicinal chemistry as the design and synthesis of biologically active molecules, no one would deny that medicinal chemistry has evolved to be the center of a vast variety of related scientific fields. Medicinal chemists connect the communities of analytical chemists, computational chemists, biochemists, chemical biologists, molecular biologists, cell biologists, structural biologists, microbiologists, pharmacologists, toxicologists, and translational medicine experts [2].

Medicinal chemistry is the subject of pharmaceutical sciences which applies the principles of chemistry and biology to certain of knowledge leading to the invention of new therapeutic agents. Bacterial infection is an exclusive natural cycle that happens due to physical, immunological, and organic signs of progress to the human body [3].

The consequences of persistent bacterial infections potentially include increased morbidity and mortality from the infection itself and also an increased risk of dissemination of disease. It is also proposed that treatment with bactericidal antibiotics may bring about expanded oxidative stress through the Fenton response [4].

It is noticed that more noteworthy quantities of persisters in *E. coli* subpopulations with ordinary morphology and lower hydroxyl extremist focuses following anti-infection treatment, contrasted and filamentous populaces with expanded hydroxyl revolutionary fixations, recommending for

oxidative stress response in persister survival [5].

When decreased concentrations of ROS (Reactive oxidative stress) is achieved, either through small reductions in oxygen tension or with the addition of thiourea, a free radical quencher, the antibiotic tolerant persister population survives in antibiotic treatment [6].

The ongoing process in the advancement of antimicrobial specialists has neglected to arrive at the assumptions about the hazardous effects and microbial resistance, which prompted a long search for novel and selective antimicrobial drugs [7].

The coumarin derivatives are excellent antibacterial profile and of its specialty that it can act through different mechanisms. The coumarin analogs are found to be useful in the therapy, prophylaxis of bacterial infections and can represent a layout for the development of novel antibacterial drugs.

Recently, many of these substituted coumarins were synthesized and proved active against the gram positive and gram negative bacterial species. This investigation also focuses the future development of the coumarin pharmacophore for antimicrobial activity. Urinary tract infections are the most serious infections among the most common bacterial infections caused by *Escherichia coli*.

Coumarin a benzopyrone derivative is extensively distributed in plant kingdom found to be most efficacious against various microbes. It is also a renowned moiety owing to its vast pharmacological characteristics [8,9].

Recently, many of these substituted coumarins were synthesized and proved active against the gram positive and gram negative bacterial species [10].

The coumarin analogs are found to be useful in the therapy, prophylaxis of bacterial infections and can represent a layout for the development of novel antibacterial drugs [11,12,13,14].

The current article specifically focuses on recent structural developments and the SAR of coumarin analogs against *E.coli* [15].

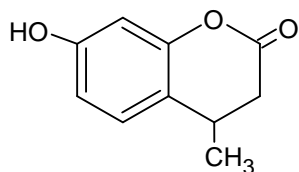
This investigation also focuses the future development of the coumarin pharmacophore for antimicrobial plant-based mixtures [16].

Urinary tract infections are the most serious infections among the most communal bacterial infections caused by *Escherichia coli* [17, 18].

The two different types of *E.coli* are type-1 and type-2. The type-1 pili is most widely distributed and uropathogenic *E. coli* binds to receptors on surface cells lining the bladder or vaginal epithelial cells allied with increased severity of UTI [19].

Moreover, the antimicrobial resistance in *E.coli* is a serious concern worldwide [20].

Thus, the *E.coli* infection treatment has been complicated for most of the first-line derivatives. Still, the popularly known drug cotrimoxazole is the only best option for *E.coli* urinary tract infections [21].

**1.1 4-METHYL-7- HYDROXY COUMARIN:**

Molecular Formula: C<sub>10</sub>H<sub>10</sub>O<sub>3</sub>

Formula Weight: 178.1846

Composition: C(67.41%) H(5.66%) O(26.94%)

Molar Refractivity: 46.75 ± 0.3 cm<sup>3</sup>

Molar Volume: 142.2 ± 3.0 cm<sup>3</sup>

Parachor: 371.2 ± 6.0 cm<sup>3</sup>

Index of Refraction: 1.571 ± 0.02

Surface Tension: 46.4 ± 3.0 dyne/cm

Density: 1.252 ± 0.06 g/cm<sup>3</sup>

Dielectric Constant: Not available

Polarizability: 18.53 ± 0.5 10<sup>-24</sup>cm<sup>3</sup>

RDBE: 6

Monoisotopic Mass: 178.062994 Da

Nominal Mass: 178 Da

Average Mass: 178.1846 Da

M+: 178.062446 Da

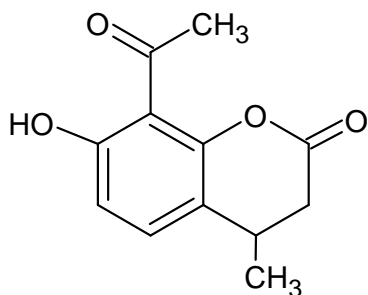
M-: 178.063543 Da

[M+H]<sup>+</sup>: 179.070271 Da

[M+H]<sup>-</sup>: 179.071368 Da

[M-H]<sup>+</sup>: 177.054621 Da

[M-H]<sup>-</sup>: 177.055718 Da

**1.2 4-METHYL-7-HYDROXY-8-ACETYL COUMARIN**

Molecular Formula: C<sub>12</sub>H<sub>12</sub>O<sub>4</sub>

Formula Weight: 220.22128

Composition: C(65.45%) H(5.49%) O(29.06%)

Molar Refractivity: 56.78 ± 0.3 cm<sup>3</sup>

Molar Volume: 173.7 ± 3.0 cm<sup>3</sup>

Parachor: 454.7 ± 6.0 cm

Index of Refraction: 1.567 ± 0.02

Surface Tension: 46.9 ± 3.0 dyne/cm

Density: 1.267 ± 0.06 g/cm<sup>3</sup>

Dielectric Constant: Not available

Polarizability: 22.50 ± 0.5 10<sup>-24</sup>cm<sup>3</sup>

RDBE: 7

Monoisotopic Mass: 220.073559 Da

Nominal Mass: 220 Da

Average Mass: 220.2213 Da

M+: 220.07301 Da

M-: 220.074107 Da

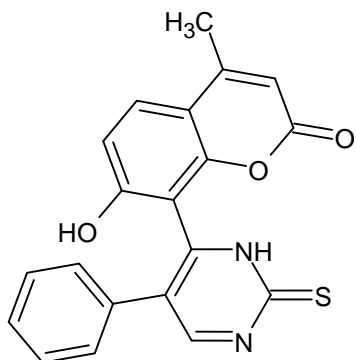
[M+H]<sup>+</sup>: 221.080835 Da

[M+H]<sup>-</sup>: 221.081932 Da

[M-H]<sup>+</sup>: 219.065185 Da

[M-H]<sup>-</sup>: 219.066282 Da

## 1.3 4-METHYL-7-HYDROXY-8-PYRIMIDINECOUMARIN



Molecular Formula:  $C_{20}H_{15}N_2O_3$

Formula Weight: 378.3514

Composition: C(69.56%) H(4.38%) N(12.17%) O(13.90%)

Molar Refractivity:  $95.95 \pm 0.3 \text{ cm}^3$

Molar Volume:  $252.8 \pm 3.0 \text{ cm}^3$

Parachor:  $720.3 \pm 6.0 \text{ cm}^3$

Index of Refraction:  $1.683 \pm 0.02$

Surface Tension:  $65.9 \pm 3.0 \text{ dyne/cm}$

Density:  $1.366 \pm 0.06 \text{ g/cm}^3$

Dielectric Constant: Not available

Polarizability:  $38.03 \pm 0.5 \cdot 10^{-24} \text{ cm}^3$

RDBE: 15

Monoisotopic Mass: 345.111341 Da

Nominal Mass: 345 Da

Average Mass: 345.3514 Da

M+: 345.110793 Da

M-: 345.11189 Da

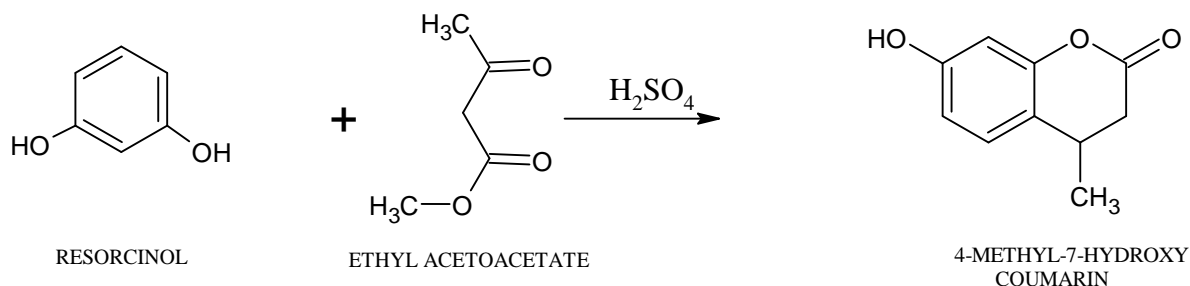
[M+H]<sup>+</sup>: 346.118618 Da

[M+H]<sup>-</sup>: 346.119715 Da

[M-H]<sup>+</sup>: 344.102968 Da

[M-H]<sup>-</sup>: 344.10

### 1.4 PECKMAN CONDENSATION:



The Pechmann reaction introduces one of the most significant and simple methods for the synthesis of a variety of heterocyclic compounds, particularly coumarin derivatives.

The **Pechmann condensation reaction** was discovered by the German chemist Hans von Pechmann is a synthesis of coumarins, starting from a phenol and a carboxylic acid or ester containing a  $\beta$ -carbonyl group. The condensation is performed under acidic conditions using lewis acid and bronsted acid .lewis acid are heterogeneous catalyst and bronsted acid are homogeneous catalyst. The condensation was performed under acidic conditions [22].

### 1.5 MECHANISM:

The mechanism involves an esterification/transesterification followed by attack of the activated carbonyl ortho to the oxygen to generate the new ring. In the reaction of resorcinol and beta-ketoesters and  $\text{Con.H}_2\text{SO}_4$  (Sulfuric acid) yields a chrysochrome. This reaction is called **Simonis chromone cyclization**. The ketone in the ketoester is activated by  $\text{Con.H}_2\text{SO}_4$  (Sulfuric acid) for reaction with the resorcinol hydroxyl group first, the ester group in it is then activated for electrophilic attack of the arene[23].



**ENZYME:**

DNA gyrase is the bacterial enzyme responsible for converting circular DNA to a negatively supercoiled form. We show that the synthesis of DNA gyrase is itself controlled by DNA supercoiling; synthesis is highest when the DNA template is relaxed. The rates of synthesis in vivo of both the A and B subunits of DNA gyrase are increased up to 10-fold by treatments that block DNA gyrase activity and decrease the supercoiling of intracellular DNA. Similarly, efficient synthesis of both gyrase subunits in a cell-free S-30 extract depends on keeping the closed circular DNA template in a relaxed conformation. The results suggest that DNA supercoiling in *E. coli* is controlled by a homeostatic mechanism. Synthesis of the RecA protein and several other proteins is also increased by treatments that relax intracellular DNA [24].

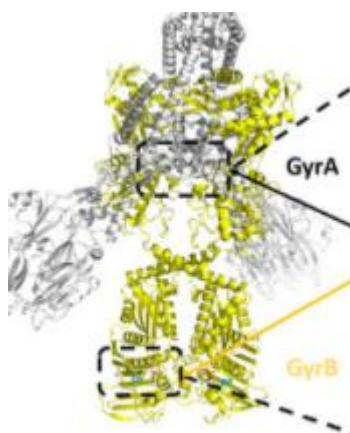


**Figure 1.** Structure of DNA gyrase B

Our first series of dual GyrA and GyrB inhibitor hybrids was designed by combining the GyrA inhibitor ciprofloxacin. Then the hybrids were tested against bacteria, we showed that in the bacteria they only bound to GyrA, and not to GyrB, which means that the observed antibacterial activity was mainly due to the ciprofloxacin part that interacted with GyrA. In the present series, we combined our balanced dual-targeting GyrB with potent antibacterial activity against Gram-positive and Gram-negative strains with ciprofloxacin **Figure 1.** [25].

In the discovery of new and complementary antibacterial agents, phytochemicals that show antibacterial activity can be examined for potential inhibition of bacterial target proteins such as peptide deformylase (PDF), topoisomerase IV (TopoIV), DNA gyrase B (GyrB), protein tyrosine

phosphatase (Ptp), UDP-galactopyranosemutase (UGM), cytochrome P450 (CYP121), and NAD<sup>+</sup>-dependent DNA ligase, as well as phytochemical inhibitors of bacterial efflux pumps or quorum sensing proteins, or agents that enhance the immune system [26].

Escherichia coli DNA gyrase catalyzes negative supercoiling of closed duplex DNA at the expense of ATP. Two additional activities of the enzyme that have illuminated the energy coupling component of the supercoiling reaction are the DNA-dependent hydrolysis of ATP to ADP and P(i) and the alteration by ATP of the DNA site specificity of the gyrase cleavage reaction.

This cleavage of both DNA strands results from treatment with sodium dodecyl sulfate of the stable gyrase-DNA complex that is trapped by the inhibitor oxolinic acid. Either ATP or a nonhydrolyzable analogue, adenylyl-5'-yl-imidodiphosphate, shifts the primary cleavage site on ColE1 DNA. The prevention by novobiocin and coumermycin of this cleavage rearrangement places the site of action of the antibiotics at a reaction step prior to ATP hydrolysis [27].

## 1.6 QSAR APPROACH AND 2D QSAR STUDIES:

The Quantitative structure-activity relationship, which is a critical stage in the development and optimization of lead compounds and, as a result, improving their biological activity, is one of the rational and successful strategies in drug development. We used QSAR approach for antimicrobial activity in this work, and we have provided a complete QSAR analysis using "QSARINS" for antimicrobial activity. PADEL software was used to calculate the 2D Descriptors. It predicts the relationships between substituents and biological activity, allowing for the estimation of bioactivities for newly designed compounds based entirely on software parameters [28, 29].

The antimicrobial activity of these derivatives were predicted using the generated QSAR equations. The present study is aimed at developing novel antimicrobial agents using the 4-Methyl-7 hydroxy-8-pyrimidine as parent nucleus.

## 1.7 DOCKING:

Docking is a procedural method to predict the preferred orientation of one molecule to another when bound forming a stable complex. Docking is important in Drug designing which is used for calculating the binding alignment of small molecular drugs or inhibitors to their protein targets and can predict affinity and activity of complex formed. Molecular docking is an attractive scaffold to understand drug biomolecular interactions for the rational drug design and discovery, as well as in the mechanistic study by placing a molecule (ligand) into the preferred binding site of the target specific region of the DNA/protein (receptor) mainly in a non-covalent fashion to form a stable complex of potential efficacy and more specificity. The information obtained from the docking technique can be used to suggest the binding energy, free energy and stability of complexes. At present, docking technique is utilized to predict the tentative binding parameters of ligand-receptor complex beforehand. The main objective of molecular docking is to attain ligand-receptor complex with optimized conformation and with the intention of possessing less binding free energy.

Molecular docking can demonstrate the feasibility of any biochemical reaction as it is carried out before experimental part of any investigation. There are some areas, where molecular docking has revolutionized the findings. In particular, interaction between small molecules (ligand) and protein target (may be an enzyme) may predict the activation or inhibition of enzyme. Such type of information may provide a raw material for the rational drug designing. Some of the major applications of molecular docking are Lead optimization, Hit identifications, Drug- DNA interaction.

## 1.8 DRUG FILTERS:

ChemSketch ACD/ChemSketch Freeware is a drawing package that allows you to draw chemical structures including organics, organometallics, polymers and Markush structures. It also includes features such as calculation of molecular properties (e.g. molecular weight, density, molar refractivity, etc.), 2D and 3D structure cleaning and viewing, functionality for naming structures (fewer than 50 atoms and 3 rings), and prediction of log P.

### Swiss ADME:

A free webtool to evaluate pharmacokinetics, drug-likeness and medicinal chemistry friendliness of small molecules. It allows to compute physicochemical descriptors as well as to predict ADME parameters, pharmacokinetic properties, druglike nature and medicinal chemistry friendliness of one or multiple small molecules to support drug discovery.

### ProTox II:

ProTox-II, a virtual lab for the prediction of toxicities of small molecules. The prediction of compound toxicities is an important part of the drug design development process. ProTox-II incorporates molecular similarity, fragment propensities, most frequent features and (fragment similaritybased CLUSTER cross-validation) machine-learning, based a total of 33 models for the prediction of various toxicity endpoints such as acute toxicity, hepatotoxicity, cytotoxicity, carcinogenicity, mutagenicity, immunotoxicity, adverse outcomes (Tox21) pathways and toxicity targets.

### PreADMET:

PreADMET is a web-based application for predicting ADME data and building drug-like library using *in silico* method. It predicts permeability for Caco-2 cell, MDCK cell and BBB (blood-brain barrier), HIA (human intestinal absorption), skin permeability and plasma protein binding.

# REVIEW OF LITERATURE

## 2. REVIEW OF LITERATURE

1. Coumarin bridged with theophylline through a methyl linker (**Figure 2**) have been reported with improved antibacterial activity. Mangasuli *et.al.* (2018) synthesized and reported the invitro effect against gram positive and gram negative bacteria including *Escherichia coli*. [30]

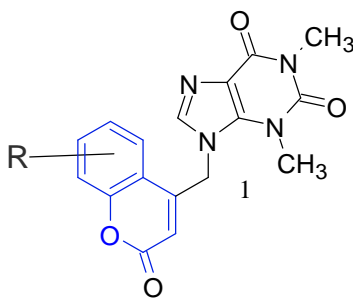


(Figure 2)

1. Liu *et al.*, (2018) reported the structure based drug design and synthesis of six series of 70 novel coumarin-pyrazole carboxamide derivatives and evaluated for its *invitro* antibacterial activity. Among them, sixteen derivatives were found to possess improved antibacterial activity against *Escherichia coli*. [31]

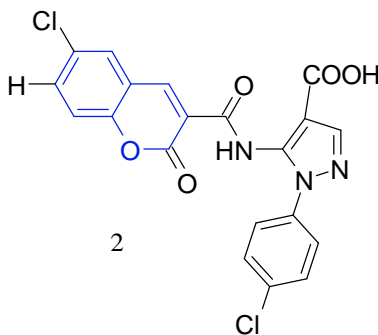


(Figure 3)

2. The silver salt of benzimidazolium with coumarin complexes demanding antibacterial activity by Achar *et al.*, (2017a) synthesized and characterized a series of new sterically modulated chlorocoumarin-substituted (benz)imidazolium bromide and hexafluorophosphate salts and their mono- and bis-N-heterocyclic carbene





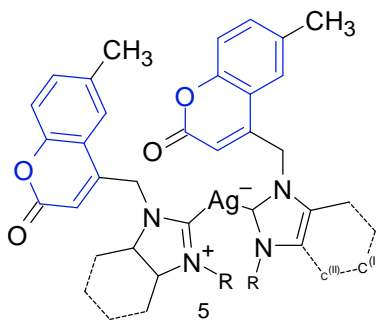


(Figure 6)

5. Priyanka *et al.*, have constructed fourteen 7-coumarinyl oxy amino propanol derivatives (Figure 6) and screened against bacterial strains. To improve the efficacy and selectivity of the new pharmacophores docking studies are considered to be supportive tools. The docking studies against *E.coli* DNA gyrase B structure obtained from the Protein Data Bank [PDB ID: 1KZN, *E.coli*].[35]

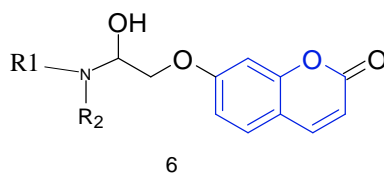


(Figure 7)

6. The spectacular hastening of microwave assisted synthesis was used to prepare novel cyanopyridine and furan coumarin derivatives 5a-5m. The synthesized compounds were evaluated for its antibacterial activity by broth dilution method. From the antibacterial study it was noted that compounds bearing methyl, methoxy and hydroxy substitution (Figure 7) were very effective against *E.coli*.[36]

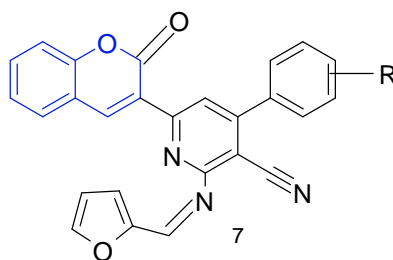


(Figure 8)

7. The literature reports of Aksungur *et al.*, describes the synthesis and antimicrobial screening of two coumarin-indole conjugate fluorescent dyes (**Figure 8**) having donor-acceptor-donor system. The invitro antibacterial study for the synthesised compounds (CI-1 and CI-2) were tested against certain strains of bacteria using Ampicillin and chloramphenicol as the standard drug.[37]

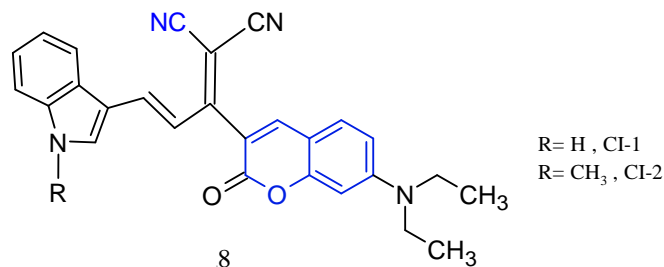


(Figure 9)

8. The Schiff base coumarin complexes synthesized by Mahendra raj and Mruthyunjayaswamy *et al.*, were complexed with a series of metal (II) complexes with donor ligands containing indole and coumarin moieties. An intermediate ligand was prepared by the reaction of methanolic solution 5-substituted-3-phenyl-1H-indole-2-carbohydrazide with 4-methyl-7-chloro 8-formyl coumarin (**Figure 9**) in the presence of glacial acetic acid then Schiff base ligand reacted with respective metal chlorides in methanolic solution to obtain the corresponding metal complexes of indole carmax hydrazide coumarin derivatives.[38]

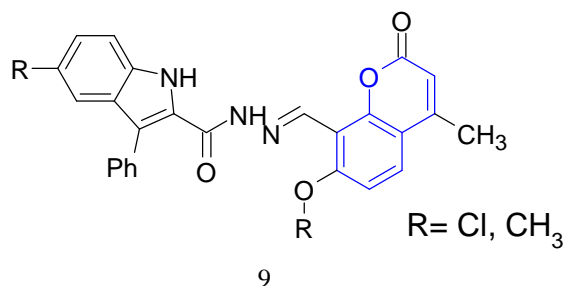
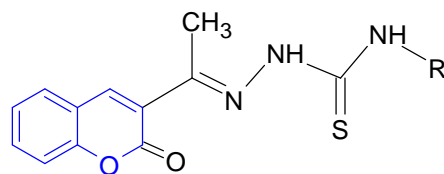


(Figure 10)

9. An intermediate 3-acetyl coumarin was prepared by eco-friendly novel method using starch sulfuric acid (SSA) or cellulose sulfuric acid (CSA) catalyst *via* Pechmann condensation reaction. All the synthesised compounds exhibited appreciable antimicrobial potential against *E.coli*. The activity was compared with three standard

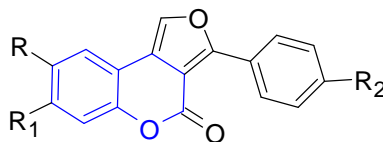
drugs Ampicillin, Ciprofloxacin and Chloramphenicol. The compounds with Chloro, methoxy and hexyl substitution in the Coumarin-thiosemicarbazone moiety exhibited potent activity against *E.coli*. [39]



10

(Figure 11)

10. The synthesis of various 3-aryl-furo[3,2-c]coumarins were carried out by the reaction of substituted 4-hydroxyl coumarin with appropriate 2-aryl-methyl-bromide and 2-aryl-1-nitroethenes (**Figure 11**) in acetic acid and ammonium acetate through Feist-benary reaction. Among these two methods, in the method of feist benary condition, furan-coumarin-derived products had good yields. From the *invitro* antibacterial study it can be inferred that compound with 4-methyl phenyl substitution at the coumarin-furan moiety exhibited higher antibacterial activity against *E.coli*. [40]



11

(Figure 12)

11. 2,6 -bis (1-coumarin-2-yl)-4-(4-substituted phenyl) derivatives (**Figure 12**) were prepared by Chichibabin reaction and checked for antibacterial property. The synthesised was done by the condensation of 3-acetyl coumarin or 5-bromo 3-acetyl coumarin with substituted aromatic aldehydes and ammonium acetate under acidic conditions. The bacterial culture was inoculated on nutrient (Merck) agar-diffusion method at three different concentrations. [41]

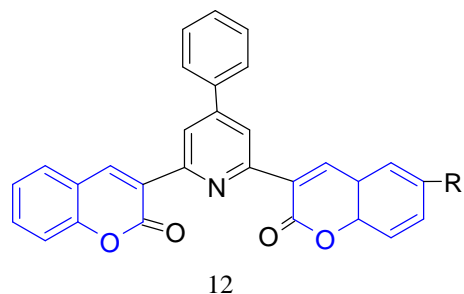


(Figure 13)

12. The simple, calorically efficient and solvent-free condensation of 2-amino-3-cyano-6-methyl-4-phenyl-4H-pyran-5-ethyl-carboxylate derivatives with coumarin-3-carboxylic acid employing pentafluorophenyl ammonium triflate was reported by M. Ghashang *et al.*, The ethyl-5-(4-bromophenyl)-7-methyl-4-oxo-2-(2-oxo-2H-chromen-3-yl)-4,5-dihydro-3H-pyrano[2,3-d]pyrimidine-6-carboxylate derivatives (Figure 13) prepared by Muller Hinton broth Serial dilutions method.[42]

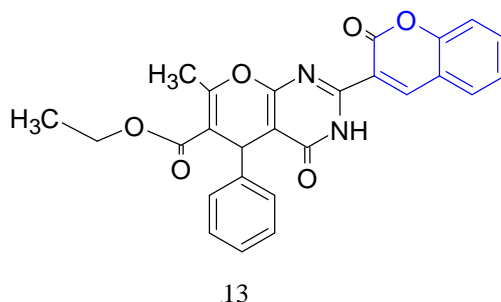
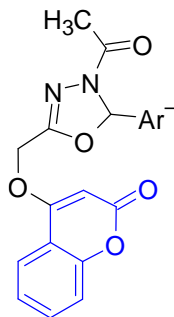


(Figure 14)

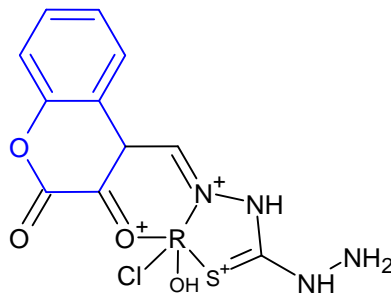
13. The 4-hydroxycoumarin was used as a starting material for the preparation of 4-(4-acetyl-5-substituted-4,5-dihydro-1,3,4-oxodiazol-2-yl)methoxy)-2H-chromen-2-one (Figure 14). The derivatives were studied for the antibacterial activity by Hamdi *et al.*[43]



14

(Figure 15)

14. The complexes of thiosemicarbazone ligand were investigated. The metals such as Cu(II), Ni(II), Co(III), Cr(III) and Fe(III) complexes with substitution of 3-hydroxy-coumarin-3-thiocarbohydrazide, (Figure 15) HL, ligand in the molar ratio 1:1 was synthesized. The clear zone of inhibition was found around the disc for the HL and its [Co(L)(H<sub>2</sub>O)Cl<sub>2</sub>].EtOH complex. [44]



15

(Figure 16)

15. An efficient method of synthesis and antimicrobial effect was completed for coumarin hydrazone compounds. The chloro substituted coumarin compound (2-(1-(6-chloro-2-oxo-2H chromen-3-yl) ethylidene)hydrazinyl)quinoxalin-2(1H)-one derivatives (Figure 16). The derivatives were substituted with several electron withdrawing and electron donating groups. [45]

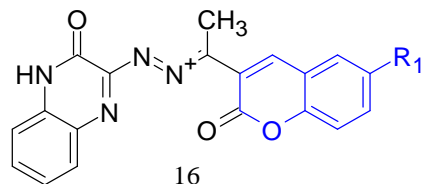


(Figure 17)

16. A new lineage of coumarin derivatives with 3-acetyl-4-dimethylamino phenyl chalcone were combined with aryl and heteroaryl aldehydes using piperidine as a base (Figure 17). The antibacterial study was assessed by methylhydroxide 0.5 mg/mL solution and was tested for antimicrobial activity by disc diffusion assay method. From the reports it is clear that, the antibacterial activity of the chloro substituted coumarin bearing naphthyl and chalcone analogue and also the coumarin derived 4-dimethylamino phenyl chalcone had a outstanding antibacterial activity against *E.coli*. [46]

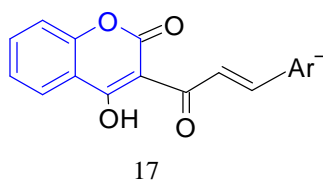


(Figure 18)

17. The Schiff bases and their complexes had been studied for their antibacterial activity. The antibacterial activity of the Co(II) and Ni(II) complexes of 4-methyl-7-hydroxy coumarin thiosemicarbazone derivatives to form the complexes the Schiff

base complexes from methylthiosemicarbazone and 5-formyl-6-hydroxy coumarin/8-formyl-7-Hydroxy-4-methylcoumarin.[47]

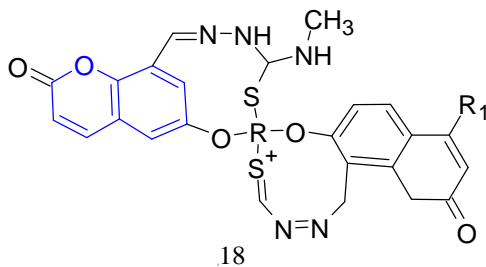


(Figure 19)

18.A substitution of amino derivatives of 4-hydroxycoumarins were studied and reported for the antibacterial activity by Vukovic *et al.*, The newly synthesized unsubstituted phenyl, tolyl residue in aniline with the substitution of aminoalkyl, hydroxyl derivatives (Figure 19)[48].

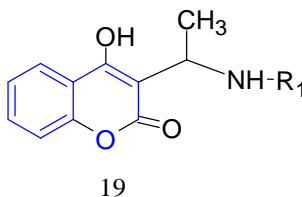


(Figure 20)

19.The chelation complexes of the coumarin thiosemicarbazone derivatives was reported on the synthesized antibacterial activity of Schiff base complexes from 5-amino-1,3,4-thiadiazole-2-thiol and 8-formyl-7hydroxy4methylcoumarin/8acetyl7hydroxy-4-methylcoumarin compound Of cobalt complexes of (E)- N- (3-chlorophenyl) -2 (1 (7hydroxy 4methyl 2oxo 2Hchromen 8yl) ethylidene) hydrazine carbothioamide (Figure 20).[45]

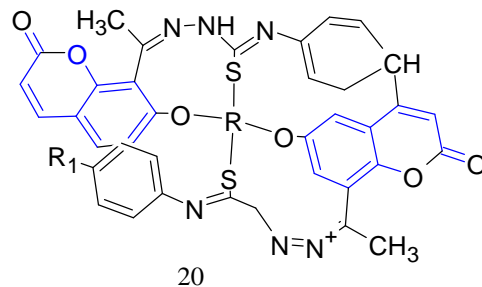


(Figure 21)

20. New transitional metal complexes derived from 3-aryl-azo-4-hydroxy coumarin. The synthesized complexes from with cobalt complexes of (E)-3-((4-chlorophenyl) diazenyl) -4-hydroxy -2H -chromen-2 -one and (E)-3-((4-methoxyphenyl) diazenyl)-4-hydroxy-2H-chromen-2-one derivatives (Figure 21) [49].

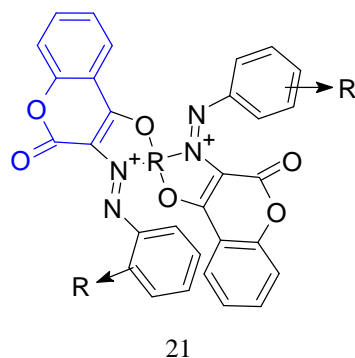


(Figure 22)

21. The determination of antibacterial activity of coumarin bearing triazine derivatives were given by Patel *et al.*, They worked on the preparation of 2-[4-cyano (3trifluoromethyl)phenylamino]4-(4quinoline /coumarin-4-yloxy) -6 - (fluoropiperaziny) -s-triazines and 4((4((3,4dimethyl phenyl) amino) - 6 - (4-



phenylpiperazinyl )4,5dihydro1,3,5triazin 2yl) oxy) naphthalene -2(1*H*)-one derivatives (**Figure 22**). The effect was screened by using paper disc diffusion technique and agar streak dilution method [50].

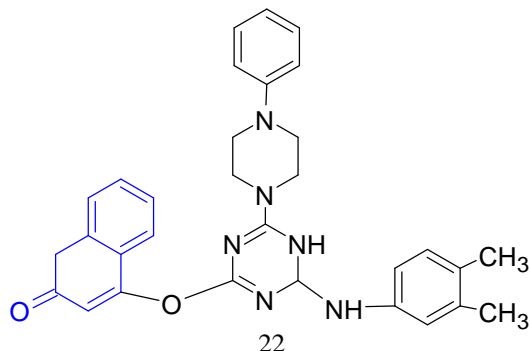


(**Figure 23**)

22. The characterization of metal complexes of Schiff base with coumarin derivatives by **involves** the preparation of Cu(II), Ni(II) and Co(II) complex-schiff base ligand reacted with respective metal. The corresponding metal of complexes was derived from 8-formyl-7-hydroxy 4-methyl coumarin with benzylamine derivatives (**Figure 23**). The coordination phenolic hydroxy group of coumarin and nitrogen of azomethine groups [51].

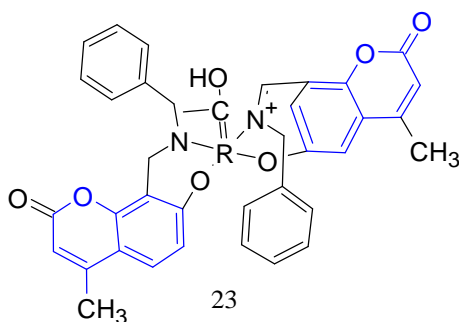


(**Figure 24**)

23. The impact of different substitution on coumarin with imidazolium methyl were reported by Achar *et al.*, They synthesized and evaluated the biological activity of the imidazolium and benzimidazolium hexafluorophosphate salts bearing

6-methylcoumarin, 6-chlorocoumarin and 5,6-benzannulated coumarin (**Figure 24**). The coumarin substituted N-heterocyclic carbene (NHC) ligand was formed with silver(I) complex, and then the silver complex of 6-methyl coumarin [52].

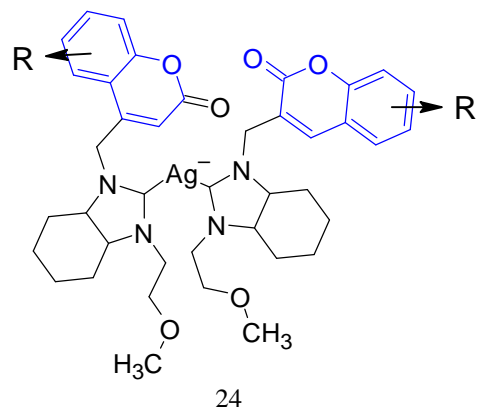


(**Figure 25**)

24. The coordination complexes of coumarin Schiff base derivatives were prepared by Patil *et al.*, The Schiff base metal complexes were liberated by the condensation of respective coumarin 3-carbohydrazide with 2-hydroxy naphthaldehyde 5 derivatives (**Figure 25**). In the tautomerism sulphur play major role for formation of metal complexes. The reported compounds were studied for *in vitro* antimicrobial activity [53].

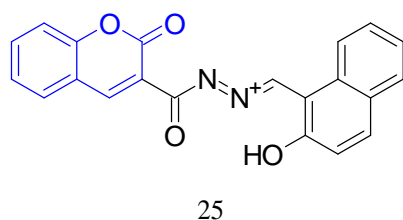


(**Figure 26**)

## **AIM AND OBJECTIVE**

## 2. AIM AND OBJECTIVE:

Bacterial infections have a large impact on public health. Many factors lead to the development of bacterial infection and disease. Bacteria are transmitted to humans through air, water, food, or living organisms.

More than **1.2 million** people and potentially millions more died in 2019 as a direct result of antibiotic-resistant bacterial infections, according to the most comprehensive estimate to date of the global impact of antimicrobial resistance (AMR).

The principal modes of transmission of bacterial infection are contact, airborne, droplet, vectors. Preventive measures have a dramatic impact on morbidity and mortality. Such measures include water treatment, immunization of animals and humans, personal hygiene measures.

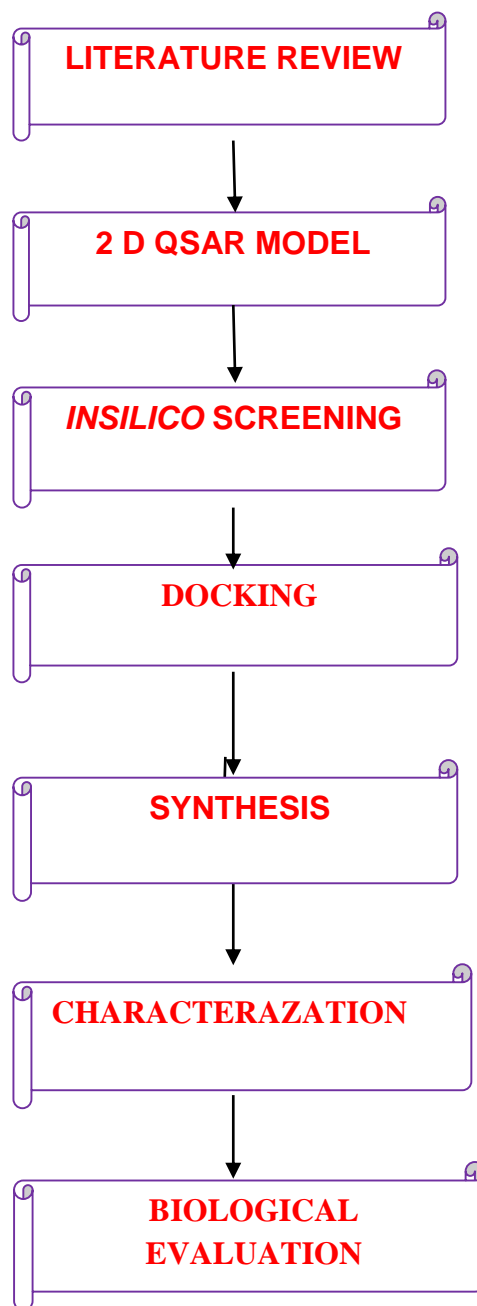
Bacterial resistance to antibiotics is a growing concern mandating their intelligent use. Despite the advancement in the knowledge of biochemical processes associated with bacterial disease, the successful treatment of bacterial disease remains a significant challenge because of the resistance associated with the clinical use of Regular antibacterial agents.

Hence, the design and development of new drugs for antibiotics agents remains to be an important and challenging task for medicinal chemists worldwide.

- To develop a 2D QSAR model using DTC laboratory
- To design peckmann condensation of 4 methyl, 7 hydroxy coumarin derivatives using chemsketch.
- To perform docking studies for all designed compounds with DNA gyrase using Autodock 4.
- To synthesize 4-methyl-7-hydroxy-8-(5)-substituted-pyrimidine-2-thiolcoumarin derivatives based on docking score.
- To characterize the synthesized compounds using IR, NMR, Mass spectrometry.
- To evaluate antibacterials activity of the synthesized compounds

## **PLAN OF STUDY**

#### 4. PLAN OF STUDY:



## **MATERIALS AND METHODS**

## 5. MATERIALS AND METHODS:

### 5.1 2D QSAR MODEL:

The structures and biological activity of the above mentioned derivatives are shown in Table 1. The biological activities of the derivatives expressed in terms of IC<sub>50</sub> (μM, half maximal inhibitory concentration) is converted to logarithmic pIC<sub>50</sub> and it is taken as dependent variable in 2D-QSAR model.

The structure of the compounds was built with ACD/Chemsketch Freeware and saved in .mol file format. The molecular descriptors for the studied compound were calculated using Padel-descriptor 2.21 software.

QSAR studies were carried out using QSARINS software. The Genetic algorithm (GA) and multiple linear regression (MLR) methods were used in QSARINS [56] to construct QSAR models using experimental biological activities and molecular descriptors.

In order to obtain significant model, the descriptors with constant, semi-constant (80%) values and pair-wise correlation more than 0.85, were excluded.

And the remaining descriptors were used as input for model development. The data was splitted according to a random percentage method where, approximately 20% compounds were retained in test set (13) and remaining 80% (52) compounds were used for model development (ref).

Parameters such as: all subset until 1, genetic iteration: 10000 with maximum of 5 variables were chosen and other parameters were set as default.

The applicability domain [57] of QSAR model was used to verify the prediction reliability, to identify the problematic compounds and to predict the compounds with acceptable activity that falls within this domain.

The leverage approach allows the determination of the position of new chemical in the QSAR model, i.e., whether a new chemical will lie within the structural model domain or outside of it.

Furthermore, the leverage approach along with the William plot is used to determine the applicability in all QSAR models. To construct the William plot, the leverage  $h_i$  for each chemical compound, in which QSAR model was used to predict its activity, was calculated according to the following equation:



$$h_i = x_i^T (X^T X)^{-1} x_i$$

Where  $x_i$  is the descriptor vector of the considered compound and  $X$  is the descriptor matrix derived from the training set descriptor values and the warning leverage ( $h^*$ ) was determined as

$$h^* = 3(p+1)/n$$

Where  $n$  is the number of training compounds,  $p$  is the number of predictor variables. The defined applicability domain (AD) was then visualized via a Williams plot, the plot of the standardized residual versus the leverage values ( $h$ ).

A compound with  $h_i > h^*$  seriously influences the regression performance and may be excluded from the applicability domain, but it doesn't appear to be an outlier because its standardized residual may be small.

Moreover, a value of 3 for standardized residuals is commonly used as a cut-off value for accepting predictions, because points that lie with  $\pm 3$  standardized residual from the mean cover 99% of the normally distributed data.

The best model was selected based on statistical parameters such as observed squared correlation coefficient ( $r^2 > 0.6$ ), which is a relative measure of the quality of fit.

The cross leave one out squared correlation coefficient ( $q^2$ ) should be high for predicting the goodness of the QSAR model, and the difference between  $q^2$  and  $r^2$  should not be more than 0.3. The standard error of estimate (SEE  $< 0.3$ ) represents an absolute measure of prediction accuracy.

### **QSAR VALIDATION:**

Validation is carried out to assess the QSAR model's predicting capacity. Internal and external validation are the two sorts of validation methodologies. The Leave One Out (LOO) approach is used for internal validation. The best model was chosen based on a number of statistical metrics, including the square of the correlation coefficient ( $r^2$ ), and the cross-validated squared correlation coefficient ( $r^2_{cv}$ ) was used to determine the quality of each model.

**Leave one out cross-validation (LOOCV)**

Leave one out cross-validation is one of the most effective methods for validation of a model with a small training data set. Leave one out cross validation technique was employed to determine the predictive power of the model. This was evaluated by using this mathematical expression;

$$Q^2_{cv} = \frac{1 - \sum(Y_{pred} - Y_{exp})^2}{2 - \sum(Y_{exp} - Y_{training})^2}$$

Where  $Y_{pred}$ ,  $Y_{exp}$  and  $Y_{training}$  represents the experimental, the predicted and mean values of experimental activity of training set compounds

**External validation ( $r^2_{cv}$ ):**

For external validation, the activity of each molecule in the test set was predicted using the. The regression coefficient ( $r^2_{cv}$ ) value is calculated as follows:

$$r^2_{cv} = \frac{1 - \sum(Y_{pred}(\text{test}) - Y(\text{test}))^2}{\sum(Y(\text{test}) - Y(\text{training}))^2}$$

Where  $r^2_{cv}$  refers cross validated regression coefficient,  $Y_{test}$  and  $Y_{pred}$  are observed and predicted activity of the molecule in the test set, respectively, and  $Y(\text{training})$  is the average activity of all molecules in the training set. Both, summations are over all molecules in the test set.

## 5.2 DESIGN OF COMPOUNDS:

Based on the 2D QSAR results, 12 compounds were designed using Chems sketch software and physicochemical properties were calculated for all compounds.

### MOLAR REFRACTIVITY:

Molar refractivity,  $A$ , is a measure of the total polarizability of a mole of a substance and is dependent on the temperature, the index of refraction, and the pressure.

The molar refractivity is defined as

$$A = 4\pi N_A \alpha / 3$$

Where  $N_A \approx 6.0221023$  is the Avogadro constant and  $\alpha$  is the mean polarizability of the molecule.

### MOLAR VOLUME:

The molar volume, symbol  $V_m$ , is the volume occupied by one mole of a substance (chemical element or chemical compound) at a given temperature and pressure. It is equal to the molar mass ( $M$ ) divided by the mass density ( $\rho$ ). It has the SI unit cubic meters per mole ( $m^3/mol$ ), although it is more practical to use the units cubic decimetres per mole ( $dm^3/mol$ ) for gases and cubic centimeters per mole ( $cm^3/mol$ ) for liquids and solids. The molar volume of a substance can be found by measuring its molar mass and density then applying the relation.

$$V_m = M/\rho$$

### INDEX OF REFRACTION:

The refractive index or index of refraction of a material is a dimensionless number that describes how light propagates through that medium. It is defined as

$$n = c/v$$

Where,  $c$  is the speed of light in vacuum and  $v$  is the phase velocity of light in the medium.

**SURFACE TENSION:**

Surface tension is the elastic force of a fluid surface which makes it acquire the least surface area possible. Surface tension has the dimension of force per unit length, or of energy per unit area.

**POLARIZABILITY:**

Polarizability is the ability to form instantaneous dipoles. It is a property of matter. Polarizabilities determine the dynamical response of a bound system to external fields and provide insight into a molecule's internal structure. In a solid, polarizability is defined as the dipole moment per unit volume of the crystal cell.

**PARACHOR:**

It is an empirical constant for a liquid that relates the surface tension to the molecular volume and that may be used for a comparison of molecular volumes under conditions such that the liquids have the same surface tension and for determinations of partial structure of compounds by adding values obtained for constituent atoms and structural features called also molar parachor, molecular parachor. Parachor is a quantity defined according to the formula:

$$P = \sqrt[4]{\gamma} \cdot M / d$$

Where:  $\sqrt[4]{\gamma}$  is the fourth root of surface tension

M is the molar mass

D is the density.

**DENSITY:**

The density, or more precisely, the volumetric mass density, of a substance is its mass per unit volume.

$$\rho = m/V$$

**DIELECTRIC CONSTANT:**

Substances have capacity to produce dipoles in another molecule. Dielectric constant is a measure of this capacity and it is a physical property. It is affected by both the attractive forces that exist between atoms and also molecules. It is denoted by  $\epsilon$ .

### 5.3 IN SILICO SCREENING OF DESIGNED COMPOUNDS:

In silico is an expression meaning "performed on computer or via computer simulation" in reference to biological experiments. When lead molecules have been identified, they have to be optimized in terms of potency, selectivity, pharmacokinetics (i.e.) absorption, distribution, metabolism and excretion (ADME) and toxicology before they can become candidates for drug development. In silico approaches to predict pharmacokinetic parameters (ADME) were pioneered by Lipinski et al. By studying the physicochemical properties of >2000 drugs from the WDI (World Drug Index, Derwent Information, London), which can be assumed to have entered Phase II human clinical trials (and therefore must possess drug-like properties), the so-called 'rule-of five' was derived to predict oral bioavailability (intestinal absorption) of a compound that can be considered as the major goal of drug development. The ADME properties of the designed compounds were evaluated using Swiss ADME and PreADMET online softwares. Toxicity of all the designed compounds was evaluated by using ProTox II software.

#### SwissADME:

#### Lipinski's rule of five:

Lipinski's rule of five also known as the Pfizer's rule of five or simply the rule of five (RO5) is a rule of thumb to evaluate drug likeness or determine if a chemical compound with a certain pharmacological or biological activity has chemical properties and physical properties that would make it a likely orally active drug in humans.

The rule Lipinski's rule states that, in general, an orally active drug has no more than one violation of the following criteria:

1. No more than **5** hydrogen bond donors (the total number of nitrogen–hydrogen and oxygen–hydrogen bonds).
2. No more than **10** hydrogen bond acceptors (all nitrogen or oxygen atoms).
3. A molecular mass less than **500** daltons.
4. An octanol-water partition coefficient log P not greater than **5**.

### **Ghose Filter:**

This filter defines drug-likeness constraints as follows:

- ✓ Calculated log P is between -0.4 and 5.6
- ✓ Molecular weight is between 160 and 480
- ✓ Molar refractivity is between 40 and 130
- ✓ The total number of atoms is between 20 and 70.

### **Veber Filter:**

The molecules fitting to these two properties have a high probability of good oral bioavailability.

- ✓ Rotatable bond: max. 12
- ✓ Polar Surface Area: max. 140Å<sup>2</sup>

### **Egan Rule**

Predicts good or bad oral bioavailability.

- ✓  $0 \geq \text{TPSA} \leq 132$
- ✓  $-1 \geq \log P \leq 6$ .

### **Polar surface area (PSA) or topological polar surface area (TPSA):**

It is a measure of apparent polarity of a molecule is defined as the surface sum overall polar atoms, primarily oxygen and nitrogen, also including their attached hydrogen atoms. PSA is a commonly used for the optimization of a drug's ability to permeate cells. Molecules with a polar surface area of greater than 140 angstroms squared tend to be poor at permeating cell membranes. For molecules to penetrate the blood–brain barrier (and thus act on receptors in the central nervous system), a PSA less than 90 angstroms squared is usually needed. Topological PSA (TPSA, fast 2D calculation).

**ADME Guideline:**

✓  $TPSA < 140 \text{ \AA}^2$  good intestinal absorption.

✓  $TPSA < 70 \text{ \AA}^2$  good brain penetration.

**Lipophilicity:**

Lipophilicity is the ability of a molecule to mix with an oily phase rather than with water, is usually measured as partition coefficient,  $P$ , between the two phases and is often expressed as  $\log P$ . Lipophilicity has also been found to affect a number of pharmacokinetic parameters: higher lipophilicity ( $\log P > 5$ ) gives, in general, lower solubility, higher permeability in the gastrointestinal tract, across the blood–brain barrier and other tissue membranes, higher affinity to metabolizing enzymes and efflux pumps, and higher protein binding. Low lipophilicity can also negatively impact permeability and potency and thus results in low BA and efficacy.

**Partition coefficient,  $P$ :**

It is defined as a particular ratio of the concentrations of a solute between the two solvents (a biphasic or liquid phases), specifically for un-ionized solutes, and the logarithm of the ratio is thus  $\log P$ . When one of the solvents is water and the other is a non-polar solvent, then the  $\log P$  value is a measure of lipophilicity or hydrophobicity.

✓  $\log P_{oct/wat} = \log \frac{[\text{solute}]_{\text{unionized octanol}}}{[\text{solute}]_{\text{unionized water}}}$

✓  $\log P_{oct/wat} = \log \frac{C_O}{C_W}$

Lipophilicity not only impacts solubility but also influences permeability, potency, selectivity, absorption, distribution, metabolism, and excretion (ADME) properties and toxicity. A desired  $\log P$  value (octanol-water partition coefficient) is no more than 5.



### **Water Solubility:**

Water solubility is a measure of the amount of chemical substance that can dissolve in water at a specific temperature. Solubility is common physicochemical parameter for drug discovery compounds. Determination of the aqueous solubility of the drug candidate is an important analysis as it reflects the bioavailability of the compound.

### **Log S:**

The aqueous solubility of a compound significantly affects its absorption and distribution characteristics. Typically, a low solubility goes along with a bad absorption and therefore the general aim is to avoid poorly soluble compounds. Log S value is a unit stripped logarithm (base 10) of the solubility measured in mol/liter. Log S value should be greater than -4.

### **Rotatable Bonds:**

The bioavailability of a drug like molecule is related with its rotatable bond number. Less than seven rotatable bonds are essential for good bioavailability. Many highly potent molecules carry more than 10 rotatable bonds and still administered through oral route.

### **Hydrogen bond acceptors and donors:**

12 or fewer H-bond donors and acceptors will have a high probability of good oral bioavailability.

### **PreADMET Drug-Likelihood:**

Drug likeness is a qualitative concept used in drug design for how "druglike" a substance is with respect to factors like bioavailability. It is estimated from the molecular structure before the substance is even synthesized and tested. The most well-known rule relating the chemical structures to their biological activities is Lipinski's rule and it is called the 'rule of five'. Another well-known rule is the Lead-like rule. PreADMET contains drug-likeness prediction module based on these rules.

### **ADME Prediction:**

Numerous in vitro methods have been used in the drug selection process for assessing the intestinal absorption of drug candidates. Among them, Caco2-cell model and MDCK (Madin-Darby canine kidney) cell model has been recommended as a reliable invitro model for the prediction of oral drug absorption. In absorption, this module provides prediction models for in vitro Caco2-cell and MDCK cell assay. Additionally, *in silico* HIA (human intestinal absorption) model and skin permeability model can predict and identify potential drug for oral delivery and transdermal delivery. In distribution, BBB (blood brain barrier) penetration can give information of therapeutic drug in the central nervous system (CNS), plasma protein binding model in its disposition and efficacy. In order to build these QSAR models, genetic functional approximation is used to select relevant descriptors from all 2D descriptors that calculated by Topo mol module, followed by Resilient back-propagation (Rprop) neural network to develop successful nonlinear model.

### **Toxicity prediction:**

In silico toxicity prediction will have more and more importance in early drug discovery since 30% of drug candidates fail owing to these issues.

### **ProTox II:**

ProTox II, a virtual lab for the prediction of toxicities of small molecules. The prediction of compound toxicities is an important part of the drug design development process. Computational toxicity estimations are not only faster than the determination of toxic doses in animals, but can also help to reduce the amount of animal experiments. ProTox II incorporates molecular similarity, fragment propensities, most frequent features and (fragment similarity based CLUSTER cross-validation) machine-learning, based a total of 33 models for the prediction of various toxicity endpoints such as acute toxicity, hepatotoxicity, cytotoxicity, carcinogenicity, mutagenicity, immunotoxicity, adverse outcomes (Tox21) pathways and toxicity targets.

**Acute toxicity:**

The acute toxicity models are developed based on chemical similarities between compounds with known toxic effects and the presence of toxic fragments.

**Toxicity targets:**

The prediction of toxicity targets is based on 15 different targets from the Novartis in vitro safety panels of the protein targets linked to adverse drug-reactions.

**Hepatotoxicity:**

Drug-induced hepatotoxicity is a significant cause of acute liver failure and one of the major reasons for the withdrawal of drugs from the market. Drug-induced liver injury (DILI) is either a chronic process or a rare event. However, prediction of DILI is important and one of the safety concerns for the drug developers, regulators and clinicians. The data for the prediction of DILI are taken from DILIRank and the NIH Liver Tox database. The ProTox-II hepatotoxicity prediction model has a balanced accuracy of 82.00% on cross-validation and 86.00% on external validation. The AUC–ROC scores of cross-validation and external validation are 0.86 and 0.91 respectively. The kappa value is 0.69 for the model.

**Toxicological end points:**

Carcinogenicity Chemicals that can induce tumors or increase the incidence of tumours are referred as carcinogens. The data for the prediction of carcinogenicity are collected from the Carcinogenic Potency Database (CPDB) and CEBS database. The ProTox-II carcinogenicity prediction model has a balanced accuracy of 81.24% on cross-validation and 83.30% on external validation. The AUC–ROC scores of cross-validation and external validation are 0.85 and 0.87 respectively. The kappa value is 0.69 for the model.

### **Mutagenicity:**

Chemicals that cause abnormal genetic mutations such as changes in the DNA of a cell are referred as mutagens. Such changes can cause harm to the cells and result in certain disease, e.g. cancer. ProTox-II, mutagenicity prediction is based on the benchmark data set from Ames test as well as CEBS database. The ProTox-II mutagenicity prediction model has a balanced accuracy of 84.00% on cross-validation and 85.00% on external validation. The AUC–ROC scores of cross- validation and external validation are 0.90 and 0.91 respectively. The kappa value is 0.69 for the model.

### **Cytotoxicity:**

Prediction of cytotoxicity is important to screen compounds that can cause undesired and desired cell damage, the latter as in the case of the tumour cells. The ProTox-II cytotoxicity model is based on data extracted from the Chemical European Biology Laboratory (ChEMBL) database. All compounds with an IC<sub>50</sub> value of less than or equal to 10  $\mu$ M in the in vitro toxicity assay against HepG2 cells are considered as positively cytotoxic. The ProTox-II cytotoxicity prediction model has a balanced accuracy of 85.00% on cross- validation and 83.60% on external validation. The AUC–ROC scores of cross-validation and external validation are 0.89 and 0.90 respectively. The kappa value is 0.69 for the model.

### **Immunotoxicity:**

The adverse effect of xenobiotics on the immune system is called immunotoxicity. The immunotoxicity model is based on immune cell cytotoxicity data obtained from the U.S. National Cancer Institute's (NCI) public database. Growth inhibition (GI<sub>50</sub>) values from the B-cell line RPMI-8226 are used and compounds with GI<sub>50</sub> values below 10  $\mu$ M are defined as toxic. The ProTox-II immunotoxicity prediction model has a balanced accuracy of 74.00% on cross-validation and 70.00% on external validation. The AUC–ROC scores of cross- validation and external validation are 0.76 and 0.74 respectively. The kappa value is 0.35 for the model.

### **Toxicological pathways:**

Toxicology in the 21st Century (Tox21) platform, the US toxicology initiative which was started in 2008, provides a library of 10 000 chemical data, screened in high-throughput assays against a panel of 12 different biological target-based pathways, that involve two major groups of adverse outcome pathways (AOPs): the nuclear receptor pathway and the stress response pathway. ProTox-II, prediction of chemical compounds active in toxicological pathways is based on the Tox21 dataset.

### **Nuclear receptor signaling pathways:**

There are seven target-pathway based models under nuclear receptor signaling pathways: aryl hydrogen receptor (AhR), androgen receptor (AR), androgen receptor ligand binding domain (AR-LBD), aromatase, estrogen receptor alpha (ER), estrogen receptor ligand binding domain (ER-LBD), and peroxisome proliferator activated receptor gamma (PPAR-Gamma). All the models have a balanced accuracy of >80% and AUC–ROC values within a range of 0.75–0.90 for both cross-validation and external validation. The kappa values are in a range of 0.60–0.80.

### **Stress response pathways:**

There are five target-pathway based models under stress response pathways: Nuclear factor (erythroid-derived 2)-like 2/antioxidant responsive element (ARE), heat shock factor response element (HSE), mitochondrial membrane potential (MMP), phosphoprotein tumor suppressor (p53), and ATPase family AAA domain-containing protein 5 (ATAD5). All the models have a balanced accuracy of >80% and AUC–ROC values within the range of 0.80– 0.90 for both cross-validation and external validation. Except for HSE the value for ROC– AUC is 0.79. The kappa values are in a range of 0.60–0.80.

### **Prediction models:**

All the newly added prediction models on the ProTox-II platform are based on machine learning algorithms. A Random Forest (RF) algorithm is used to construct the classification and prediction models for hepatotoxicity, cytotoxicity, mutagenicity, and carcinogenicity. The RF-based models are constructed using 500 decision trees and GINI index criterion.

The advantage of using RF-based classifier is that it tends to avoid overfitting. For the construction of theTox21 based toxicological pathway prediction, an ensemble approach is used including RF and Support Vector Machine (SVM) classifiers.

The radial basis function (RBF) is used as kernel function for the SVM algorithm. Immunotoxicity prediction model is based on Bernoulli–Naive Bayes algorithm, as explained in the published work.

Here, two different fingerprints are used: MACCS molecular fingerprints-166 bits and Morgan circular fingerprints-2048 bits (<http://www.rdkit.org/>).

These two fingerprints have shown an optimal performance for prediction of chemical activity. Additionally, a selective oversampling of minority class is introduced in the construction of the models.

For each of the prediction end-points, the active (positive) and inactive (negative) data are fragmented using RECAP and ROTBONDS fragmentation methods. The propensity score (PS) for each of the uniquely occurring fragments in both the sets is computed. Only those molecules having the highest propensity scores for fragments conserved for the active class are oversampled and added into model construction.

The same ratio of active and inactive compounds was maintained for all the folds of cross-validation, using the fragmentbased similarities between the compound.

### **Toxic doses and Toxicity classes:**

Toxic doses are often given as LD50 values in mg/kg body weight. The LD50 is the median lethal dose meaning the dose at which 50% of test subjects die upon exposure to a compound.

Toxicity classes are defined according to the globally harmonized system of classification of labelling of chemicals (GHS). LD50 values are given in [mg/kg]:

- Class I: fatal if swallowed ( $LD50 \leq 5$ )
- Class II: fatal if swallowed ( $5 < LD50 \leq 50$ )
- Class III: toxic if swallowed ( $50 < LD50 \leq 300$ )
- Class IV: harmful if swallowed ( $300 < LD50 \leq 2000$ )
- Class V: may be harmful if swallowed ( $2000 < LD50 \leq 5000$ )
- Class VI: non-toxic ( $LD50 > 5000$ )

## 5.4 DOCKING:

Docking is a method which predicts the preferred orientation of one molecule to a Second when bound to each other to form a stable complex. Knowledge of the preferred orientation in turn may be used to predict the strength of association or binding affinity between two molecules using, for example, scoring functions.

In this study, pyrX is used to perform docking studies. Docking studies were performed with the active site of DNA gyrase (PDB ID: 6F86) (**Figure:27**). Protein was downloaded from RCSB and used for docking analysis. This molecular docking study was performed using the selected protein from the protein data bank (PDB ID: 6F86).

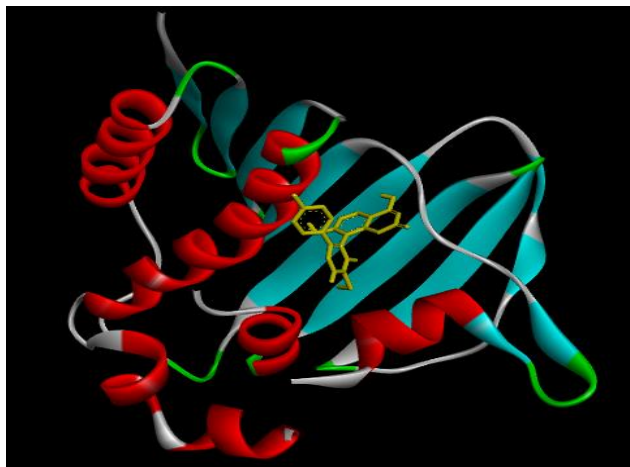
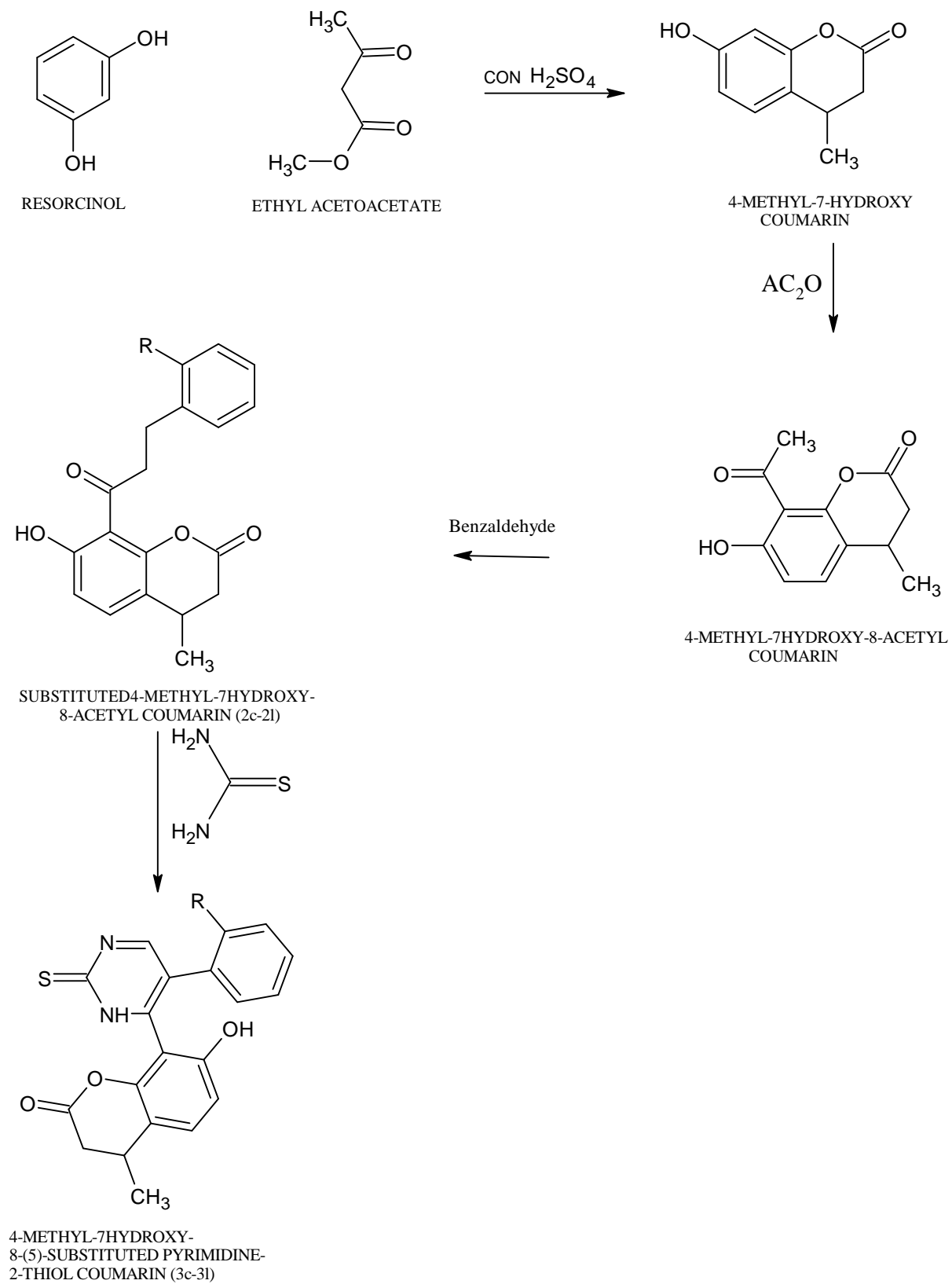


(Figure:27)



5.5 SYNTHESIS:



## **GENERAL PROCEDURES FOR SYNTHESIS:**

### **STEP 1: SYNTHESIS OF 4-METHYL-7-HYDROXY COUMARIN:**

Mix about 9 ml of con.  $\text{H}_2\text{SO}_4$  which is chilled to about 4.5 degree. Add 2.2gm of resorcinol powder dissolved in 2.6ml of ethyl acetoacetate is added in with continuous mechanical stirring taking care that the temperature does not increase about 10 degree further stirring is continued for 30-40 minutes to ensure the completeness of condensation reaction pass this mixture into crushed ice water the product separate out. The product is filtered by suction and wash with cold water.

### **STEP2: ACETYLATION OF 4-METHYL-7-HYDROXY COUMARIN:**

Dissolve 1gm (the molecular weight is unknown) of the compound in 5ml of 3M sodium hydroxide (NaOH) solution. Add 10-20gm of crushed ice followed by 1.5gm(1.5ml) of acetic anhydride. Shake the mixture vigorously for 30-60 seconds. The acetate separates in a practically pure condition either at once or after acidification by the addition of a mineral acid. Collect the acetyl product is filtered.

### **STEP3: SUBSTITUTION OF 4-METHYL-7-HYDROXY-8-ACETYL COUMARIN:**

A mixture of equimolar amount of acetyl coumarin and the corresponding aromatic aldehyde(5mmol) (1ml) were dissolved in 10ml of ethanol containing catalytic amount of potassium hydroxide KOH (0.1ml) was irradiated for an appropriate time of 5-6 minutes in (225) watt in a 10ml closed vial using CEM microwave system.

### **STEP4:4-METHYL-7-HYDROXY-8-(5)-SUBSTITUTED-PYRIMIDINE-2-THIOL COUMARIN:**

Substituted 4-methyl-7-hydroxy-8-acetyl coumarin (0.01mol), thiourea (0.015mol, 0.96gm) and sodium hydroxide (0.045mol, 0.40gm) were mixed carefully with a little water. Obtained mixture was irradiated about 2-3 minutes in microwave oven at 750 watts. The mixture had become dark-yellow. Cooled it to room temperature, recrystallized from solvent system of ethanol.

**5.6 CHARACTERIZATION:**

All the synthesized compounds were characterized by using FT-IR,  $^1\text{H}$ -NMR,  $^{13}\text{C}$ -NMR, MASS Spectroscopy.

**INFRARED SPECTROSCOPY:**

The infrared spectroscopy is one of the most powerful analytical techniques, this offers the possibility of chemical identification. The most important advantages of infrared spectroscopy over the other usual methods of structural analysis are that it provides useful information about the functional groups present in the molecule quickly. The technique is based upon the simple fact that a chemical substance shows marked selectable absorption in the infrared region. After absorbing IR radiations the molecules of a chemical compound exhibit small vibrations, giving rise to closely packed absorption bands called as IR absorption spectrum which may extend over a wide wavelength range. Various bands will be present in IR spectrum which corresponds to the characteristic functional groups and bonds present in a chemical substance. Thus an IR spectrum of a chemical compound is a fingerprint for its identification.

**NMR SPECTROSCOPY:**

It is the branch of spectroscopy in which radiofrequency waves induces transitions between magnetic energy levels of nuclei of a molecule. The magnetic energy levels are created by keeping nuclei in a magnetic field. Without the magnetic field the spin states of nuclei are degenerated i.e., possess the same energy and the energy level transition is not possible. The energy level transition is possible with the application of external magnetic field which requires different Rf radiation to put them into resonance. This is a measurable phenomenon. It is a powerful tool for the investigation of nuclei structure.  $^1\text{H}$ NMR and  $^{13}\text{C}$ NMR Spectras of the prepared derivatives were done by using 400-MHz and 500-MHz Bruker spectrometer using internal standard as tetra

methyl silane.  $^1\text{H}$  and  $^{13}\text{C}$  NMR Spectral were taken with dimethyl sulphoxide (DMSO) as a solvent and the data of chemical shift were shown as delta values related to trimethylsilane (TM) in ppm.

### **MASS SPECTROSCOPY:**

Mass spectrometer performs three essential functions. First, it subjects molecules to bombardment by a stream of more amounts of energy electrons, converting some of the molecules to ions, which are then accelerated in a field of electric. Second, the ions which are accelerated are divided according to their ratios of mass to charge in an electric or magnetic field. Finally the ions that have particular mass-to-charge ratio are detected by a device which can count the number of ions striking it. The detector's output is amplified and fed to a recorder. The trace from the recorder is a mass spectrum a graph of particles detected as a function of mass-to- charge ratio. The Mass spectra of the synthesized compounds were taken using Agilent spectrometer.

## 5.7 BIOLOGICAL ACTIVITIES

### PRINCIPLE

The antimicrobials present in the given sample were allowed to diffuse out into the medium and interact in a plate freshly seeded with the test organisms. The resulting zones of inhibition will be uniformly circular as there will be a confluent lawn of growth. The diameter of zone of inhibition can be measured in millimeters.

### MATERIALS REQUIRED

(*E.coli*- 443) was purchased from MTCC, Chandihar, India. Nutrient Agar medium, Nutrient broth, Gentamicin antibiotic solution was purchased from Himedia, India. Test samples, petri-plates, test tubes, beakers conical flasks were from Borosil, India. Spirit lamp, double distilled water.

### 1. AGAR- WELL DIFFUSION METHOD

#### a. Nutrient Agar Medium

The medium was prepared by dissolving 2.8 g of the commercially available Nutrient Agar Medium (HiMedia) in 100ml of distilled water. The dissolved medium was autoclaved at 15 lbs pressure at 121°C for 15 minutes. The autoclaved medium was mixed well and poured onto 100mm petriplates (25-30ml/plate) while still molten.

#### b. Nutrient broth

Nutrient broth was prepared by dissolving 2.8 g of commercially available nutrient medium (HiMedia) in 100ml distilled water and boiled to dissolve the medium completely. The medium was dispensed as desired and sterilized by autoclaving at 15 lbs pressure (121°C) for 15 minutes.

### PROCEDURE

Petri plates containing 20 ml nutrient agar medium were seeded with 24 hr culture of bacterial strains were adjusted to 0.5 OD value according to McFarland standard, (*E.coli*- 443) Wells were cut and concentration of sample 3k, 3h and 3j (500, 250, 100 and 50 µg/ml) was added. The plates were then incubated at 37°C for 24 hours. The antibacterial

activity was assayed by measuring the diameter of the inhibition zone formed around the wells. Gentamicin antibiotic was used as a positive control. The values were calculated using Graph Pad Prism 6.0 software (USA).

#### **Procedure for MIC:**

MIC values are used to determine susceptibilities of bacteria to drugs and also to evaluate the activity of new antimicrobial agents.

#### **Materials Required:**

*E.coli*(MTCC. No. 443) was purchased from MTCC, Chandihar, India. Nutrient broth, Gentamicin antibiotic solution was purchased from Himedia, India. Sterile 96 well plates were purchased from Tarsan, India. Conical flasks was from Borosil, India. Spirit lamp, double distilled water and Test samples.

#### **Procedure:**

The broth microdilution assay method was used to determine the MICs for the susceptibility of *E.coli* (MTCC. No. 443) in sterile disposable flat-bottomed 96-well microtiter plates. Briefly, the 0.5 McFarland inoculum suspensions were further diluted 1:100 in nutrient broth before inoculation, 50  $\mu$ L of the bacterial suspension was seeded into a 96-well plate containing 50  $\mu$ L of test sample with serial concentrations. The final inoculum of the bacteria was approximately  $5 \times 10^5$  CFU/mL. The final concentrations of 3k (500, 250, 125, 62.5 and 31.25  $\mu$ g/mL). The broad-spectrum antibiotic Ciprofloxacin was chosen for testing as a control and the concentration of antibiotic in the well was 100  $\mu$ g/mL. The plates were then incubated at 37 °C for 18–24 h. The results were read at 600 nm using a microplate reader. Changes of color were observed and recorded. All the tests were done in triplicates.

(% inhibition) = [(absorbance of control- absorbance of reaction mixture)/absorbance of control] X 100

*Escherichia coli* ATCC 25922 is used for evaluating antibacterial activity via minimum concentration of inhibition. *E.coli* ATCC 25922 quinolone resistant recommended CLSI control strain used worldwide for antimicrobial susceptibility testing (including quinolones).

## RESULTS AND DISCUSSION

## 6. RESULTS AND DISCUSSION

### 6.1 QSAR MODEL RESULTS:

In this study, 2D QSAR was used for designing the drug molecule. A reported series of 12 substituted 4-methyl-7-hydroxy-8-(5)-pyrimidine-2-thiolcoumarin derivatives as antibacterial agents. It was used to study 2D-QSAR models [21]. The chemical structures and pharmacological activity of coumarin derivatives are shown in Table 1.

The substituted coumarin derivatives structure was drawn with ACD/Chemsketch Freeware and saved in .mol file format. The molecular descriptors for the studied compound were calculated using Padel-descriptor 2.21 software.

Totally 1043 descriptors including 2D and 3D properties can be for all the compounds. For developing 2D-QSAR model, this data set is split into training set (23 compounds) to create a model and a test set (5 compounds) for external validation of the predictive ability of the 2D QSAR model.

The therapeutic activities of the coumarin derivatives expressed in terms of IC<sub>50</sub> (μM, half maximal inhibitory concentration) is converted to logarithmic pIC<sub>50</sub> and it is taken as dependent variable in 2D-QSAR model [51].

If model descriptor contains the missing value and zero value should be removed. The multiple linear regression method was performed to determine the relationship between descriptors as independent variable and biological activity of the compounds of the training set as dependent variables using DTC laboratory. Validation is done to evaluate the predictive ability of the obtained QSAR model by internal and external validation.

The best QSAR model was selected based on r<sup>2</sup> value (r<sup>2</sup> > 0.8).

The chemical structures of the compounds with their pIC<sub>50</sub> values are shown in **Table 1**.

$$\text{PIC}_{50} = 10.7615 + 0.0004(\text{AATSC1p}) + 16.9538(\text{VE3\_Dzv}) + 0.0375(\text{SaaaC}) - 607.7200(\text{JGI8})$$
$$R^2 = 0.9201 \text{----- (Equation 1)}$$



The william plot of equation 1 show two outlier by removing the out lier it is possible to achieve 3 best equation without out lier is more acceptable compared to other equations due to the increased importance of  $r^2$ ,  $q^2$  and decreased values of RMSE, being much less (<0.3).

2D-QSAR models were generated to determine the effect of structural features coumarin as antibacterial agents.

$$\text{PIC50} = -10.7615 + 0.0004(\text{ATSe4V}) + 16.9538(\text{GATS2E}) + 0.0375(\text{VE3DZM}) - 607.7200(\text{AVP-7})$$

$$R^2 = 0.9388 \text{ ----- (Equation 2)}$$

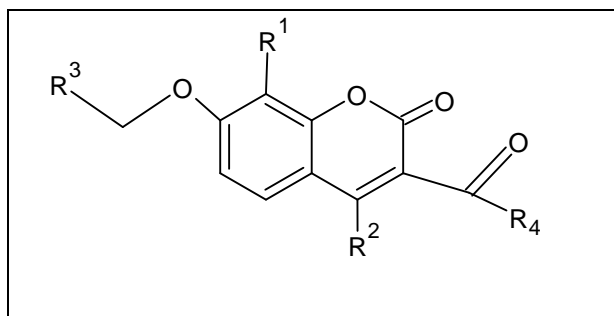
$$\text{PIC50} = -10.2873 + 14.7501(\text{GATS2E}) + 0.0374(\text{VE3DZM}) - 0.1012(\text{C36P2}) - 443.7566(\text{AVP-7})$$

$$R^2 = 0.9348 \text{ ----- (Equation 3)}$$

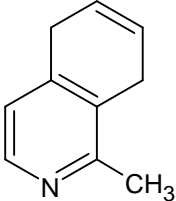
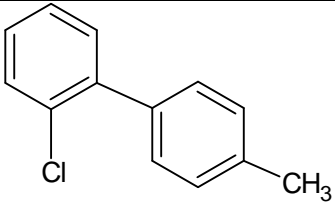
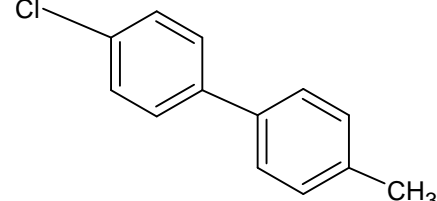
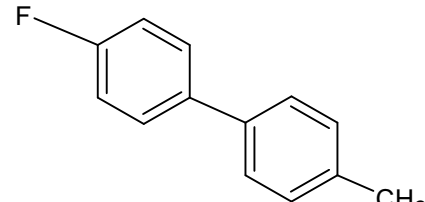
$$\text{PIC50} = -9.996 + 0.505(\text{AATSC4V}) + 17.2475(\text{GATS2E}) + 0.0373(\text{VE3DZM}) - 746.3481(\text{AVP-7})$$

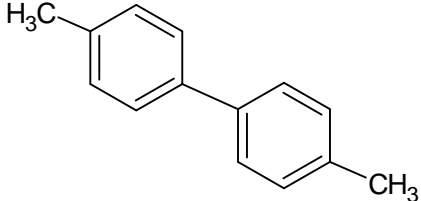
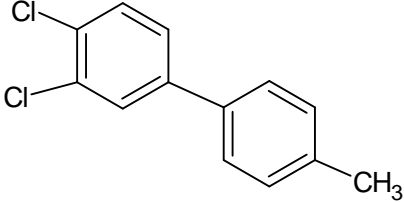
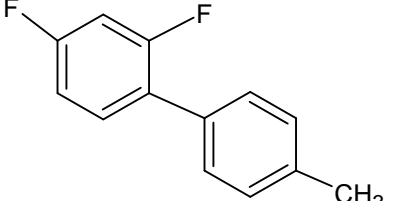
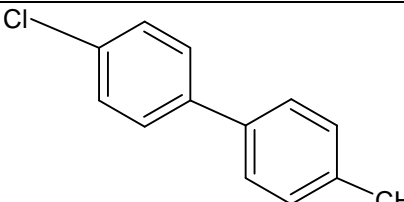
$$R^2 = 0.9347 \text{ ----- (Equation 4)}$$

From the correlation, there is inverse relationship between ATSe4V, GATS2E, VE3DZM, AVP-7 descriptors and biological activity values. There is a direct relationship between molar volume, GATS2E, VE3DZM, C36P2, AVP-7) descriptors and biological activity values. There is a direct relationship between volume, AATSC4V, GATS2E, VE3DZM, AVP-7 descriptors and biological activity with different correlation coefficients.

TABLE 1: PIC<sub>50</sub> values of reported hybrids.

Compound id	R1	R2	R3	R4	PIC <sub>50</sub>	PIC <sub>50</sub>
1	CH <sub>3</sub>	CH <sub>3</sub>	1-Naphthyl	OH	6	- 5.22185
2	CH <sub>3</sub>	CH <sub>3</sub>		OH	>100	-4
3	CH <sub>3</sub>	CH <sub>3</sub>		OH	>100	-4
4	CH <sub>3</sub>	CH <sub>3</sub>	Phenyl	OH	85	- 4.07058
5	CH <sub>3</sub>	CH <sub>3</sub>	4-pyridyl	OH	>100	-4
6	CH <sub>3</sub>	CH <sub>3</sub>	2-Naphthyl	OH	9	5.04576
7	CH <sub>3</sub>	CH <sub>3</sub>		OH	56	- 4.25181
8	CH <sub>3</sub>	CH <sub>3</sub>		OH	>100	-4
9	CH <sub>3</sub>	CH <sub>3</sub>		OH	>100	-4

10	CH <sub>3</sub>	CH <sub>3</sub>		OH	>100	-4
11	H	CH <sub>3</sub>	9 – anthracenyl	OH	7.2	- 5.14267
12	CH <sub>3</sub>	CH <sub>3</sub>	1,2- biphenyl	OH	10.2	-4.9914
13	H	CH <sub>3</sub>	1,2 –biphenyl	OH	19	- 4.72125
14	CH <sub>3</sub>	CH <sub>3</sub>	1,3-biphenyl	OH	15	- 4.82391
15	CH <sub>3</sub>	CH <sub>3</sub>	1,3-biphenyl	OH	7.5	- 5.12494
16	H	CH <sub>3</sub>	1,4-biphenyl	OH	9.7	- 5.01323
17	H	CH <sub>3</sub>	1,4-biphenyl	OH	3	- 5.52288
18	CH <sub>3</sub>	CH <sub>3</sub>		OH	3.8	- 5.42022
19	H	CH <sub>3</sub>		OH	1.5	- 5.8239 1
20	CH <sub>3</sub>	CH <sub>3</sub>		OH	5.1	- 5.2924 3

21	CH <sub>3</sub>	CH <sub>3</sub>		OH	6.1	- 5.2146 7
22	CH <sub>3</sub>	CH <sub>3</sub>		OH	3	- 5.5228 8
23	CH <sub>3</sub>	CH <sub>3</sub>		OH	9	- 5.0457 6
24	CH <sub>3</sub>	CH <sub>3</sub>		OH	>100	-4
25	CH <sub>3</sub>	CH <sub>3</sub>	1,4-biphenyl	OH	>100	-4
26	CH <sub>3</sub>	CH <sub>3</sub>	1,4-biphenyl	OH	1.8	- 5.7447
27	CH <sub>3</sub>	CH <sub>3</sub>	1,4-biphenyl	OH	9	5.0457 6
28	CH <sub>3</sub>	CH <sub>3</sub>	1,4-biphenyl	OH	2	- 5.6989
29	CH <sub>3</sub>	CH <sub>3</sub>	1,4-biphenyl	OH	21	- 4.6777 8
30	CH <sub>3</sub>	CH <sub>3</sub>	1,4-biphenyl	OH	2	- 5.6989
31	CH <sub>3</sub>	CH <sub>3</sub>	1,4-biphenyl	OH	5	- 5.3010

Fitting criteria and internal validation values for model 2 is good. Compared to previous model, it shows slight improvements in external validation parameter values, without any outliers in the William's plot. The descriptor correlation matrix of model 2 was given in **Table 2**. Experimental and predicted activities of original dataset compounds are given **Table 1**.

**TABLE 2:** Descriptor correlation matrix for the best model

	GATS2e	VE3_Dzm	C3SP2	AVP-7
GATS2e	1			
VE3_Dzm	0.265	1		
C3SP2	-0.2456	-0.366	1	
AVP-7	0.3495	-0.2398	0.5002	1

From the correlation, it is clear that there is inverse relationship between ATSe4V, GATS2E, VE3DZM, AVP-7 descriptors and biological activities values. The direct relationship was found between GATS2E, VE3DZM, C36P2, AVP-7 descriptors and biological activity. The model 2 equation is more acceptable due to high  $R^2$ ,  $Q^2$  values and low error values such as s, RMSE, MAE parameters. Based on the final model 2, pMIC values for all compounds were calculated and shown in **Table 3**. And the internal and external parameters are shown in **Table 4**.

**TABLE 3:** predicted activities of designed compounds by best equation

Compound no.	pIC <sub>50</sub> (predequ1)	pIC <sub>50</sub> (pred equ 2)	pIC <sub>50</sub> (pred equ 3)
1	-1.35164	-4.84707	-4.3107
2	-4.21584	-1.8769	-0.88307
3	-0.75339	-5.81851	-5.42674
4	-5.38303	-3.22812	-2.51824
5	-2.5995	-4.61742	-3.8422
6	-3.69699	-4.82543	-4.30515
7	-4.25219	-1.26649	-0.39202
8	-0.47735	-4.74396	-4.11811
9	-4.13862	-5.7416	-5.43435
10	-5.45641	-5.01532	-4.60423
11	-4.50001	-5.11207	-4.81115
12	-4.60045	-10.2873	-9.9996

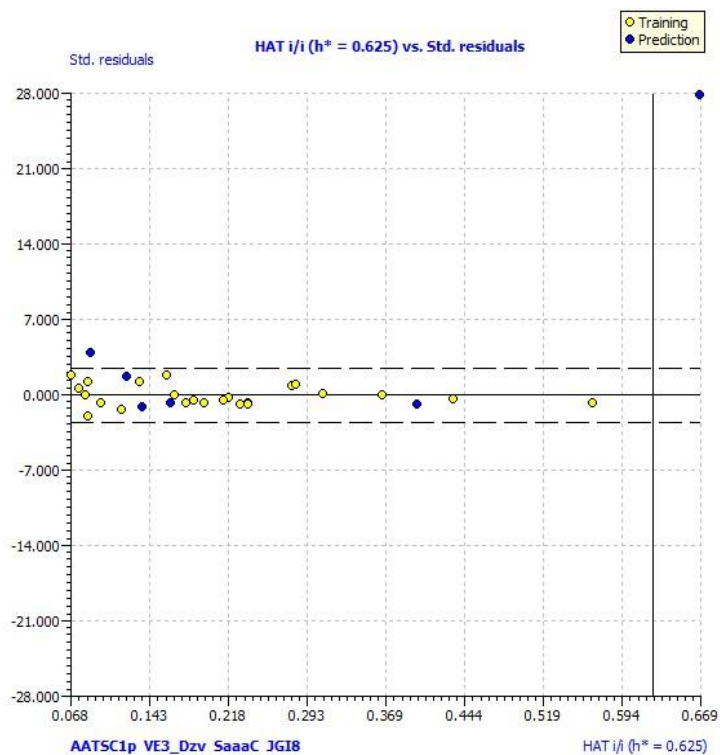


Figure .28 williams plot for equation 1

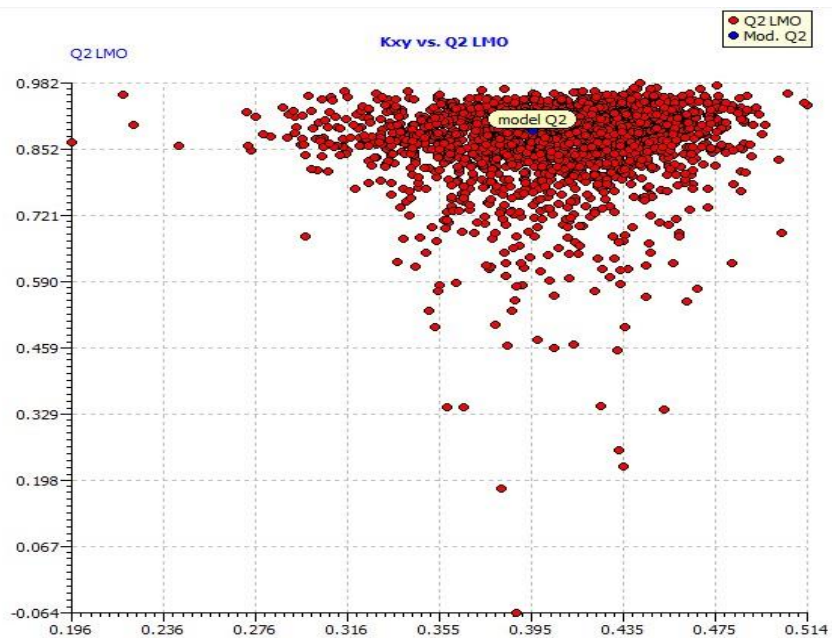


Figure 28. The LMO Scatter plot for equation 1

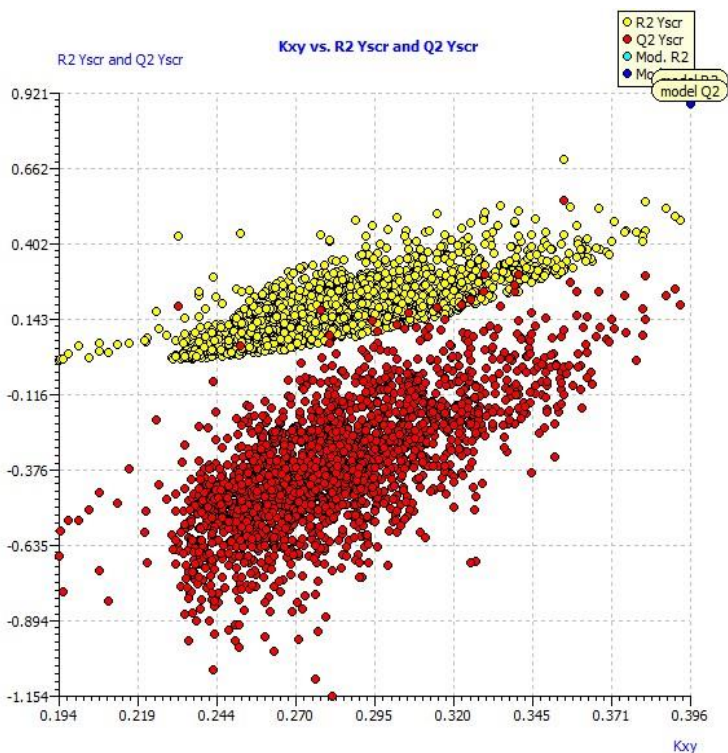


Figure 28. Y-scramble plot for equation 1

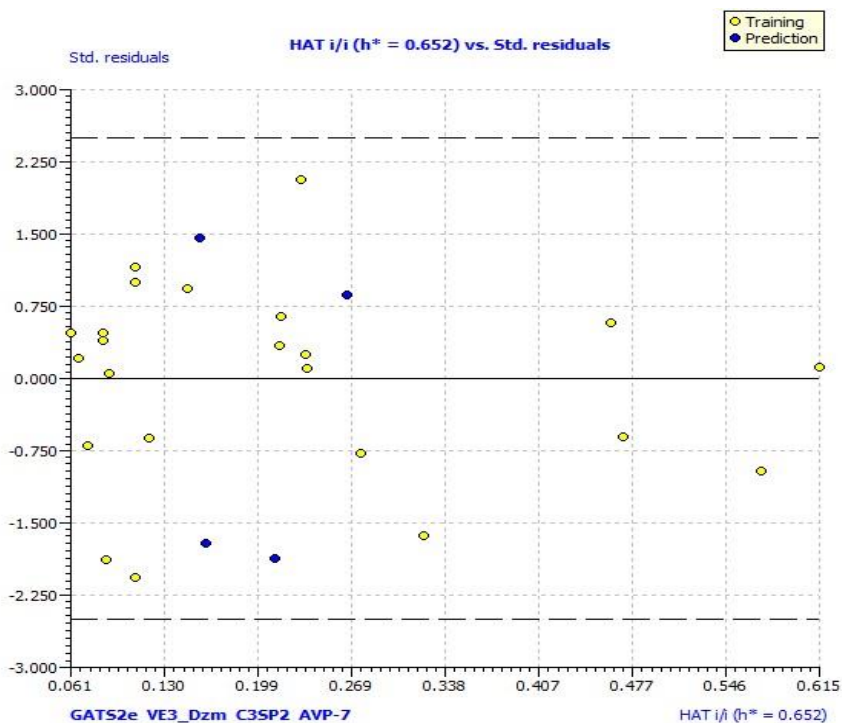


Figure. 29 williams plot for equation 2



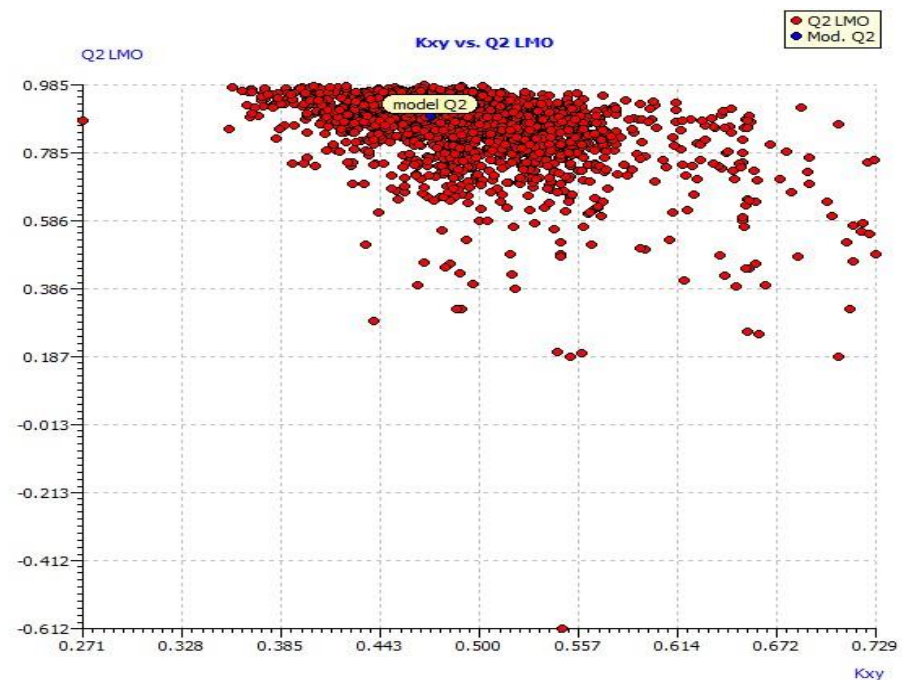


Figure29: The LMO Scatter plot for equation 2

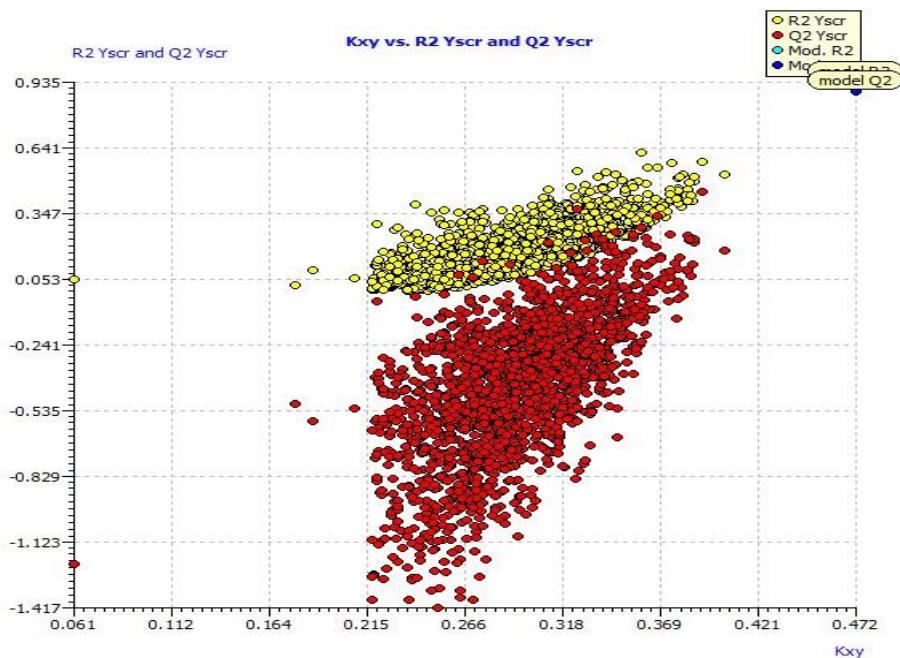


Figure 29: Y-scramble plot for equation 2

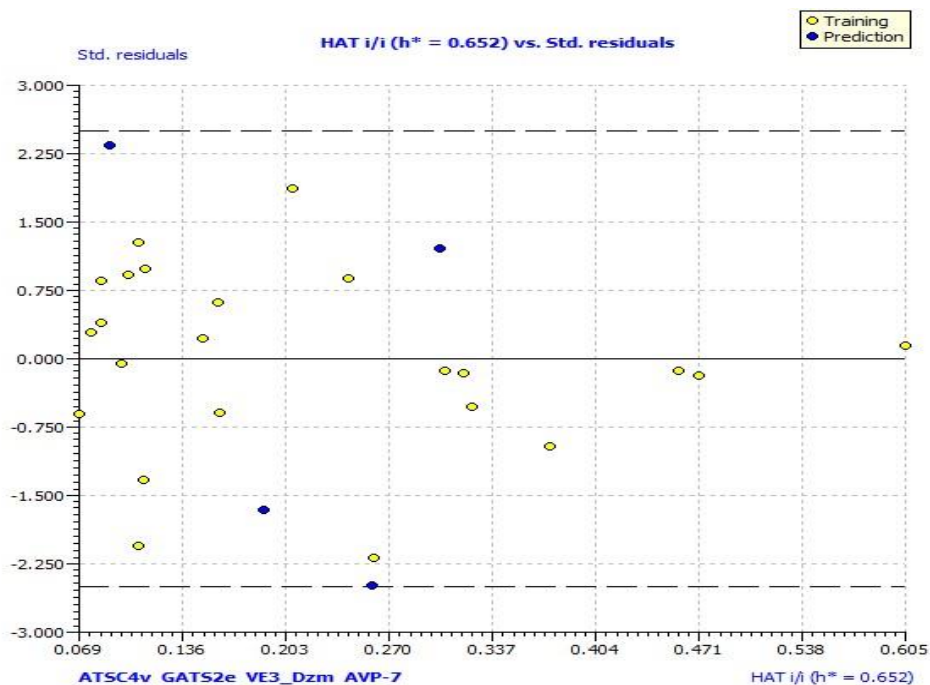


Figure. 30 williams plot for equation 3

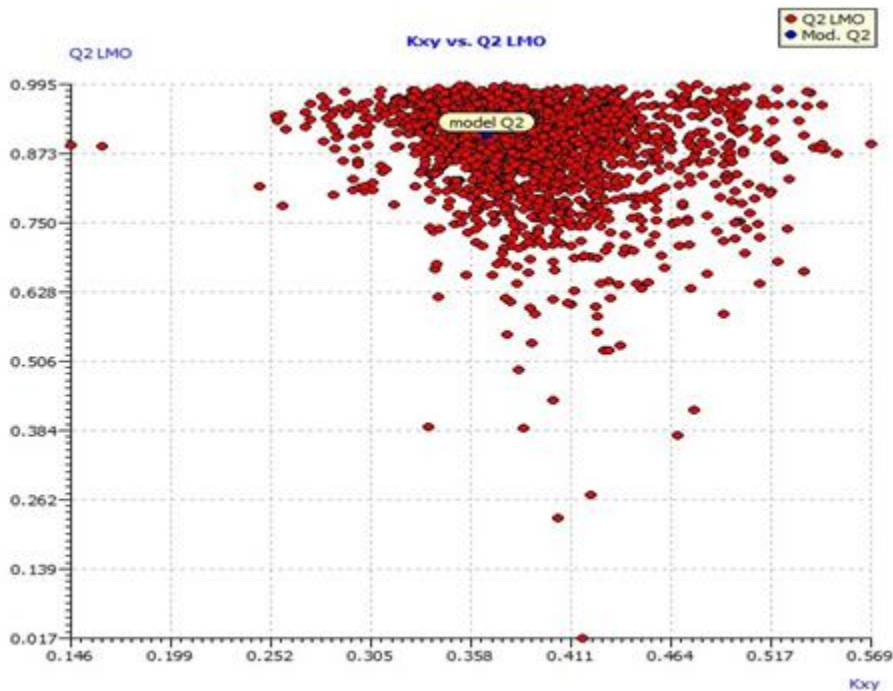


Figure .30 The LMO Scatter plot for equation 3

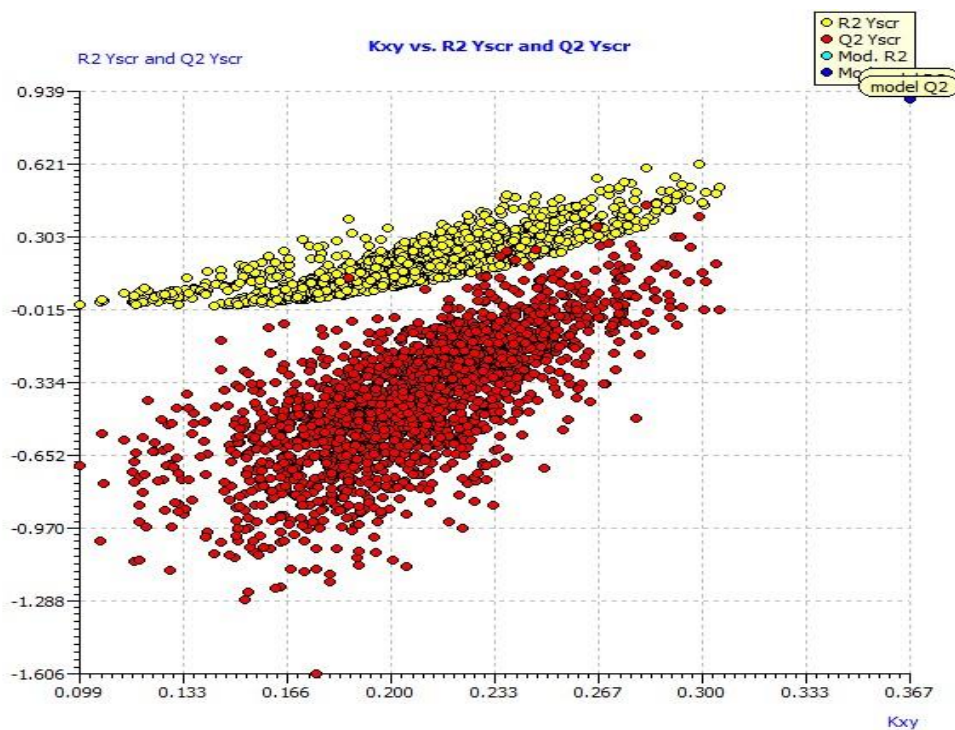


Figure 30: Y-scramble plot for equation 3

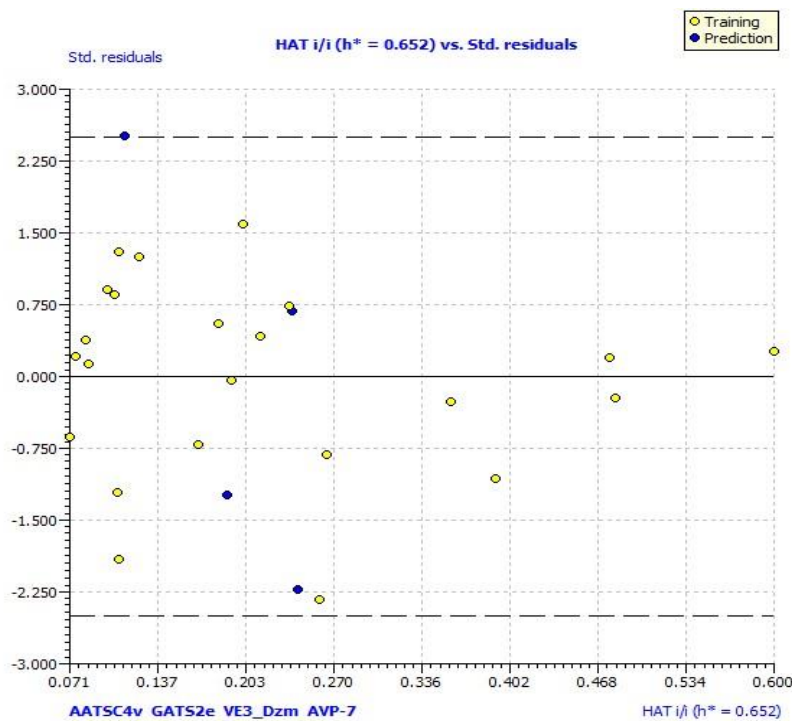


Figure .31 williams plot equation 4

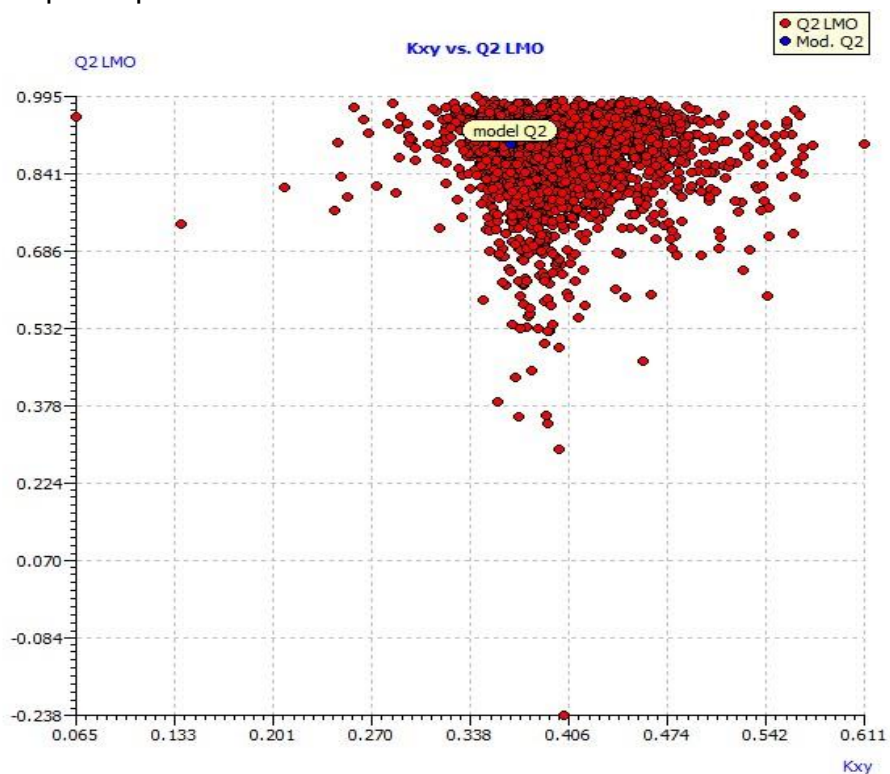


Figure 31. The LMO Scatter plot for equation 4

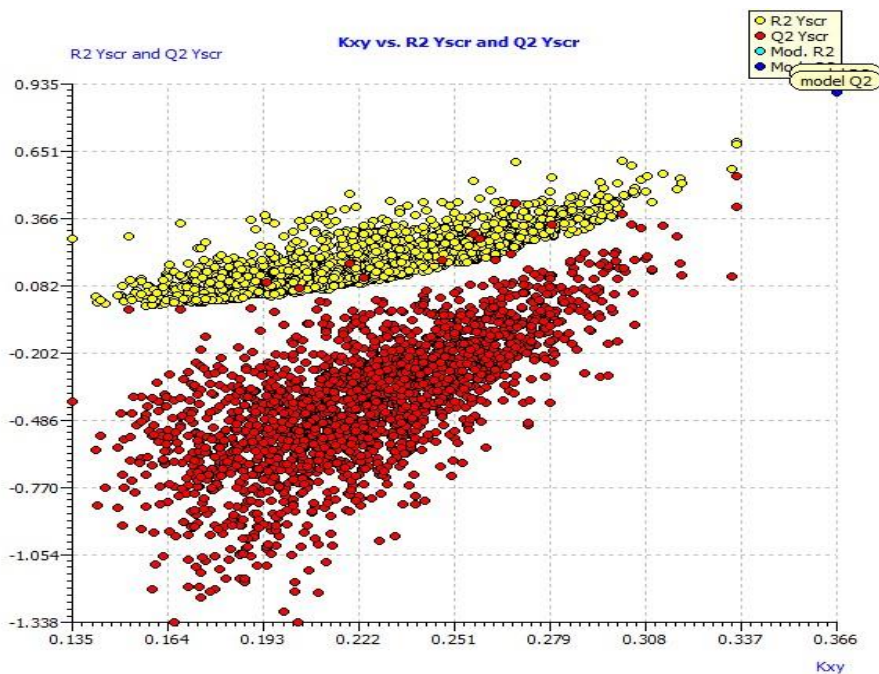
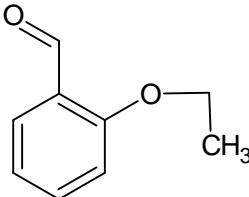
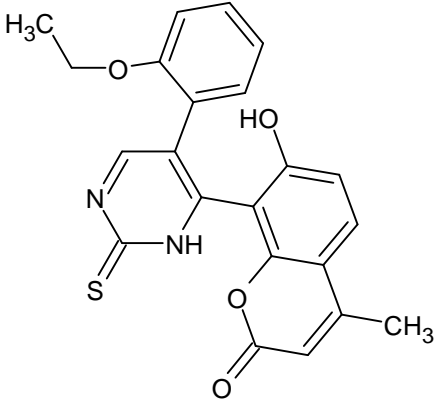
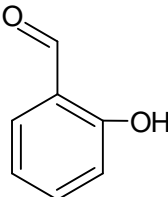
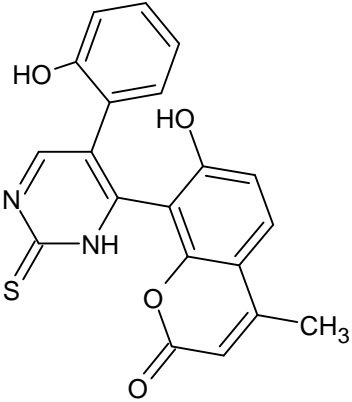
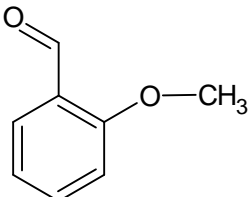
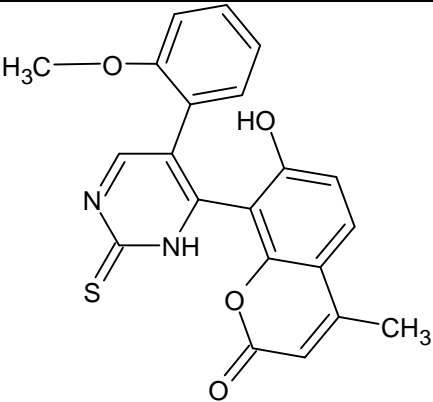


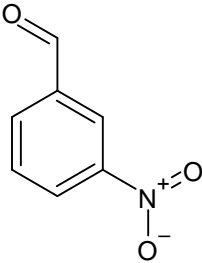
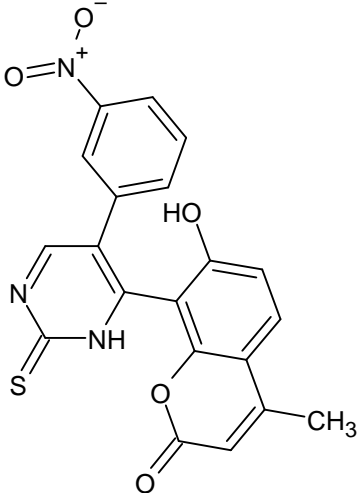
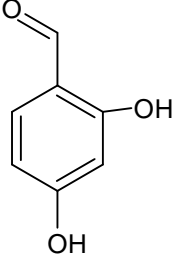
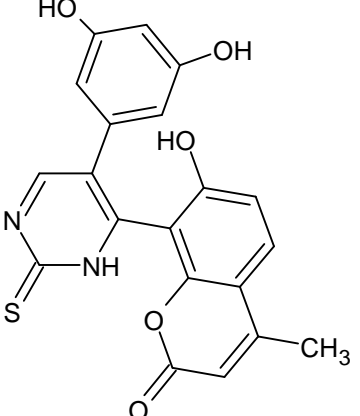
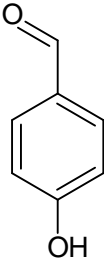
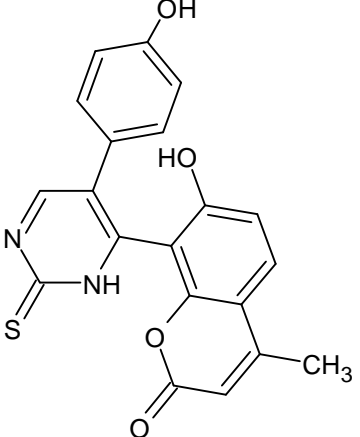
Figure. 31Y-scramble plot for equation 4

## 6.2. DESIGN OF COMPOUNDS

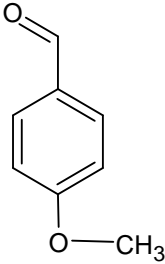
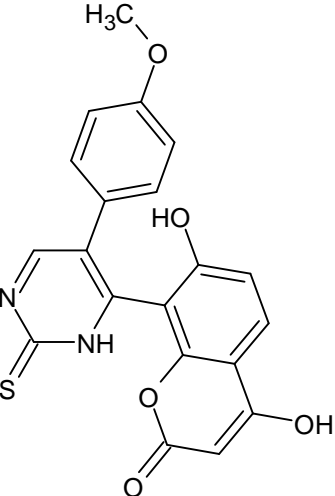
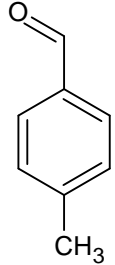
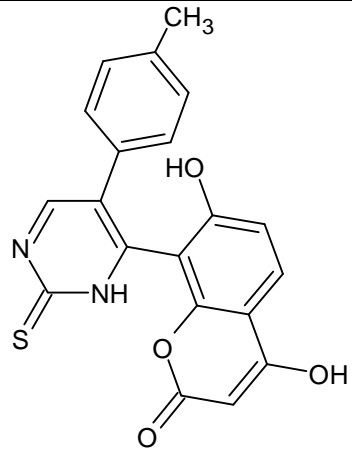
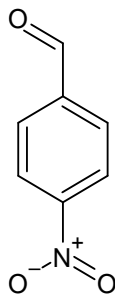
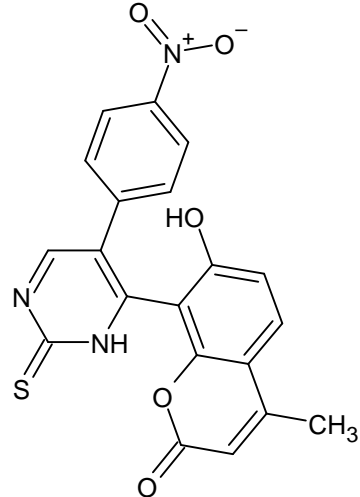
35 compounds were designed using Chemskech software and physicochemical properties were calculated for all compounds. The designed compounds and their predicted pMIC using model 2 was given in **Table:4**

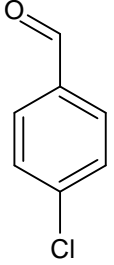
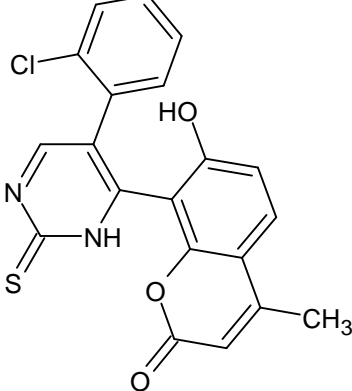
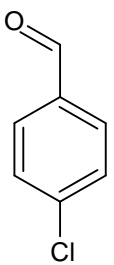
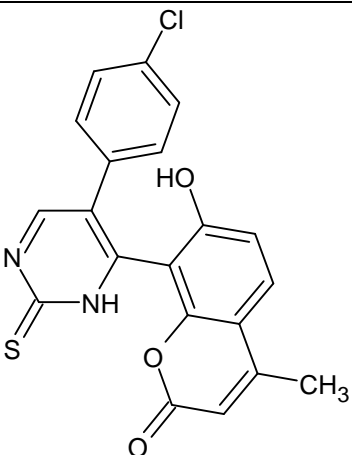
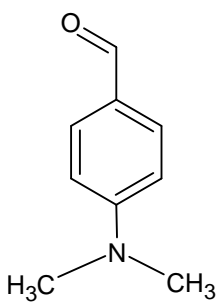
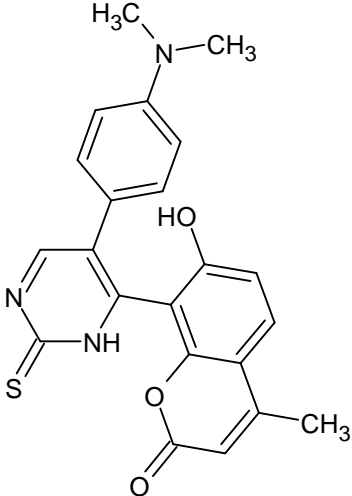
**Table 4: Structures of the predicted compounds 3a-3l**

Compound No.	DERIVATIVES	Structure	PIC <sub>50</sub>
3a			-4.84707
3b			-1.8769
3c			-5.81851

<b>3d</b>	 <p>Chemical structure of 3-nitrobenzaldehyde: A benzene ring with an aldehyde group (-CHO) at the 1-position and a nitro group (-NO<sub>2</sub>) at the 3-position.</p>	 <p>Chemical structure of a complex heterocyclic molecule: A central benzothiazine ring system (6-membered ring with N and S) is substituted with a 4-nitrophenyl group at the 2-position, a 2-hydroxyphenyl group at the 4-position, and a 6-methyl-2-pyrone ring at the 5-position.</p>	-3.22812
<b>3e</b>	 <p>Chemical structure of 3,4-dihydroxybenzaldehyde: A benzene ring with an aldehyde group (-CHO) at the 1-position and hydroxyl groups (-OH) at the 3 and 4 positions.</p>	 <p>Chemical structure of a complex heterocyclic molecule: A central benzothiazine ring system (6-membered ring with N and S) is substituted with a 2,3-dihydroxyphenyl group at the 2-position, a 2-hydroxyphenyl group at the 4-position, and a 6-methyl-2-pyrone ring at the 5-position.</p>	-4.61742
<b>3f</b>	 <p>Chemical structure of 4-hydroxybenzaldehyde: A benzene ring with an aldehyde group (-CHO) at the 1-position and a hydroxyl group (-OH) at the 4-position.</p>	 <p>Chemical structure of a complex heterocyclic molecule: A central benzothiazine ring system (6-membered ring with N and S) is substituted with a 4-hydroxyphenyl group at the 2-position, a 2-hydroxyphenyl group at the 4-position, and a 6-methyl-2-pyrone ring at the 5-position.</p>	-4.82543



<b>3g</b>	 <p>Chemical structure of 4-methoxybenzaldehyde: A benzene ring with an aldehyde group (-CHO) at the top and a methoxy group (-OCH<sub>3</sub>) at the para position.</p>	 <p>Chemical structure of a complex heterocyclic molecule. It features a central benzothiazine ring system fused to a benzene ring and a pyridone ring. A 4-methoxyphenyl group is attached to the benzothiazine ring. The pyridone ring has a hydroxyl group (-OH) at the 2-position. The benzene ring has a hydroxyl group (-OH) at the 6-position.</p>	-1.26649
<b>3h</b>	 <p>Chemical structure of 3-methylbenzaldehyde: A benzene ring with an aldehyde group (-CHO) at the top and a methyl group (-CH<sub>3</sub>) at the meta position.</p>	 <p>Chemical structure of a complex heterocyclic molecule. It features a central benzothiazine ring system fused to a benzene ring and a pyridone ring. A 3-methylphenyl group is attached to the benzothiazine ring. The pyridone ring has a hydroxyl group (-OH) at the 2-position. The benzene ring has a hydroxyl group (-OH) at the 6-position.</p>	-4.74396
<b>3i</b>	 <p>Chemical structure of 4-nitrobenzaldehyde: A benzene ring with an aldehyde group (-CHO) at the top and a nitro group (-NO<sub>2</sub>) at the para position.</p>	 <p>Chemical structure of a complex heterocyclic molecule. It features a central benzothiazine ring system fused to a benzene ring and a pyridone ring. A 4-nitrophenyl group is attached to the benzothiazine ring. The pyridone ring has a hydroxyl group (-OH) at the 2-position. The benzene ring has a methyl group (-CH<sub>3</sub>) at the 6-position.</p>	-5.7416

<b>3j</b>	 <p>Chemical structure of 4-chlorobenzaldehyde: A benzene ring with an aldehyde group (-CHO) at the top and a chlorine atom (-Cl) at the para position (bottom).</p>	 <p>Chemical structure of a complex heterocyclic molecule: A central benzothiazine ring system (6-membered ring with N and S) is substituted with a 2-chlorophenyl group at the 4-position, a 2-hydroxyphenyl group at the 5-position, and a 2-methyl-4-pyridone ring at the 6-position.</p>	-5.01532
<b>3k</b>	 <p>Chemical structure of 4-chlorobenzaldehyde: A benzene ring with an aldehyde group (-CHO) at the top and a chlorine atom (-Cl) at the para position (bottom).</p>	 <p>Chemical structure of a complex heterocyclic molecule: A central benzothiazine ring system (6-membered ring with N and S) is substituted with a 4-chlorophenyl group at the 4-position, a 2-hydroxyphenyl group at the 5-position, and a 2-methyl-4-pyridone ring at the 6-position.</p>	-5.11207
<b>3L</b>	 <p>Chemical structure of N,N-dimethyl-4-formylbenzamide: A benzene ring with an aldehyde group (-CHO) at the top and a dimethylamino group (-N(CH<sub>3</sub>)<sub>2</sub>) at the para position (bottom).</p>	 <p>Chemical structure of a complex heterocyclic molecule: A central benzothiazine ring system (6-membered ring with N and S) is substituted with a 4-(dimethylamino)phenyl group at the 4-position, a 2-hydroxyphenyl group at the 5-position, and a 2-methyl-4-pyridone ring at the 6-position.</p>	-10.2873



### 6.3 *IN SILICO* SCREENING OF DESIGNED COMPOUNDS

The molecular properties were calculated using Molinspiration and tabulated in **Table 5**.

Molinspiration software was used to evaluate molecular properties such as miLogP, no. of rotatable bonds, molecular weight and volume of designed compounds and its results were tabulated (table). No violations was reported with the designed compounds.

The bioactivity scores of the synthesized complexes were calculated for different parameters such as binding to G protein-coupled receptor (GPCR) ligand and nuclear receptor ligand, ion channel modulation, kinase inhibition, protease inhibition, and enzyme activity inhibition. The bioactivity score is given in **Table 5**. If the bioactivity score is more than 0.0, then the complex is active; if it is between -5.0 and 0.0, then the complex is moderately active, and if the bioactivity score is less than -5.0, then it is inactive. The synthesized compounds were found to be moderately bioactive (<0) towards all the enzyme considered for the study.

The Pharmacokinetic properties such as TPSA, No. of H-bond acceptor/donor, Molar refractivity, logP, Bioavailability score, GI absorption, of the designed compounds were evaluated using SWISS ADME and software and their results were tabulated(**Table 5,6**). TPSA has been used as descriptor for characterizing absorption and passive transportation properties through biological membranes, allowing a good prediction of transport of candidate drugs in the intestines and through the blood-brain barrier. Compounds with TPSA values within the range 140 Å<sup>2</sup> have good intestinal absorption. TPSA (Total Polar Surface Area) of our designed compounds were found to be in the range of 100-215 Å<sup>2</sup>. Except the molecules 3d, 3e remaining was expected to possess good intestinal absorption.

Lipophilicity (logP) plays an important role in the absorption, distribution, metabolism, excretion, and toxic effects of a drug. LogP of the designed compounds was found to be in the range of 1-5. So there is a strong lipophilic character of the molecule plays a major role in producing the antimicrobial effect.

Molar refractivity is related, not only to the volume of the molecules but also to the London dispersive forces that act in the drug-receptor interaction. All the designed compounds were within the normal range of 40-130 J mol<sup>-1</sup> K<sup>-1</sup>. The majority of compounds have bioavailability score of **0.55** which indicates a good pharmacokinetic property.

Antibacterial agents generally possess greater number of hydrogen bond acceptors. All the designed compounds have hydrogen bond donors in the range of 1-4 and 4-9 hydrogen bond acceptors. This obeys Lipinski rule of five. Molecular weight of the most designed compounds was around 500 daltons and its results were tabulated (**Table 6,7**).

CaCo<sup>2</sup> is primarily used as a model of the intestinal epithelial barrier. It is used to predict *in vivo* absorption of the drugs. All the synthesized compounds are found to be with high absorption predicted permeability of >10 x 10<sup>-6</sup> cm/s and good Human Intestinal Absorption (HIA) and its results were tabulated (**Table 9**).

Cytochrome P450 enzymes are essential for the metabolism of many medications. Knowledge of the most important drugs metabolized by cytochrome P450 enzymes, as well as the most potent inhibiting and inducing drugs, can help minimize the possibility of adverse drug reactions and interactions. From synthesized compounds 3n, 3y are 2C9 inhibitor and most of the designed compounds are weakly CYP3A4 substrate.

Toxicity of all the designed compounds were evaluated by using two softwares ProTox II and Pre ADMET and its results were tabulated (**Table 8,11**). Drug likeness results were evaluated the qualified compound are used to design the compounds were tabulated (**Table 10**) According to Pre ADMET toxicity study- all the synthesized compounds was found to be non-mutagenic, non-carcinogenic with medium risk of hERG inhibition.

Protox II results shows predicted LD50 mg/kg of class 5 for the synthesized compounds without any toxicity.

**Table 5: Physicochemical parameters obtained from MOLINSPIRATION for the designed compounds 3a-3l**

Compound	MilogP	TPSA Å	N Atom	Molecular Weight	No.of violation	No.rotable bonds	Volume
3a	3.95	111.4	29	389.40	0	4	341.31
3b	3.30	122.4	27	361.35	0	2	341.31
3c	3.58	111.4	28	375.38	0	3	306.98
3d	3.50	148.0	29	390.35	0	3	324.29
3e	2.54	142.7	28	377.35	0	2	322.29
3f	3.09	122.4	27	361.35	0	2	314.99
3g	3.53	148.0	29	377.35	0	3	306.98
3h	4.20	102.2	27	361.35	0	2	322.29
3i	4.25	102.2	27	390.35	0	2	312.49
3j	3.67	105.4	29	378.80	0	3	344.86
3k	3.55	105.4	27	378.80	0	3	317.62
3l	3.76	103.5	27	388.42	0	2	320.21

## BIOACTIVITY SCORE

Compound	GPCR ligand	Ion channel modulator	Kinase inhibitor	Nuclear receptor ligand	Protease inhibitor	Enzyme inhibitor
3a	-0.14	-0.36	0.29	-0.02	-0.38	0.20
3b	-0.14	-0.36	0.29	-0.02	-0.38	0.20
3c	-0.10	-0.33	0.38	-0.03	-0.32	0.26
3d	-0.11	-0.36	0.36	-0.04	-0.37	0.24
3e	-0.23	-0.37	0.27	-0.14	-0.42	0.16
3f	-0.09	-0.32	0.42	-0.01	-0.32	0.28
3g	-0.08	-0.32	0.43	0.00	-0.30	0.29
3h	-0.23	-0.37	0.25	-0.14	-0.42	0.15
3i	-0.10	-0.35	0.43	-0.04	-0.34	0.24
3j	-0.09	-0.34	0.40	-0.04	-0.32	0.23
3k	-0.07	-0.33	0.34	-0.05	-0.34	0.24
3l	0.10	-0.38	0.45	-0.06	-0.32	0.26

Table 6: SWISS ADME results of the predicted compounds 3a-3l:

Cmpd No.	Lipinski	Ghose	Veber	Egan	Muegge	Bioavailability score	GI absorption	BBB permeation	P-gp substrate	Log kP cm/s	Synthetic accessibility score
3a	Yes	Yes	Yes	Yes	Yes	0.55	High	No	Yes	-6.51	3.56
3b	Yes	Yes	Yes	yes	Yes	0.55	High	No	Yes	-6.86	3.36
3c	Yes	Yes	Yes	Yes	Yes	0.55	High	No	Yes	-6.76	3.47
3d	Yes	Yes	No	No	Yes	0.55	High	No	Yes	-6.89	3.43
3e	Yes	Yes	No	No	Yes	0.55	High	No	Yes	-7.2	3.44
3f	Yes	Yes	Yes	yes	Yes	0.55	High	No	Yes	-6.84	3.35
3g	Yes	Yes	No	No	Yes	0.55	High	No	Yes	-6.89	3.39
3h	Yes	Yes	Yes	Yes	Yes	0.55	High	No	Yes	-6.4	3.67
3i	Yes	Yes	Yes	Yes	Yes	0.55	High	No	Yes	-6.75	3.33
3j	Yes	Yes	Yes	yes	Yes	0.55	High	No	Yes	-6.26	3.36
3k	Yes	Yes	Yes	yes	Yes	0.55	High	No	Yes	-6.26	3.36
3l	Yes	Yes	Yes	yes	Yes	0.11	High	No	Yes	6.67	3.55

Table 7: Bioavailability of the predicted compounds 3a-3l

Comd. code.	Formula	Molecular weight (g/mol)	Num. heavy atoms	Num. aromatic heavy atoms	Fraction Csp3	Number rotatable bonds	N0.H bond acceptors	Number H bond donors	Molar refractivity	TPSA(Å)
3a	C22H19N2O4S	389.4	29	22	0.14	4	6	2	111.64	111.47
3b	C20H15N2O4S	361.35	27	22	0.05	2	6	3	102.36	122.47
3c	C21H17N2O4S	378.38	28	22	0.1	3	6	2	106.83	111.47
3d	C20H14N2O5S	390.35	29	22	0.05	3	7	2	109.16	116.49
3e	C20H15N2O5S	377.35	28	22	0.05	2	7	4	104.39	148.06
3f	C20H15N2O4S	361.38	27	22	0.05	2	6	3	102.36	142.7
3g	C20H14N2O5S	390.35	29	22	0.05	3	7	2	109.16	122.47
3h	C22H15N2O3S	379.8	27	22	0.05	2	5	2	107.71	148.06
3i	C17H15N2O3S	362.37	27	22	0.05	2	5	2	102.16	102.24
3j	C20H15CLN2O3S	396.8	29	22	0.05	3	5	3	105.35	162.31
3k	C20H14CLN2O3S	396.8	27	22	0.05	3	6	2	105.35	102.24
3l	C22H20N3O3S	388.42	29	22	0.14	2	5	3	1114.55	105.48

Table 8: protox II results of the predicted compounds 3a-3l

Compound No	Predicted LD50 mg/kg	Predicted toxicity class	Carcinogenicity	Immunotoxicity	Mutagenicity	Cytotoxicity
3a	1050	4	Active	Inactive	Inactive	Inactive
3b	1500	3	Inactive	active	Inactive	Inactive
3c	3500	5	Inactive	Inactive	Inactive	Inactive
3d	2000	4	Inactive	Inactive	Active	Inactive
3e	1150	3	Inactive	active	Inactive	Inactive
3f	2000	3	Inactive	Inactive	Inactive	active
3g	1500	3	Active	Inactive	Active	Inactive
3h	4000	5	Inactive	Inactive	Inactive	Inactive
3i	1450	4	Active	Inactive	Inactive	active
3j	3500	5	Inactive	Inactive	Inactive	Inactive
3k	4000	5	Inactive	Inactive	Inactive	Inactive
3l	5000	5	Inactive	Inactive	Inactive	Inactive

**Table 9: ADME Result of the predicted compounds 3a-3l**

Compounds	Caco2	CYP inhibition				CYP substrate		HIA	MDCK
		2C19	2C9	2D6	3A4	2D6	3A4		
3a	22.2815	Inhibitor	Inhibitor	Inhibitor	Inhibitor	Non	Non	100	204.401
3b	19.7118	Inhibitor	Inhibitor	Non	Inhibitor	Non	Weakly	92.21328	23.0193
3c	19.3599	Inhibitor	Inhibitor	Non	Non	Inhibitor	Non	95.75044	16.4323
3d	17.7015	Non	Inhibitor	Non	Inhibitor	Non	Weakly	87.1427	0.16112
3e	20.6186	Non	Inhibitor	Non	Non	Non	Weakly	95.58819	0.348343
3f	20.9989	Inhibitor	Non	Non	Non	Non	Substrate	85.51331	17.3883
3g	19.7118	Inhibitor	Inhibitor	Non	Inhibitor	Non	Weakly	92.21548	1.67383
3h	19.248	Inhibitor	Inhibitor	Non	Non	Non	Weakly	91.23409	7.85166
3i	20.7013	Inhibitor	Inhibitor	Non	Non	Non	Weakly	92.21401	3.2089
3j	19.9692	Inhibitor	Non	Non	Non	Non	Weakly	87.1427	0.55291
3k	20.1959	Inhibitor	Inhibitor	Non	Non	Non	Weakly	95.40973	18.3219
3l	20.1959	Inhibitor	Inhibitor	Non	Non	Non	Weakly	95.40973	0.476875



Table 10: Drug-likeness Result of the predicted compounds 3a-3l

Compounds	CMC like Rule	Lead-like Rule	MDDR like Rule	WDI like Rule
3a	Qualified	Violated	Mid-structure	In 90% cutoff
3b	Qualified	Violated	Mid-structure	In 90% cutoff
3c	Qualified	Violated	Mid-structure	In 90% cutoff
3d	Not Qualified	Violated	Non-drug like	In 90% cutoff
3e	Qualified	Violated	Mid-structure	In 90% cutoff
3f	Qualified	Violated	Mid-structure	In 90% cutoff
3g	Qualified	Violated	Mid-structure	In 90% cutoff
3h	Qualified	Violated	Mid-structure	In 90% cutoff
3i	Qualified	Violated	Mid-structure	In 90% cutoff
3j	Qualified	Violated	Mid-structure	In 90% cutoff
3k	Qualified	Violated	Mid-structure	In 90% cutoff
3l	Qualified	Violated	Mid-structure	In 90% cutoff

Table 11: Toxicity Result of the predicted compounds 3a-3l

Compounds	Ames test	Carcino Mouse	Carcino Rat	hERG inhibition
3a	Non -Mutagen	Negative	Positive	Medium risk
3b	Mutagen	Negative	Negative	Medium risk
3c	Non-Mutagen	Negative	Negative	Medium risk
3d	Mutagen	Negative	Negative	High risk
3e	Mutagen	Negative	Negative	Medium risk
3f	Mutagen	Negative	Positive	Medium risk
3g	Mutagen	Negative	Negative	Medium risk
3h	Non-Mutagen	Negative	Negative	Medium risk
3i	Mutagen	Negative	Negative	Medium risk
3j	Non-Mutagen	Negative	Negative	Medium risk
3k	Non-Mutagen	Negative	Negative	Medium risk
3l	Non-Mutagen	Negative	Negative	Medium risk

## 6.4. DOCKING

Docking is a method which predicts the preferred orientation of one molecule to a second when bound to each other to form a stable complex. Knowledge of the preferred orientation in turn may be used to predict the strength of association or binding affinity between two molecules using, for example, scoring functions.

In this study, pyrx is used to perform docking studies. Docking studies were performed with the active site of DNA gyrase (PDB ID: 6F86). Protein was downloaded from RCSB and used for docking analysis. This molecular docking study was performed using the selected protein from the protein data bank (PDB ID: 6F86). The cocrystal structure of the DNA gyrase protein complexed with CWW in the active site is taken as protein. The docking for CWW (4-(4-bromanylpyrazol-1-yl)-6-(ethylcarbamoylamino)-~{N}-pyridin-3-yl-pyridine-3-carboxamide) was performed with its complex cocrystallized protein to validate the binding energy of ligand-protein interactions. The validation results showed a binding Affinity-8.4 kcal/mol CWW for indicating that this cocrystallized protein can be used for docking studies of other ligands.

The docking studies for five designed compounds having high predicted activities were done along with C14, which has high experimental biological activity. The most active compound, compound 14 in the reported series showed interaction with Lys 714 and binding affinity energy of -10.33 kcal/mol. Compounds **3c**, **3h**, **3j**, **3k**, **3l** exhibited binding energies of **-8.4**, **-8.7**, **-8.5**, **-8.2**, **-8.4** kcal/mol respectively.

Ligand 3c showed interaction in a different mode, by forming strong hydrogen-bond interactions with the coumarin ring the oxygen shows strong hydrogen-bond ARG: 76, In pyrimidine ring the nitro group hydrogen shows vander was binding with aminoacid GLUA: 50, other interaction in this compound with two amino acids AspA: 73, THRA: 165, which may describe the high predicted activity of the designed ligand. Ligand 3h showed interaction in coumarin ring the oxygen shows strong hydrogen-bond with ARG: 76. In coumarin ring the hydroxy group shows hydrogen bond with aminoacids AspA: 73. In pyrimidine ring the nitro group hydrogen shows hydrogen-bond with

aminoacids GLYA: 77, other strong hydrogen-bond with aminoacids GLUA: 50, which may describe the predicted activity of the designed ligand. The ligand 3j showed interaction in coumarin ring the oxygen shows strong hydrogen-bond with ARG: 76, In pyrimidine ring the nitro group hydrogen shows hydrogen-bond with aminoacids THRA: 165, ASNA: 46, which may describe the predicted activity of the designed ligand. The ligand 3k showed interaction in coumarin ring the oxygen shows strong hydrogen-bond with ARG: 76, In pyrimidine ring the nitro group hydrogen shows hydrogen-bond with aminoacids THRA: 165, ASNA: 46, which may describe the predicted activity of the designed ligand. The ligand 3L showed interaction in coumarin ring the oxygen shows strong hydrogen-bond with ARG: 76, ASP:49 In pyrimidine ring the nitro group hydrogen shows hydrogen-bond with aminoacids THRA: 165, ASNA: 46, which may describe the high predicted activity of the designed ligand. These results indicate that ligands can act as antibacterial agents against DNA gyrase. The interaction of ligand CWW, 3c, 3h, 3j, 3k, 3l with protein 6F86 is shown in **(Figure:32-36)**.

Table 12: Docking results of the predicted compounds 3a-3l

S. No.	Compound No.	Docking score Kcal/mol	Amino acid interaction with Distance
1.	3c	8.3	ARG76-3.074 THR165-2.42 ASP73-2.22 ASP49-4.536 PRO79-4.93
2.	3h	8.5	ASN46-2.94 GLY77-2.56 ASP49-2.54 GLU50-2.04
3.	3j	8.0	ARG76-2.77 THR165-2.34 ASN46-2.48 ASP49-4.55
4.	3k	8.0	ARG76-2.78 THR:165-2.32 ASN46-2.68
5.	3l	8.2	ASP73-2.83 ARG76-2.25 ASP49-4.56 GLU50-3.82

3c:

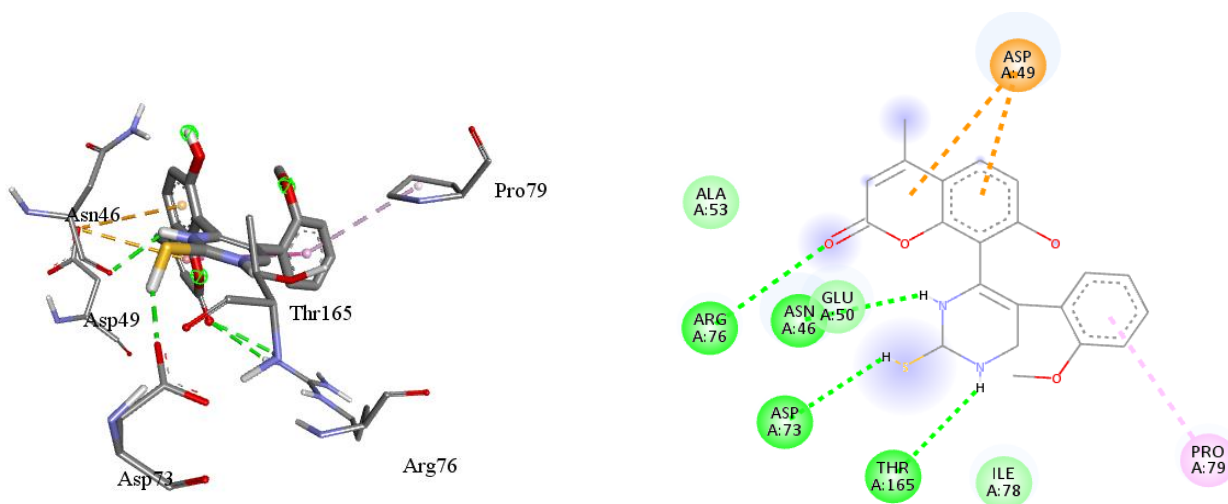


Figure.32 3D and 2D interaction of sample 3c

3h:

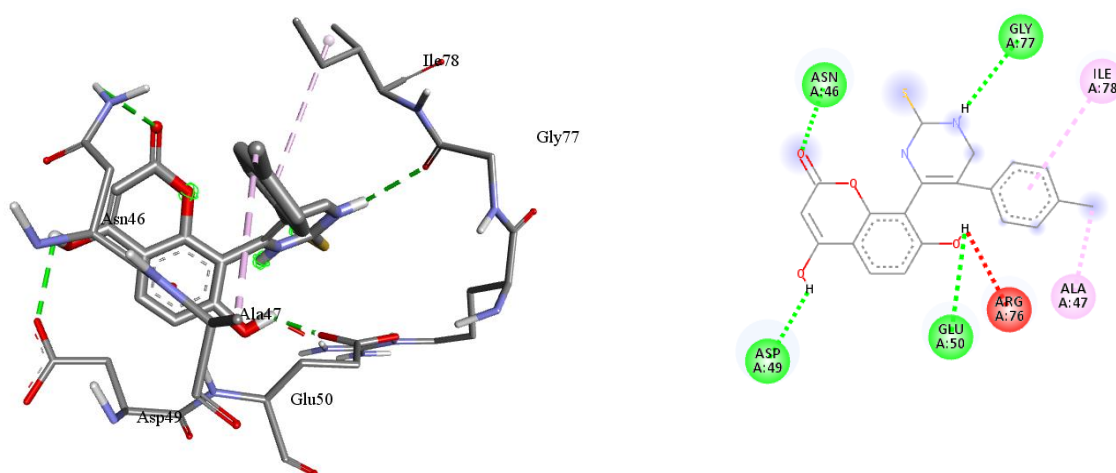


Figure.33 3D and 2D interaction of sample 3h

3j:

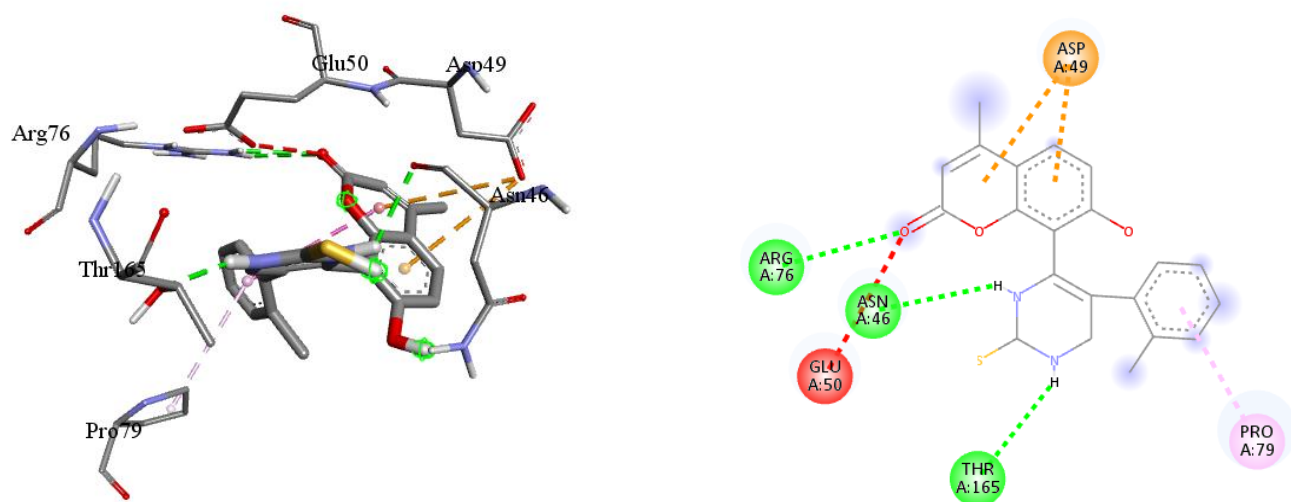


Figure.34 3D and 2D interaction of sample 3j

3k:

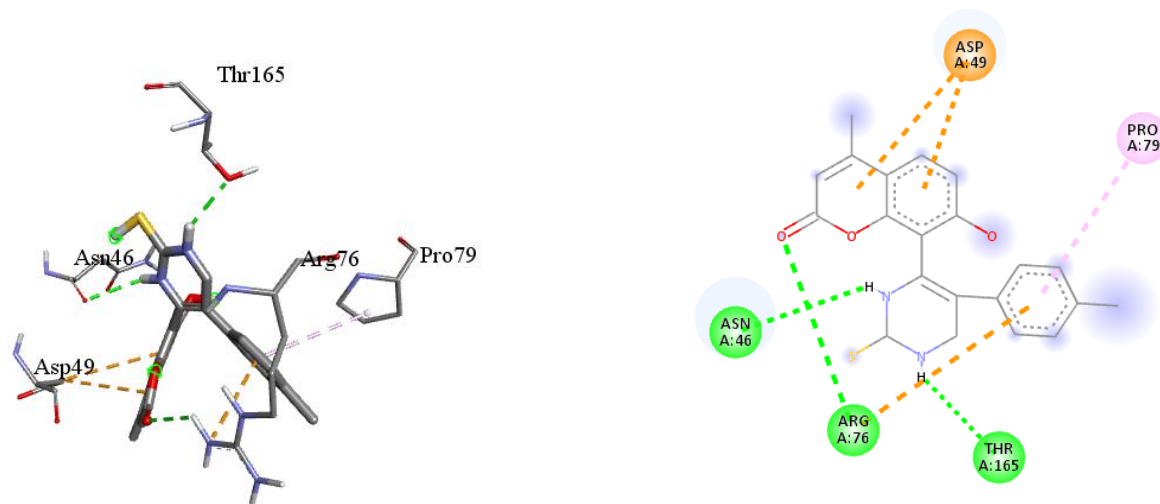


Figure.35 3D AND 2D interaction of sample 3k

3I:

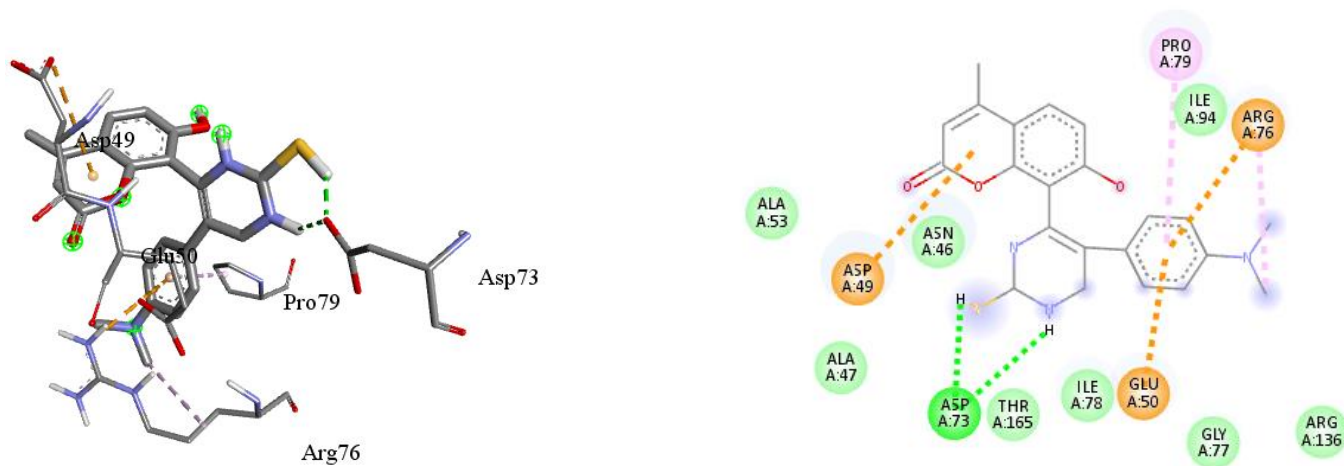


Figure.36 3D and 2D interaction of sample 3I



## 6.5 SYNTHESIS

The schematic representation for the synthesis of peckman condensation is represented in scheme 1. Peckman condensation were synthesized by reaction of resorcinol and ethylacetoacetate to form 4-methyl-7-hydroxy-coumarin. Substituted 4-methyl-7-hydroxy-8-acetyl coumarin, thiourea and sodium hydroxide were mixed carefully with a little water. Obtained mixture was irradiated about 2-3 minutes in microwave oven at 750 watts.

All the compounds were characterized by IR,  $^1\text{H}$  NMR, MS, and elemental analyses. The IR spectra of synthesized compounds showed absorption bands due to stretching vibrations of O-H, N-H and Aromatic C-H at  $375.85\text{-}3409\text{ cm}^{-1}$ ,  $3320\text{-}3140\text{ cm}^{-1}$  and  $3200\text{-}3050\text{ cm}^{-1}$  respectively. The strong absorption peak at  $1396\text{ cm}^{-1}$  is due the presence of  $\text{CH}_2$  group. The mass spectrum showed molecular ion peak which was in agreement with molecular mass of compound while the base peak was observed at 145 (100%).

## 6.7 CHARACTERIZATION INTERPRETATION

All the compounds were characterized by IR,  $^1\text{H}$  NMR, MS, and elemental analyses. The IR spectra of synthesized compounds showed absorption bands due to stretching vibrations of O-H, N-H and Aromatic C-H at  $375.85\text{-}3409\text{ cm}^{-1}$ ,  $3320\text{-}3140\text{ cm}^{-1}$  and  $3200\text{-}3050\text{ cm}^{-1}$  respectively. The strong absorption peak at  $1396\text{ cm}^{-1}$  is due the presence of  $\text{CH}_2$  group. The mass spectrum showed molecular ion peak which was in agreement with molecular mass of compound while the base peak was observed at 145 (100%).

### SYNTHESIS:4-METHYL-7-HYDROXY-{8-(5)-2-METHOXYBENZALDEHYDE}

#### PYRIMIDINE-2-THIOL COUMARIN [3C]:

2c, thiourea and sodium hydroxide were mixed carefully with a little water. Obtained mixture was irradiated about 2-3 minutes in microwave oven at 750 watts. (Figure 39), (Figure 42) The mixture had become dark-yellow; Yield: 79.4%; mp:  $184\text{-}185^\circ\text{C}$ ; FT-IR(KBr,  $\text{cm}^{-1}$ ): 3550.12(Aromatic OH), 3354.45(NH), 3177.45(Aromatic CH), 1604.26(C=N), 1548.98(N-Hbending), 1467.90(C=C), 1337.03(OH bending), 1194.23(C-O-C), 1011.77(C-S-C),  $^1\text{H}$  NMR:  $\delta$  2.508 (3H, s), 3.34(3H, s), 6.90 (1H, s), 7.67 (1H, d,  $J = 8.4\text{ Hz}$ ), 7.90-7.19 (3H, 7.97 (ddd,  $J = 8.3, 1.6, 0.5\text{ Hz}$ ), 7.01 (ddd,  $J = 7.3, 7.5, 1.4\text{ Hz}$ ), 7.12 (ddd,  $J = 8.8, 7.5, 1.6\text{ Hz}$ )), 7.26 (1H, ddd,  $J = 8.8, 1.4, 0.5\text{ Hz}$ ), 7.40 (1H, d,  $J = 8.4\text{ Hz}$ ), 8.84 (1H, ).

**SYNTHESIS:4-METHYL-7-HYDROXY-{8-(5)-4-METHYLBENZALDEHYDE}****PYRIMIDINE-2-THIOL COUMARIN [3h]:**

2h, thiourea and sodium hydroxide were mixed carefully with a little water. Obtained mixture was irradiated about 2-3 minutes in microwave oven at 750 watts. (Figure 40) The mixture had become dark-brown; Yield: 85.5%; mp:179-183°C; FT-IR (KBr, cm<sup>-1</sup>): 3757.82(Aromatic OH), 3338.64(NH), 3060.57(Aromatic CH), 1632.34(C=N), 1592.55(N-Hbending), 1494.85(C=C), 1339.53(OH bending),1186.72(C- O-C), 999.31(C-S-C), <sup>1</sup>H NMR: δ 2.509 (3H, s), 6.623 (1H, s), 7.777 (1H, d, *J* = 8.3 Hz), 7.737 (2H, ddd, *J* = 7.702,1Hz), 7.683, 7.49 (1H, d, *J* = 8.3 Hz), 8.65 (1H, s). M+calcd for C<sub>20</sub>H<sub>14</sub>N<sub>2</sub>O<sub>4</sub>S is 378.40 found: 378.40; Anal. Calcd. for C<sub>20</sub>H<sub>14</sub>N<sub>2</sub>O<sub>4</sub>S (%): C, 63.42; H, 3.70; N,7.40; O, 16.91; S, 8.46found: C,63.42; H, 3.70; N, 7.40; O,16.691; S,8.46.

**SYNTHESIS:4-METHYL-7-HYDROXY-{8-(5)-2-CHLOROBENZALDEHYDE}****PYRIMIDINE-2-THIOL COUMARIN [3J]:**

2j, thiourea and sodium hydroxide were mixed carefully with a little water. Obtained mixture was irradiated about 2-3 minutes in microwave oven at 750 watts. (Figure 37), (Figure 41), (Figure 45) (Figure 43). The mixture had become brown; Yield: 85.5%; mp: 177-179°C; FT-IR (K Br, cm<sup>-1</sup>): 3543.45(Aromatic OH), 3338.64(NH), 3060.57(Aromatic-C-H), 1632.34(C=N),1592.55(N-Hbending), 1494.85(C=C), 1339.53(OH bending),1186.72(C- O-C), 986.31(C-S-C), M+calcd or C<sub>20</sub>H<sub>13</sub>N<sub>2</sub>O<sub>3</sub>S is 396.85 found: 396.85; Anal. Calcd. for C<sub>20</sub>H<sub>13</sub>N<sub>2</sub>O<sub>3</sub>S (%): C, 60.47; H, 3.28; Cl,8.93 N, 7.05; O, 12.09; S, 8.06 found: C, 60.47; H, 3.28; Cl,8.9; N, 7.05; O,12.09; S,8.06

**SYNTHESIS: 4-METHYL-7-HYDROXY-{8-(5)-P-CHLOROBENZALDEHYDE}****PYRIMIDINE-2-THIOL COUMARIN [3K]:**

2k, thiourea and sodium hydroxide were mixed carefully with a little water. Obtained mixture was irradiated about 2-3 minutes in microwave oven at 750 watts. (Figure.38), (Figure 44). The mixture had become brown; Yield: 85.5%; mp: 180-183°C; FT-IR(KBr, cm<sup>-1</sup>): 3645.81(Aromatic OH), 3(NH), 3060.57(Aromatic CH), 1632.34(C=N), 1592.55(N-Hbending), 1494.85(C=C), 1339.53(OH bending), 1186.72(C- O-C), 986.31(C-S-C), M+calcd or C<sub>20</sub>H<sub>13</sub>N<sub>2</sub>O<sub>3</sub>S is 396.85 found: 396.85; Anal. Calcd. For C<sub>20</sub>H<sub>13</sub>ClN<sub>2</sub>O<sub>3</sub>S (%): C, 60.47; H, 3.28; Cl, 8.93 N, 7.05; O, 12.09; S, 8.06 found: C, 60.47; H, 3.28; Cl, 8.93; N, 7.05; O, 12.09; S, 8.06.

**SYNTHESIS: 4-METHYL-7-HYDROXY-{8-(5)-P DIMETHYL AMINOBENZALDEHYDE}****PYRIMIDINE-2-THIOL COUMARIN [3L]:**

2l, thiourea and sodium hydroxide were mixed carefully with a little water. Obtained mixture was irradiated about 2-3 minutes in microwave oven at 750 watts. The mixture had become dark-yellow; Yield: 78.9%; mp: 175-179°C; FT-IR (KBr, cm<sup>-1</sup>): 3645.81(Aromatic OH), 3418.21(NH), 3015.14(Aromatic CH), 1649.51(C=N), 1598.65(N-H bending), 1421.81(C=C), 1334.41(OH bending), 1183.72(C- O-C), 984.86(C-S-C),

Figure.37 IR SPECTRUM OF SAMPLE 3J

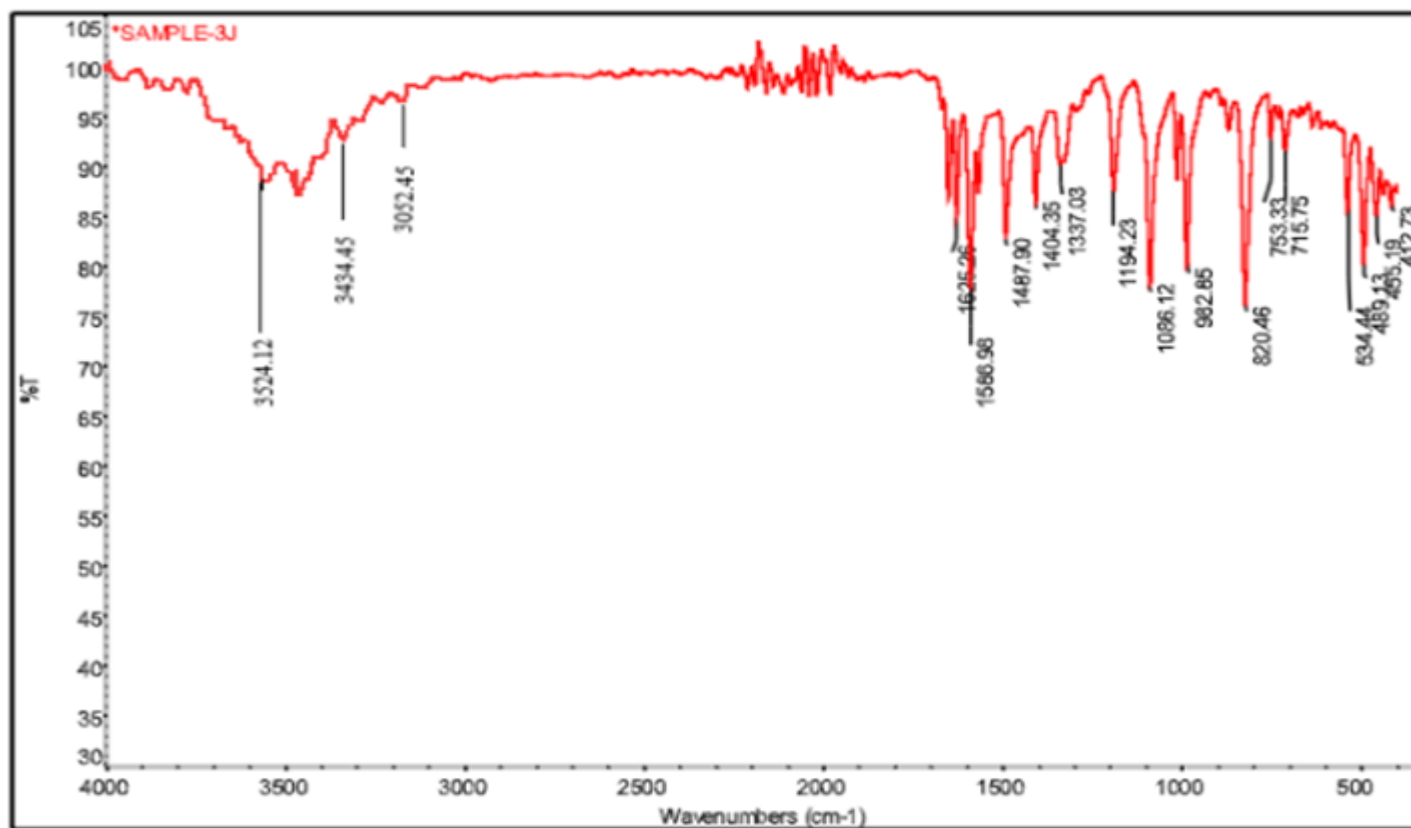


Figure.38 IR SPECTRUM OF SAMPLE 3K

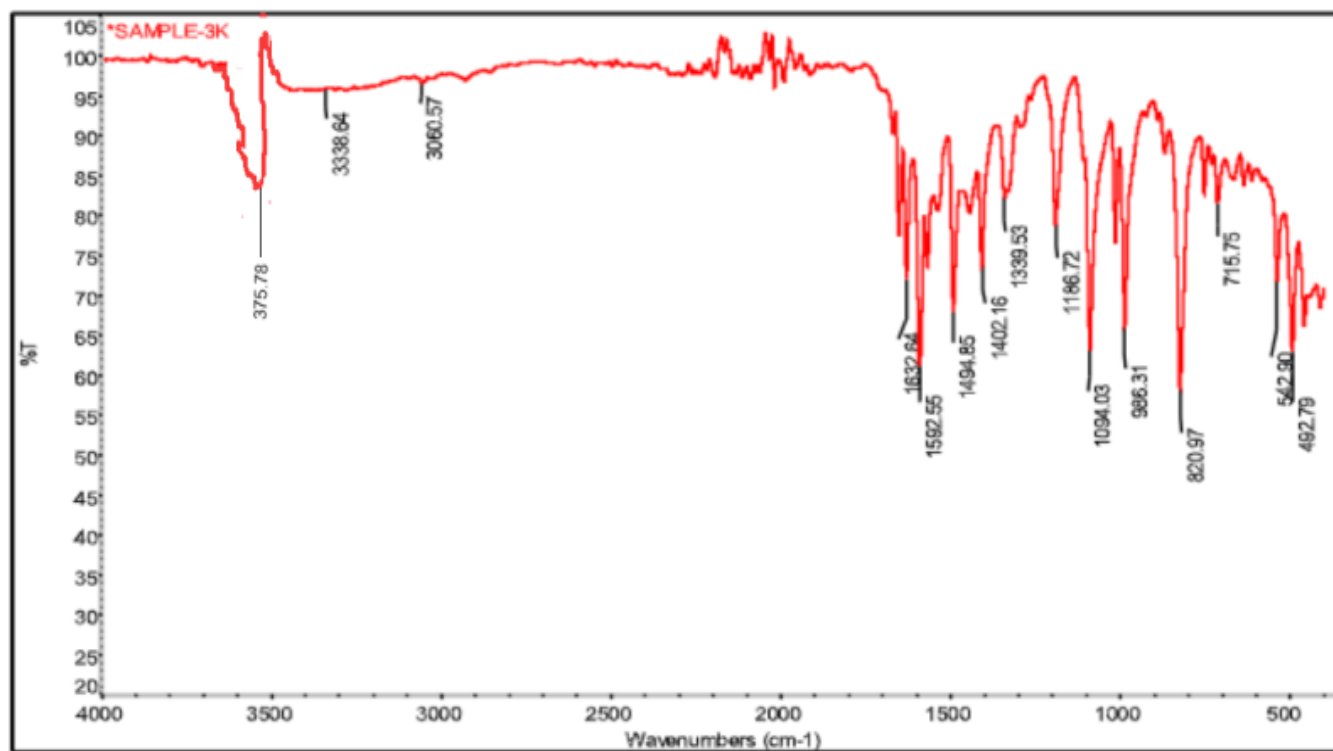


Figure.39 IR SPECTRUM OF SAMPLE 3C

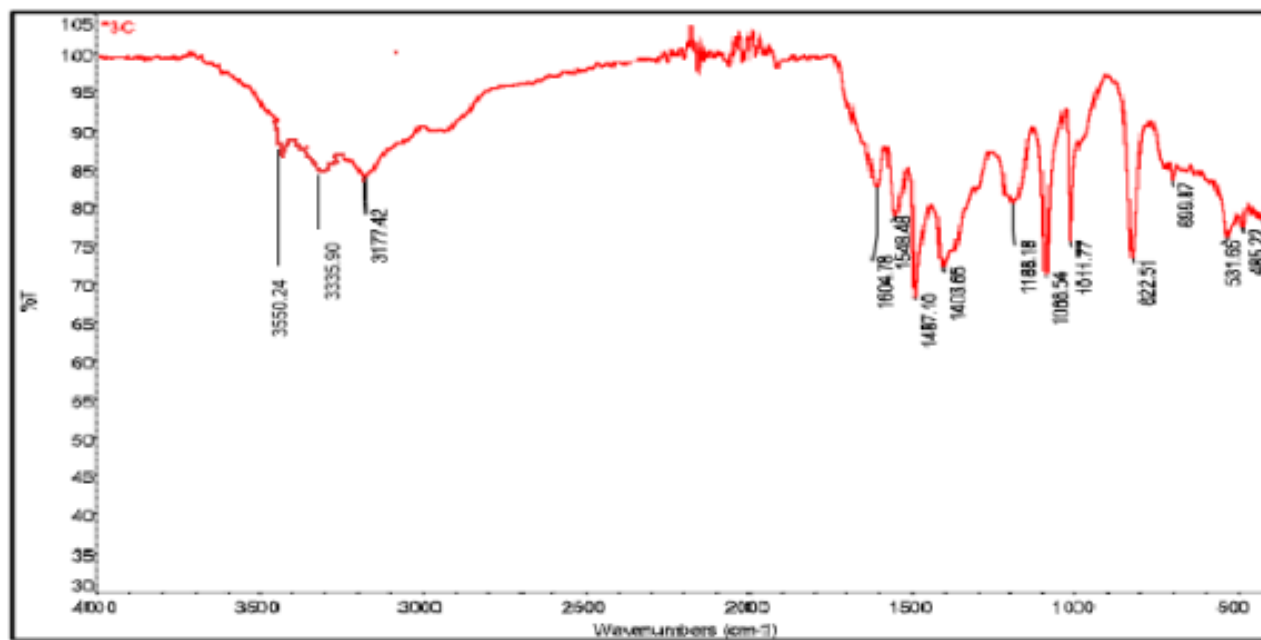


Figure.40 IR SPECTRUM OF SAMPLE 3H

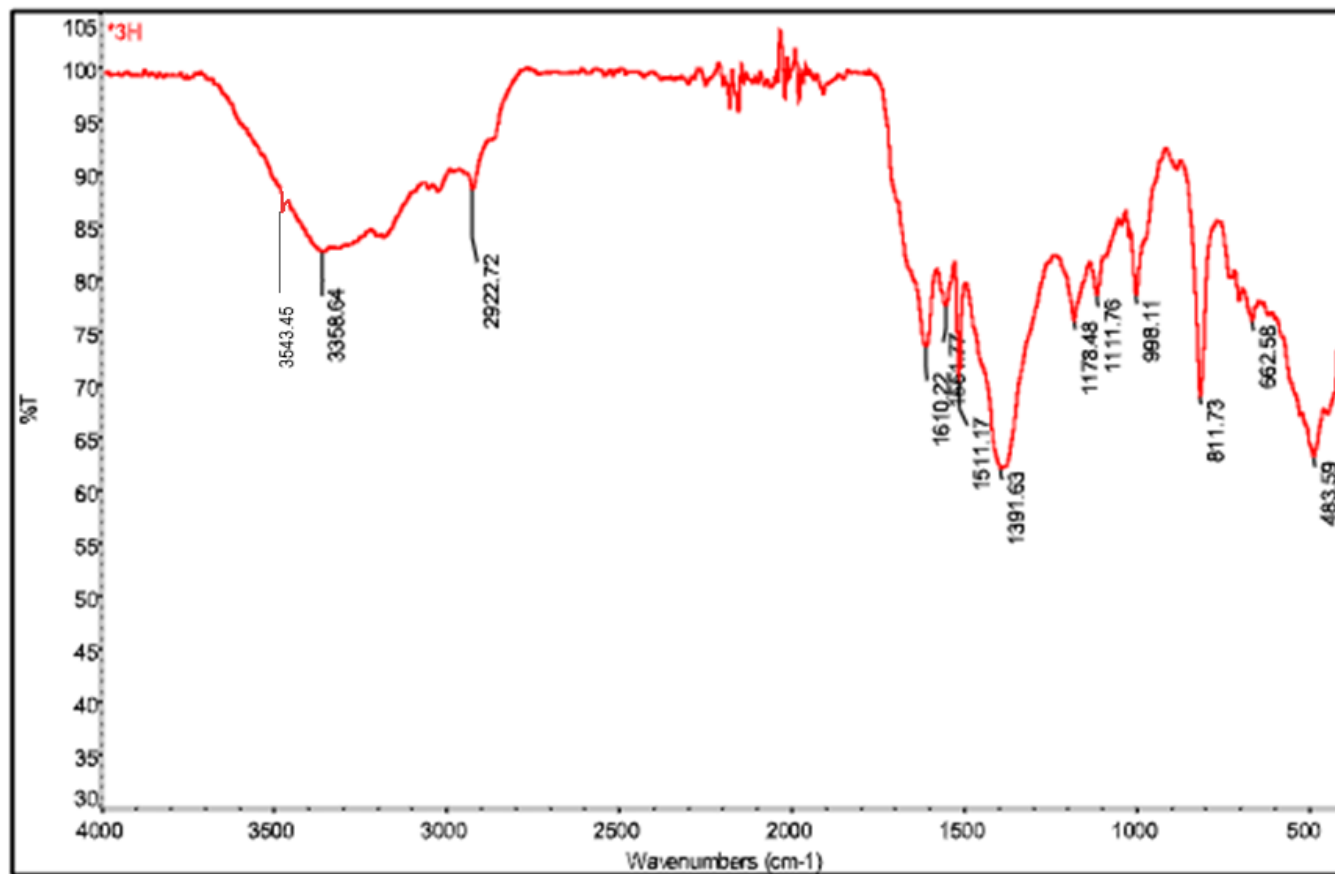




Figure.41 NMR SPECTRUM OF SAMPLE 3J

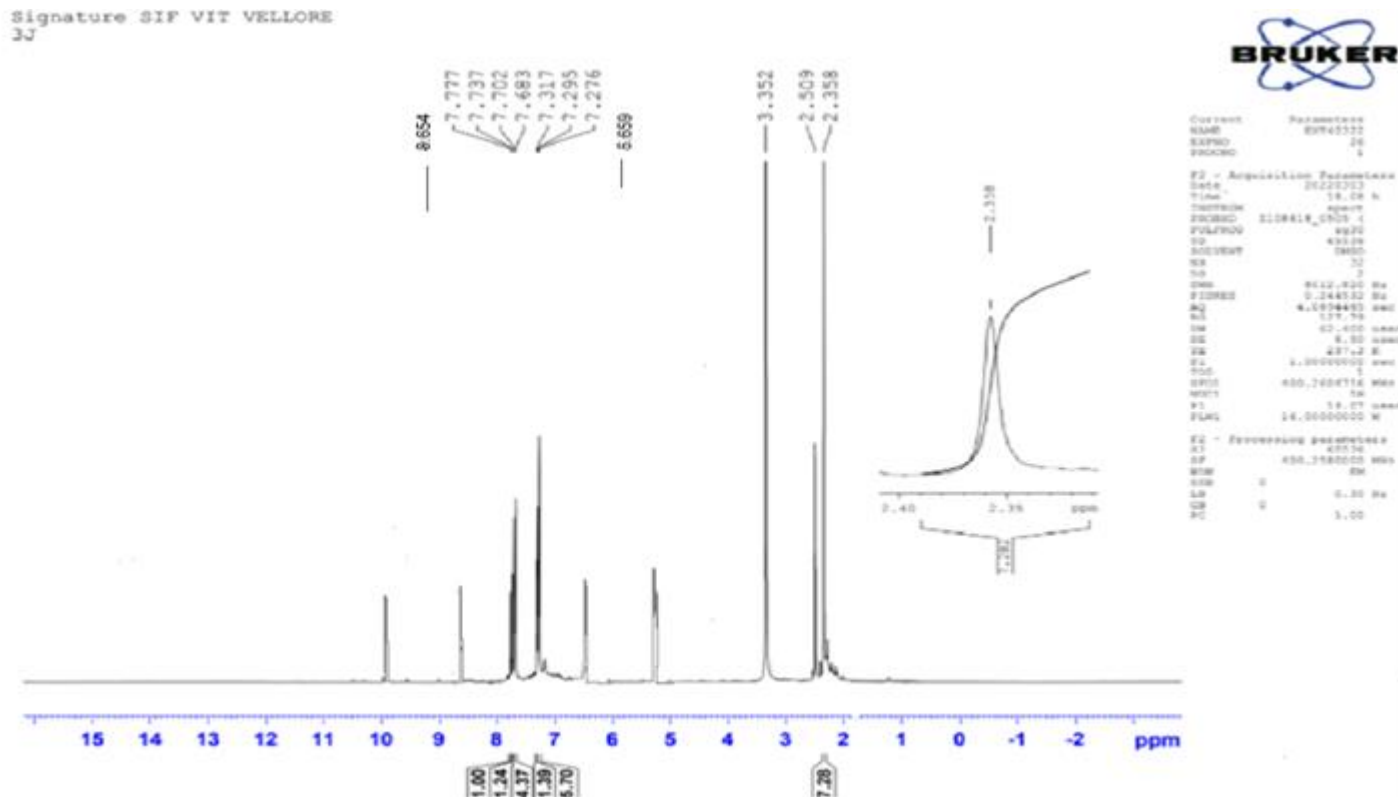
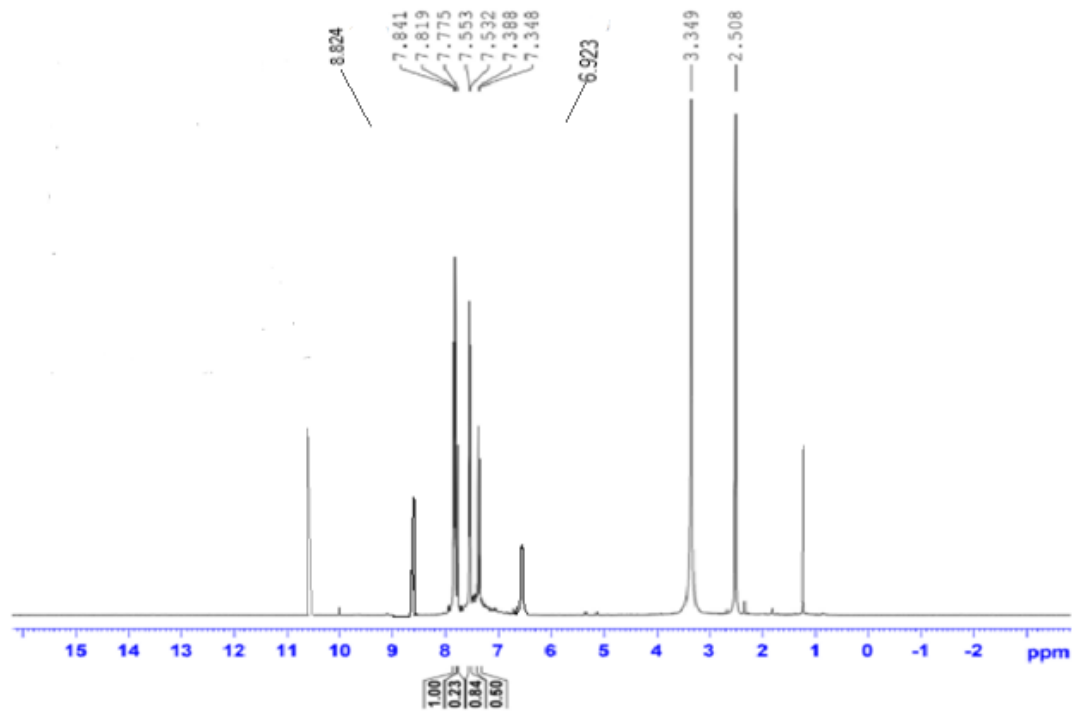


Figure.42 NMR SPECTRUM OF SAMPLE 3C

Signature SIF VIT VELLORE  
3C



Current Data Parameters  
NAME EXT40322  
EXPRO 22  
PROCNO 1

F2 - Acquisition Parameters  
Date\_ 20220903  
Time 17.56 h  
INSTRUM spect  
PROBHD E108618\_0505 1  
PULPROG zg30  
TD 65536  
SOLVENT DMSO  
NS 32  
DS 2  
SWH 8012.820 Hz  
FIDRES 0.344532 Hz  
AQ 4.0894465 sec  
RG 156.91  
DM 42.480 usec  
DE 6.50 usec  
TE 298.0 K  
UL 1.00000000 sec  
TDO 1  
SFO1 400.7604716 MHz  
NOC1 18  
F1 14.07 usec  
FLW1 16.00000000 W

F2 - Processing parameters  
SI 65536  
SF 400.7580000 MHz  
MMB SM  
SBB 0  
LB 0.30 Hz  
GB 0  
PC 1.00

Figure.43 MASS SPECTRUM OF SAMPLE 3J

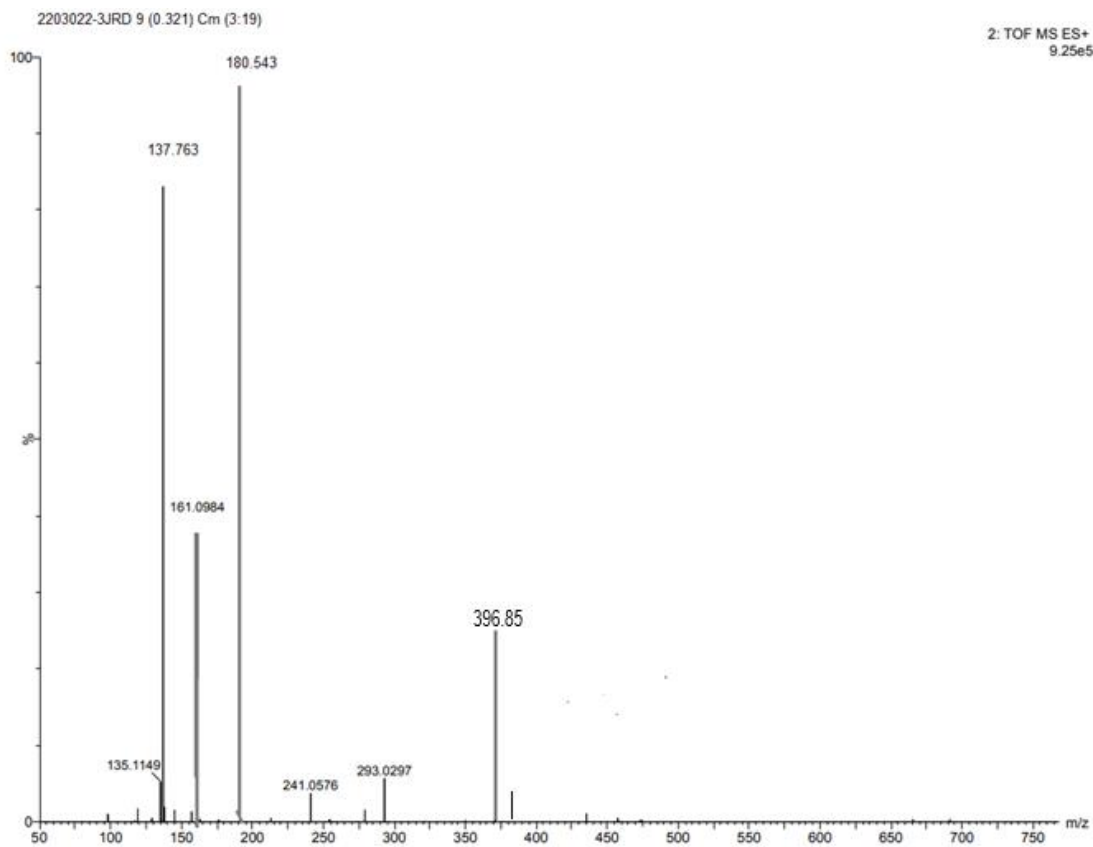


Figure.45 MASS SPECTRUM OF SAMPLE 3C

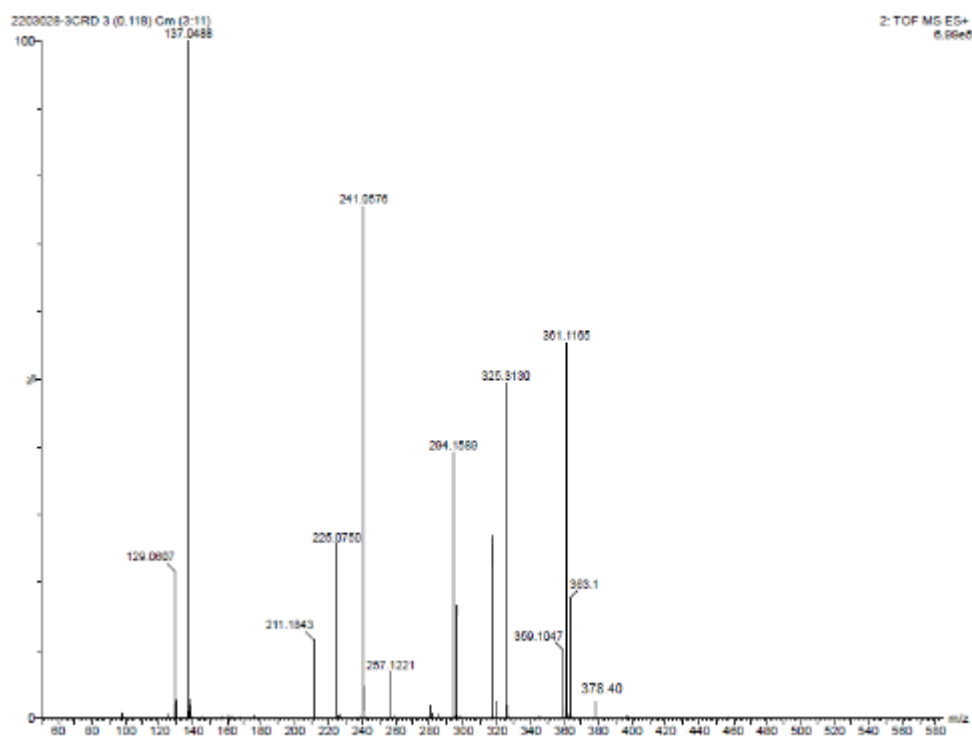
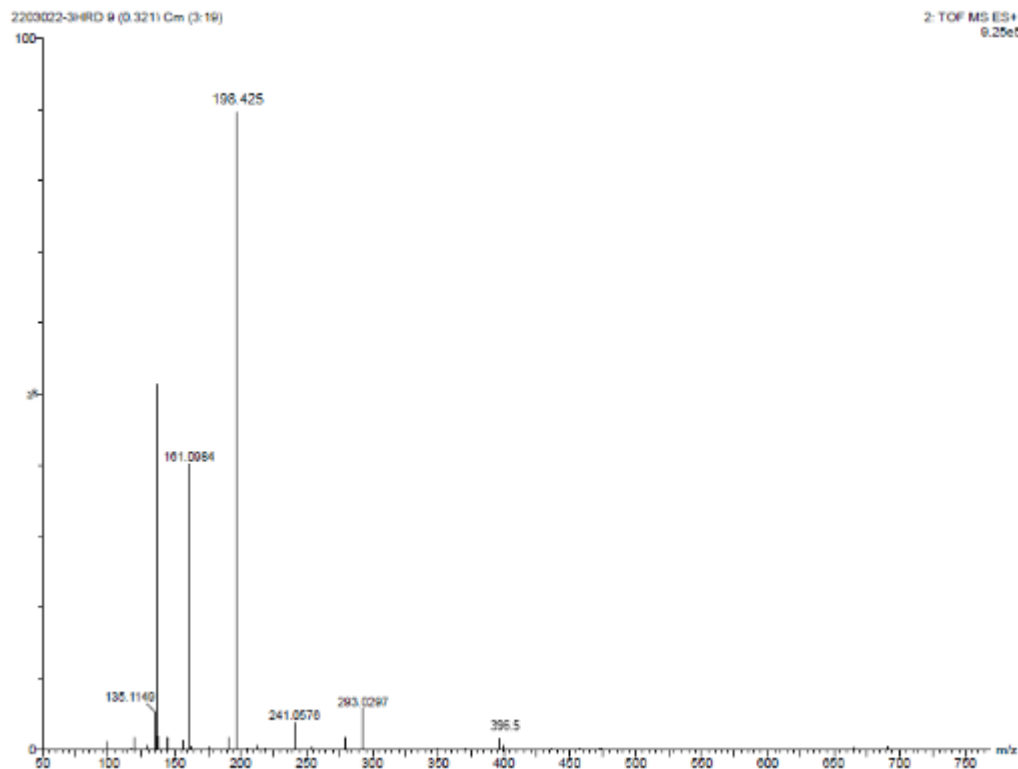


Figure.44 MASS SPECTRUM OF SAMPLE 3K



## 6.7 BIOLOGICAL STUDIES

The synthesized compounds have been subjected to antibacterial activity through Agar well diffusion method (zone of inhibition) using gentamycin as positive control for *E.coli-443* strain.

Among tested compounds, p-amino substituted compound **3J** showed potent activity of  $10.5\pm 0.7$  (500  $\mu\text{g/ml}$ ) compared to standard gentamycin against *E.coli*.

The two compounds **3H** (4-methyl) and **3K** (p-chloro) produced moderate potency of  $9.25\pm 0.35$  and  $9.5\pm 0.7$  in 500  $\mu\text{g/ml}$  respectively. Other compounds exhibited lesser activity than gentamycin against *E.coli*.

The electron donating group substituted compounds (-OH, -NH<sub>2</sub>) showed good cytotoxic activity compared to electron withdrawing group substituted compounds except ortho-chloro substituted compound. Only compound **3j** showed bacterial inhibition in all the four concentrations against *E.coli*. The antibacterial activity results are given in Table 8.

The effects of results were depicted in following figures. The results of *invitro* antibacterial activity were in agree with *in silico* docking studies.

One of the synthesis compound (**3k**) was tested for minium inhibitory concentration against e.coli

Which resulted with moderate activity at (500  $\mu\text{g/ml}$ ) of 39.10% of inhibition. The inhibitory concentration results are given in table

Among the synthesized compounds, **3j** with high potency on *E.coli- 443* is tested against the quinolone resistant strain of *E. coli* ATCC 25922.

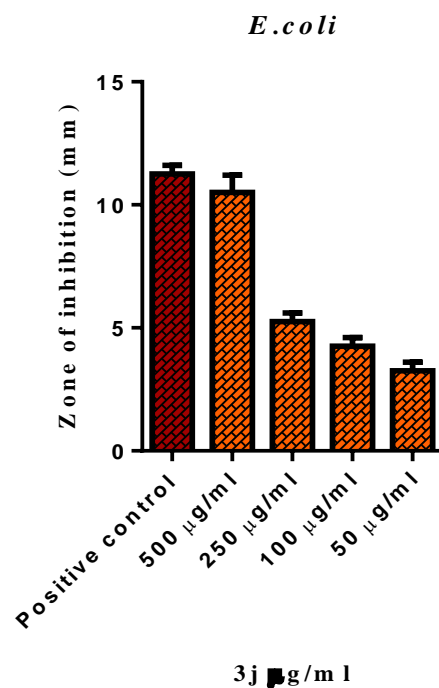
The results of compound **3y** against quinolone-resistant *E.coli* strain showed an average bacterial inhibition of  $11.5\pm 0.35$  at 500  $\mu\text{g/ml}$

**Table 13. SD± Means of zone of inhibition obtained by sample 3h, 3k and 3j against *E.coli*.**

S.No	Name of the test organism	Name of the test sample	Zone of inhibition (mm)				
			SD ± Mean				
			500 µg/ml	250µg/ml	100 µg/ml	50µg/ml	PC
1.	<i>E.coli</i>	3k	9.5±0.7	0	0	0	10.5±0.7
2.		3j	10.5±0.7	5.25±0.35	4.25±0.35	3.25±0.35	11.25±0.35
3.		3h	9.25±0.35	8.25±0.35	5.25±0.35	0	11.25±0.35
4.	Resistance	3j	11.5±0.35	6.25±0.45	3.25±0.35	0	11.5±0.7

SD – Standard Deviation, \*Significance -  $p < 0.05$ .

**Figure.46 Effect of sample 3j against *E.coli*.**



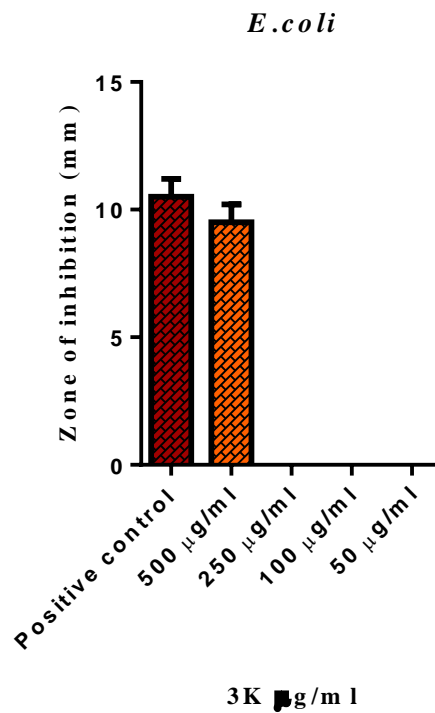


Figure.47 Effect of sample 3k against *E.coli*.

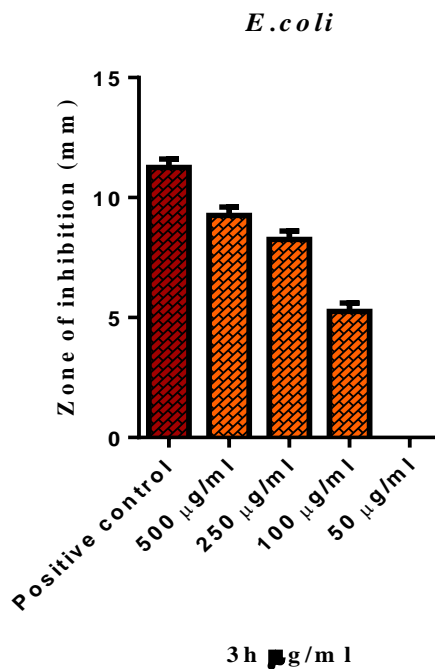
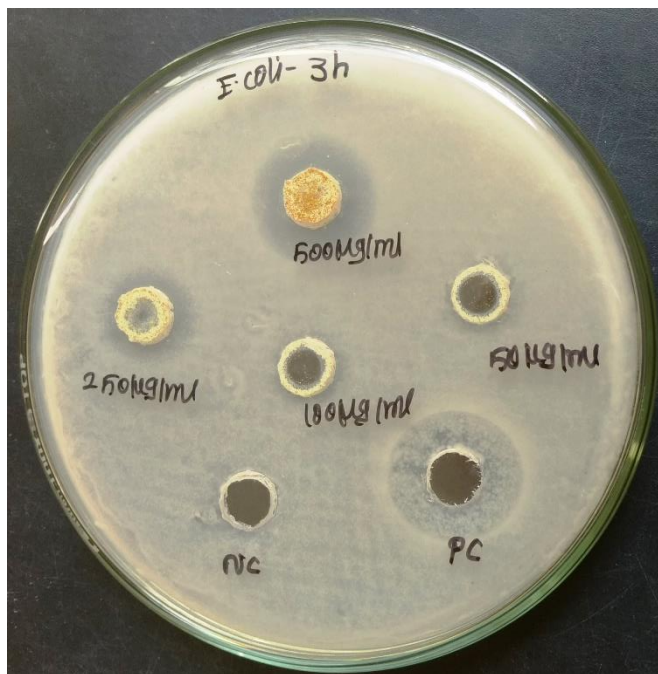
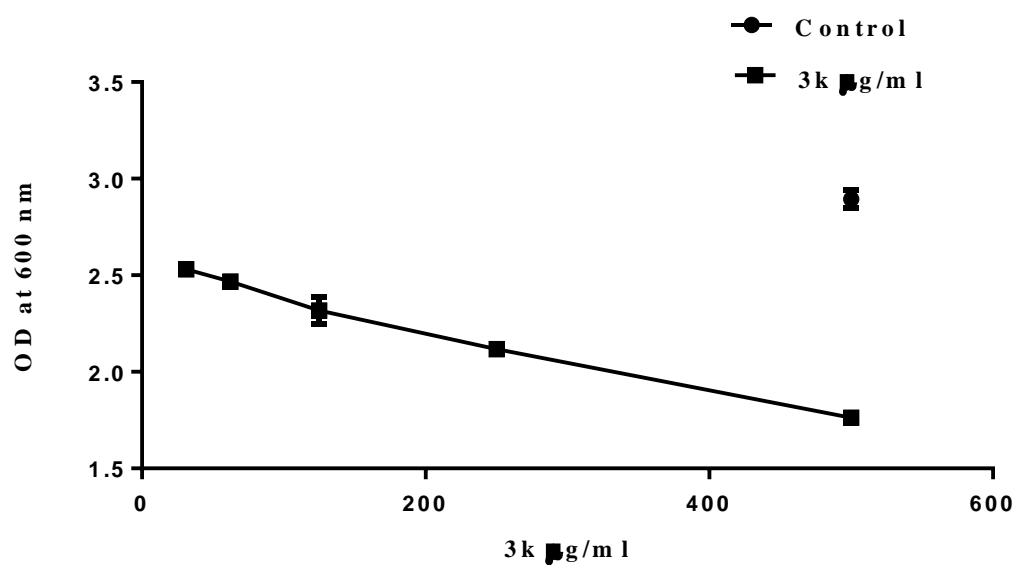


Figure.48 Effect of sample 3h against *E.coli*.



Table 14: Percentage of inhibition

S. No	Tested sample concentration ( $\mu\text{g/ml}$ )	Percentage of inhibition (in triplicates)			Mean value (%)
1.	Control	100	100	100	100
2.	500 $\mu\text{g/ml}$	37.90	39.21	40.18	39.10
3.	250 $\mu\text{g/ml}$	27.26	26.81	26.36	26.81
4.	125 $\mu\text{g/ml}$	21.90	17.27	20.52	19.90
5.	62.5 $\mu\text{g/ml}$	15.82	14.58	13.89	14.76
6.	31.25 $\mu\text{g/ml}$	11.92	13.23	12.54	12.56



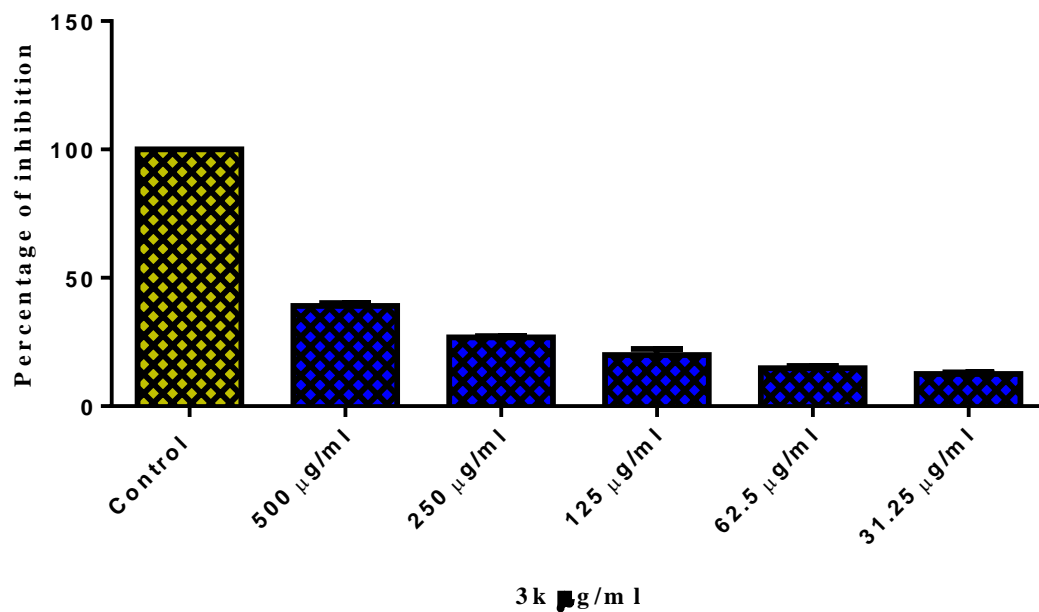


Figure.46 minium inhibitory concentration of sample 3k against *E.coli*.



## 7. CONCLUSION:

A quantitative analysis of the structure activity relationship (QSAR) was performed on a data set of 12 compounds of 4-methyl-7-hydroxy-8-pyrimidine coumarin derivatives as antibacterial agents.

The 2D-QSAR model for a series was established using multiple linear regression (MLR) methods that yielded a regression model with good predictive power. The predictability of the proposed models was demonstrated by various methods, including cross-validation, external evaluation, the root-mean-square error (RMSE) and parity plot.

All of these results showed the good statistical parameters of models to predict the activity for developing new compounds as antibacterial agents. The developed 2D-QSAR model expressed by equation 3 was used to predict the biological activity (pIC<sub>50</sub>) of newly designed 4-methyl-7-hydroxy-8-pyrimidine coumarin derivatives as antibacterial agents against DNA gyrase.

From the results, four designed compounds 3c, 3h, 3j, 3k, 3l, can act as potential antibacterial agents against DNA gyrase.

The results were acceptable giving significance to model equation descriptors supporting QSAR studies.

Thus, computer aided drug design is required to design new compounds before synthesis, thus reducing the cost by filtering the compounds. From the docking results, compounds with good docking score has been synthesized, characterized and subjected to antibacterial activity.

The results of antibacterial study explain that the synthesized active compound could serve as intermediate for generating good biological agents

## 8. BIBLIOGRAPHY

1. Holbrook SY, Garneau-Tsodikova S. What is medicinal chemistry?—Demystifying a rapidly evolving discipline!. *MedChemComm*. 2017;8(9):1739-41.
2. Walsh CT, Garneau-Tsodikova S, Gatto Jr GJ. Protein posttranslational modifications: the chemistry of proteome diversifications. *Angewandte Chemie International Edition*. 2005 Nov 18;44(45):7342-72
3. Khan IA, Kulkarni MV, Gopal M, Shahabuddin MS, Sun CM. Synthesis and biological evaluation of novel angularly fused polycyclic coumarins. *Bioorganic & medicinal chemistry letters*. 2005 Aug 1;15(15):3584-7.
4. Grant, S.S. and Hung, D.T., 2013. Persistent bacterial infections, antibiotic tolerance, and the oxidative stress response. *Virulence*, 4(4), pp.273-283
5. Kim, J.S., Heo, P., Yang, T.J., Lee, K.S., Jin, Y.S., Kim, S.K., Shin, D. and Kweon, D.H., 2011.
6. Dandriyal J, Singla R, Kumar M, Jaitak V. Recent developments of C-4 substituted coumarin derivatives as anticancer agents. *European journal of medicinal chemistry*. 2016 Aug 25;119:141-68.
7. Singh H, Singh JV, Gupta MK, Saxena AK, Sharma S, Nepali K, Bedi PM. Triazole tethered isatin-coumarin based molecular hybrids as novel antitubulin agents: Design, synthesis, biological investigation and docking studies. *Bioorganic & medicinal chemistry letters*. 2017 Sep 1;27(17):3974-9.
8. Vazquez-Rodriguez S, Lopez RL, Matos MJ, Armesto-QuintasG, Serra S, Uriarte E, Santana L, Borges F, Crego AM, Santos Y(2015) Design, synthesis and antibacterial study of new potent and selective coumarin–chalcone derivatives for the treatment of *Mycobacterium tuberculosis*. *Bioorg Med Chem* 23(21):7045–7052.
9. Azelmat J, Fiorito S, Taddeo VA, Genovese S, Epifano F, Grenier D(2015) Synthesis and evaluation of antibacterial and anti-inflammatory properties of naturally occurring coumarins. *Phytochemistry Letters* 13:399–405
10. Hryniewicz K, Szczypa K, Sulikowska A, Jankowski K, Betlejewska K, Hryniewicz W. Antibiotic susceptibility of bacterial strains isolated from urinary tract infections in Poland. *Journal of Antimicrobial Chemotherapy*. 2001 Jun 1;47(6):773-80.
11. Detsi A, Kontogiorgis C, Hadjipavlou-Litina D. Coumarin derivatives: an updated patent review (2015-2016). *Expert opinion on therapeutic patents*. 2017 Nov 2;27(11):1201-26
12. Stefanachi A, Leonetti F, Pisani L, Catto M, Carotti A. Coumarin: A natural, privileged and versatile scaffold for bioactive compounds. *Molecules*. 2018 Feb;23(2):250
13. Kaur M, Kohli S, Sandhu S, Bansal Y, Bansal G. Coumarin: a promising scaffold for anticancer agents. *Anti-Cancer Agents in Medicinal Chemistry (Formerly Current Medicinal Chemistry-Anti-Cancer Agents)*. 2015 Oct 1;15(8):1032-48

14. Dandriyal J, Singla R, Kumar M, Jaitak V. Recent developments of C-4 substituted coumarin derivatives as anticancer agents. *European journal of medicinal chemistry*. 2016 Aug 25;119:141-68
15. Hryniewicz K, Szczypa K, Sulikowska A, Jankowski K, Betlejewska K, Hryniewicz W. Antibiotic susceptibility of bacterial strains isolated from urinary tract infections in Poland. *Journal of Antimicrobial Chemotherapy*. 2001 Jun 1;47(6):773-80
16. Sahoo J, Mekap SK, Kumar PS. Synthesis, spectral characterization of some new 3-heteroaryl azo 4-hydroxy coumarin derivatives and their antimicrobial evaluation. *Journal of Taibah University for Science*. 2015 Apr 1;9(2):187-95
17. Houser JR, Barnhart C, Boutz DR, Carroll SM, Dasgupta A, Michener JK, Needham BD, Papoulas O, Sridhara V, Sydykova DK, Marx CJ. Controlled measurement and comparative analysis of cellular components in *E. coli* reveals broad regulatory changes in response to glucose starvation. *PLoS computational biology*. 2015 Aug 14;11(8):e1004400
18. Emody L, Kerényi M, Nagy G. Virulence factors of uropathogenic *Escherichia coli*. *International journal of antimicrobial agents*. 2003 Oct 1;22:29-33
19. Nofal ZM, El-Zahar MI, El-Karim A. Novel coumarin derivatives with expected biological activity. *Molecules*. 2000 Feb;5(2):99-113
20. Mangasuli, S.N., Hosamani, K.M., Devarajegowda, H.C., Kurjogi, M.M. and Joshi, S.D., 2018. Synthesis of coumarin-theophylline hybrids as a new class of anti-tubercular and antimicrobial agents. *European journal of medicinal chemistry*, 146, pp.747-756
21. Holiyachi, M., Shastri, S.L., Chougala, B.M., Shastri, L.A., Joshi, S.D., Dixit, S.R., Nagarajiah, H. and Sunagar, V.A., 2016. Design, Synthesis and Structure-Activity Relationship Study of Coumarin Benzimidazole Hybrid as Potent Antibacterial and Anticancer Agents. *ChemistrySelect*, 1(15), pp.4638-4644
22. Heravi MM, Khaghaninejad S, Mostofi M. Pechmann reaction in the synthesis of coumarin derivatives. *Advances in heterocyclic chemistry*. 2014 Jan 1;112:1-50.
23. Smith, Clare V.. "Investigating the mechanism and energy coupling of DNA gyrase." (1998).
24. Menzel R, Gellert M. Regulation of the genes for *E. coli* DNA gyrase: homeostatic control of DNA supercoiling. *Cell*. 1983 Aug 1;34(1):105-13.
25. Khan T, Sankhe K, Suvarna V, Sherje A, Patel K, Dravyakar B. DNA gyrase inhibitors: Progress and synthesis of potent compounds as antibacterial agents. *Biomedicine & Pharmacotherapy*. 2018 Jul 1;103:923-38
26. Liu H, Xia DG, Chu ZW, Hu R, Cheng X, Lv XH. Novel coumarin-thiazolyl ester derivatives as potential DNA gyrase Inhibitors: Design, synthesis, and antibacterial activity. *Bioorganic chemistry*. 2020 Jul 1;100:103907.
27. Sugino A, Higgins NP, Brown PO, Peebles CL, Cozzarelli NR. Energy coupling in DNA gyrase and the mechanism of action of novobiocin. *Proceedings of the National Academy of Sciences*. 1978 Oct 1;75(10):4838-42.

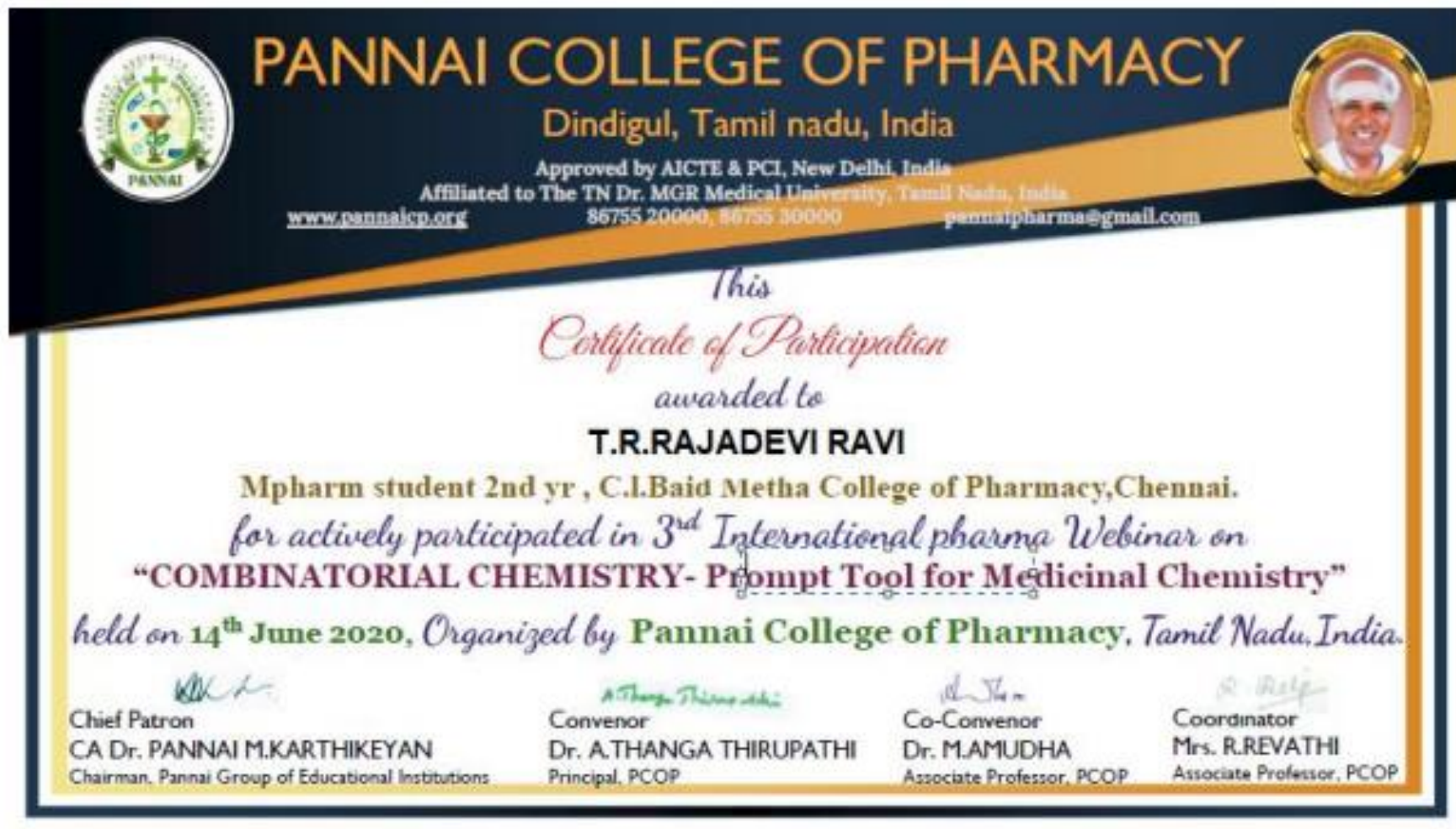
28. Mangasuli, S.N., Hosamani, K.M., Devarajegowda, H.C., Kurjogi, M.M. and Joshi, S.D., 2018. Synthesis of coumarin-theophylline hybrids as a new class of anti-tubercular and anti-microbial agents. *European journal of medicinal chemistry*, 146, pp.747-756
29. Holiyachi, M., Shastri, S.L., Chougala, B.M., Shastri, L.A., Joshi, S.D., Dixit, S.R., Nagarajiah, H. and Sunagar, V.A., 2016. Design, Synthesis and Structure-Activity Relationship Study of Coumarin Benzimidazole Hybrid as Potent Antibacterial and Anticancer Agents. *ChemistrySelect*, 1(15), pp.4638-4644
30. Achar, G., Shahini, C.R., Patil, S.A. and Budagumpi, S., 2017. Synthesis, structural characterization, crystal structures and antibacterial potentials of coumarin-tethered N-heterocyclic carbene silver (I) complexes. *Journal of Organometallic Chemistry*, 833, pp.28-42
31. Wu, Y., Vulić, M., Keren, I. and Lewis, K., 2012. Role of oxidative stress in persister tolerance. *Antimicrobial agents and chemotherapy*, 56(9), pp.4922-4926
32. Liu, B., Hu, G., Tang, X., Wang, G. and Xu, Z., 2018. 1H-1, 2, 3-Triazole-tethered Isatin-coumarin Hybrids: Design, Synthesis and In Vitro Anti-mycobacterial Evaluation. *Journal of Heterocyclic Chemistry*, 55(3), pp.775-780
33. Xu, M., Wu, P., Shen, F., Ji, J. and Rakesh, K.P., 2019. Chalcone derivatives and their antibacterial activities: Current development. *Bioorganic chemistry*, 91, p.103133
34. Liu, H., Ren, Z.L., Wang, W., Gong, J.X., Chu, M.J., Ma, Q.W., Wang, J.C. and Lv, X.H., 2018. Novel coumarin-pyrazole carboxamide derivatives as potential topoisomerase II inhibitors: Design, synthesis and antibacterial activity. *European journal of medicinal chemistry*, 157, pp.81-87.
35. Achar, G., VC, R. and Budagumpi, S., 2017. Coumarin-tethered (benz) imidazolium salts and their silver (I) N-heterocyclic carbene complexes: Synthesis, characterization, crystal structure and antibacterial studies. *Applied Organometallic Chemistry*, 31(11), p.e3770
36. Behrami A, Demaku S, Dobra Bahrije SI. Synthesis, characterization and antibacterial studies of 2-amino-5-(4-(4-amino-4-carboxy-butylamino)-3-[1-(2-hydroxy-phenylamino)-ethyl]-2-oxo-2H-chromen-7-ylamino)-pentanoic acid and its metal (II) complexes. *Int. J. Pharm. Sci. Rev. Res.* 2013;20(1):4-10.
37. Achar, G., Agarwal, P., Brinda, K.N., Malecki, J.G., Keri, R.S. and Budagumpi, S., 2018. Ether and coumarin-functionalized (benz) imidazolium salts and their silver (I)-N-heterocyclic carbene complexes: Synthesis, characterization, crystal structures and antimicrobial studies. *Journal of Organometallic Chemistry*, 854, pp.64-75
38. Patel, D., Kumari, P. and Patel, N.B., 2017. Synthesis and biological evaluation of coumarin based isoxazoles, pyrimidinthiones and pyrimidin-2-ones. *Arabian Journal of Chemistry*, 10, pp.S3990-S4001
39. Wilson, A.P.R., Livermore, D.M., Otter, J.A., Warren, R.E., Jenks, P., Enoch, D.A., Newsholme, W., Oppenheim, B., Leanord, A., McNulty, C. and Tanner, G., 2016. Prevention and control of



- multi-drug-resistant Gram-negative bacteria: recommendations from a Joint Working Party. *Journal of Hospital Infection*, 92, pp.S1-S44
40. Sahoo CR, Sahoo J, Mahapatra M, Lenka D, Sahu PK, Dehury B, Padhy RN, Paidesetty SK. Coumarin derivatives as promising antibacterial agent (s). *Arabian Journal of Chemistry*. 2021 Feb 1;14(2):102922.
41. Desai, N.C., Satodiya, H.M., Rajpara, K.M., Joshi, V.V. and Vaghani, H.V., 2017. A microwave-assisted facile synthesis of novel coumarin derivatives containing cyanopyridine and furan as antimicrobial agents. *Journal of Saudi Chemical Society*, 21, pp.S153-S162
42. Patil RB, Sawant SD. Synthesis, characterization, molecular docking and evaluation of antimicrobial activity of some 3-heteroaryl substituted chromen-2-one derivatives. *Synthesis*. 2015;7(3):471-80.
43. Aksungur, T., Aydinler, B., Seferoğlu, N., Özkütük, M., Arslan, L., Reis, Y., Açık, L. and Seferoğlu, Z., 2017. Coumarin-indole conjugate donor-acceptor system: Synthesis, photophysical properties, anion sensing ability, theoretical and biological activity studies of two coumarin-indole based push-pull dyes. *Journal of Molecular Structure*, 1147, pp.364-379
44. Achar G, Shahini CR, Patil SA, Budagumpi S. Synthesis, structural characterization, crystal structures and antibacterial potentials of coumarin-tethered N-heterocyclic carbene silver (I) complexes. *Journal of Organometallic Chemistry*. 2017 Mar 15;833:28-42.
45. Mahendra raj, K., Mruthyunjayaswamy, B.H.M., 2017. Synthesis, spectroscopic characterization, electrochemistry and biological activity evaluation of some metal (II) complexes with ON donor ligands containing indole and coumarin moieties. *J. Saudi Chem. Soc.* 1074, 572-582
46. Vekariya, R.H., Patel, K.D., Rajani, D.P., Rajani, S.D. and Patel, H.D., 2017 A one pot, three component synthesis of coumarin hybrid thiosemicarbazone derivatives and their antimicrobial evolution. *Journal of the Association of Arab Universities for Basic and Applied Sciences*, 23, pp.10-19
47. Katsori AM, Hadjipavlou-Litina D. Coumarin derivatives: an updated patent review (2012–2014). *Expert opinion on therapeutic patents*. 2014 Dec 1;24(12):1323-47.
48. Kaneria, A.R., Giri, R.R., Bhila, V.G., Prajapati, H.J. and Brahmabhatt, D.I., 2017. Microwave assisted synthesis and biological activity of 3-aryl-furo [3, 2-c] coumarins. *Arabian Journal of Chemistry*, 10, pp.S1100-S1104
49. Shirahatti AM, Kumar MK, Sachin PA, Soumya K, Kotresh O, Masuku MC. Synthesis, characterization and antimicrobial activity of some coumarin fused heterocycles.

50. Kenchappa, R., Bodke, Y.D., Chandrashekar, A., Telkar, S., Manjunatha, K.S. and Sindhe, M.A., 2017. Synthesis of some 2, 6-bis (1-coumarin-2-yl)-4-(4-substituted phenyl) pyridine derivatives as potent biological agents. *Arabian Journal of Chemistry*, 10, pp.S1336-S1344
51. Ghashang, M., Mansoor, S.S. and Aswin, K., 2014. Pentafluorophenylammonium triflate (PFPAT) catalyzed facile construction of substituted chromeno [2, 3-d] pyrimidinone derivatives and their antimicrobial activity. *Journal of advanced research*, 5(2), pp.209-218
52. Hamdi, N., Passarelli, V. and Romerosa, A., 2011. Synthesis, spectroscopy and electrochemistry of new 4-(4-acetyl-5-substituted-4, 5-dihydro-1, 3, 4-oxodiazol-2-yl) methoxy)-2H-chromen-2-ones as a novel class of potential antibacterial and antioxidant derivatives. *Comptes Rendus Chimie*, 14(6), pp.548-555
53. Li B, Pai R, Di M, Aiello D, Barnes MH, Butler MM, Tashjian TF, Peet NP, Bowlin TL, Moir DT. Coumarin-based inhibitors of *Bacillus anthracis* and *Staphylococcus aureus* replicative DNA helicase: chemical optimization, biological evaluation, and antibacterial activities. *Journal of medicinal chemistry*. 2012 Dec 27; 55(24):10896-908.







## CERTIFICATE OF PARTICIPATION

This is to certify that

**T.R. RAJADEVI RAVI**

Attended the E-Workshop on 'Structure Based and Ligand Based Drug Design'

held on 13<sup>th</sup> and 14<sup>th</sup> July 2020

*Organized by*

Department of Pharmaceutical Chemistry

JSS College of Pharmacy, Sri Shivarathreeswara Nagara, Mysuru 570015

A handwritten signature in blue ink, appearing to be 'B.R. Prashantha'.

**Dr. B.R. Prashantha Kumar**  
Organizing Secretary

A handwritten signature in blue ink, appearing to be 'G.V. Pujar'.

**Dr. G. V. Pujar**  
Convener

A handwritten signature in blue ink, appearing to be 'T.M. Pramod'.

**Dr. T. M. Pramod Kumar**  
Chairman

